Mangyeong River Hydraulic Modeling Analysis

Draft Prepared For:

Korea Institute of Construction Technology, Republic of Korea

by:

Dr. Pierre Y. Julien

Jaehoon Kim

Colorado State University

Engineering Research Center

Department of Civil and Environmental Engineering

Fort Collins, Colorado, 80523

May, 2010

ABSTRACT

There is an increase in environmental concerns about rivers and streams in South Korea. Mangyeong River is one of the main watersheds on the western central region of South Korea. When Mangyeong River was channelized in the early 1900's, an abandoned channel was formed. There is interest to restore this abandoned channel to increase flow interaction, to improve water quality, to enhance wildlife habitat, and to provide an environmental friendly site for local people. This study will be used to aid in reconnecting the abandoned channel to the main river.

This report provides a detailed study of 4.25 km of Mangyeong River from station 104+000 to the tributary of Soyang Stream at station 87+000. A Flow duration analysis was performed to obtain the discharge of 255 m^3/s with a return interval of 1.5 year. The hydraulic analysis of the Mangyeong River determines the changes in channel morphology and other important hydraulic and sediment parameters.

The hydraulic modeling analysis was performed using HEC-RAS. Hydraulic parameters were examined from upstream to downstream with discharge of 255 m^3/s and reach-averaged spatial trends were analyzed for various discharges. The results showed that the top width is 244 m, the mean flow depth is 1.11 m, the width/depth ratio is 277, the channel velocity is 1.18 m/s, Froude number is 0.42. The cross sectional area was changed most as a result of changes in various discharges. The hydraulic parameters had sudden changes in the vicinity of the three sills.

The bed material was sampled and the median grain size was obtained for the study reach. The particle size distribution indicated that the study reach is composed of very coarse gravel with a median particle diameter of 36 mm. The maximum movable grain size was estimated at 33 mm and coarser bed material will not move. The sediment load was also measured and the total load was obtained with the Modified Einstein method. When the

discharge of 255 m^3/s is applied, the total load is 6.54 thousand tons per day and the equivalent sediment concentration is 240 mg/l. In the comparison between measurement results and the HEC-RAS modeling results, total load was closer to the field measurements than any other methods. Therefore, the calculations should be based on the field measurement.

The equilibrium channel width and slope were examined at various discharges with respect to return intervals. In the equilibrium channel width analysis, the methods of Julien-Wargadalam and Lacey gave an equilibrium width of 83 m and 77m respectively compared with HEC-RAS result of 239m at the discharge of 255 m^3/s. For high discharge, the results of those two methods were closer to the HEC-RAS results. The equilibrium slope was also calculated using the Julien-Wargadalam's method. The equilibrium slope was determined as 0.00111 m/m, compared to the actual channel slope of 0.00230 m/m. The result of this method was lower than the actual slope. It is important to notice that this channel is armored and the presence of sills prevents the formation of narrower channel.

The changes in channel planform geometry were analyzed using aerial photographs from 1967 to 2003. Based on aerial photographs the channel geometry changed from meandering to straight. The observations were compared with several methods. The methods of Leopold and Wolman, Henderson, and Schumm and Khan are the best methods for identifying the planform geometry for Mangyeong River as a straight channel. This occurred because of the channelization and levee construction on the stream banks. The channel sinuosity is analyzed to 1.03. The thalweg and mean bed elevation profile were analyzed using field measurement in 1976, 1993, and 2009. Both measured profiles indicated that the channel has degraded about 2 m since 1976.

ACKNOWLEDGMENT

This work was completed with support provided by the Korea Institute of Construction Technology (KICT), Republic of Korea. The authors would like to thank Dr. Hyoseop Woo for his dedication and insight on restoration of abandoned channels. The efforts of many people inspired our work has enabled this Mangyeong River project: Dr. Honggu Yeo, Dr. Jungu Kang, and Il Hong at KICT. Dongbu Enigneering was responsible for field data collection at Mangyeong River. Finally, the authors are most grateful to Dr. Un Ji at Myongji University for the direct collaboration and participation in the discussion of the results.

TABLE OF CONTENTS

LIST OF FIGURES

LIST OF TABLES

Chapter 1 INTRODUCTION

1.1 BACKGROUND

In Korea, all rivers and streams are classified by three categories: national rivers, local rivers of first grade, and local rivers of second grade. They are divided with respect to conservation and economic management. Korean rivers are divided into six watersheds: Han River, Kum River, Youngsan River, Nakdong River, Sumjin River, and Jeju Island watershed. The Kum River watershed is located in western central part of South Korea. Mangyeong River, which is the study site, is close to the Kum River watershed. Figure 1-1 shows the six watersheds in South Korea.

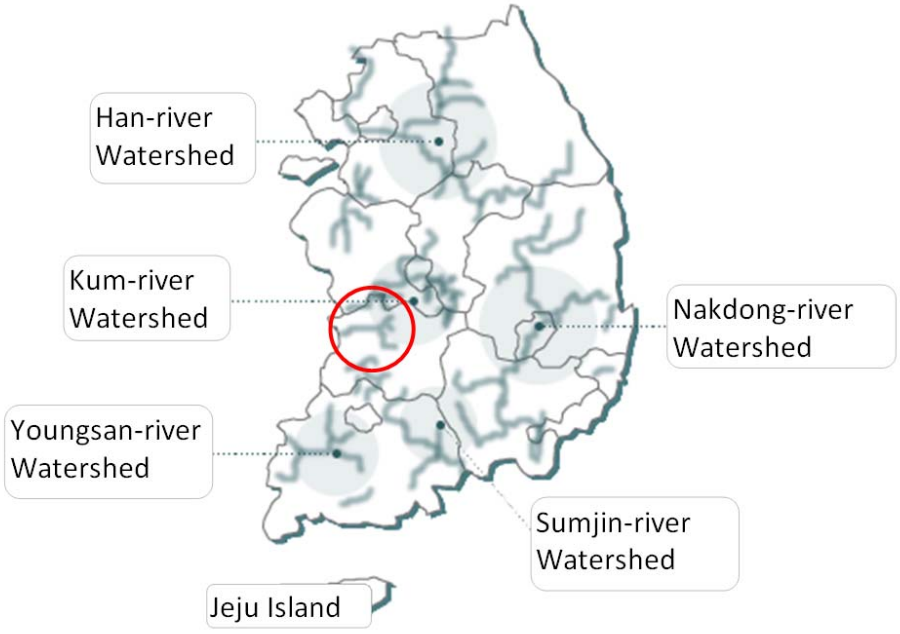

Figure 1-1: Watershed in Korea (KRA 2008)

Mangyeong River is placed in the lower part of Kum River watershed. Mangyeong River has watershed area of 1,527.1km^2, is 77.4 km long, and is located in the following provinces: Wanju-gun, Jeonju-si, Iksan-si, Gimje-si, and Gunsan-si in Jeollabuk-do.

The study site is located just upstream of Soyang Stream tributary in Guman-ri, Bongdong-eup, Wanju-gun, Jeollabuk-do. Figure 1-2 provides a location map of the site.

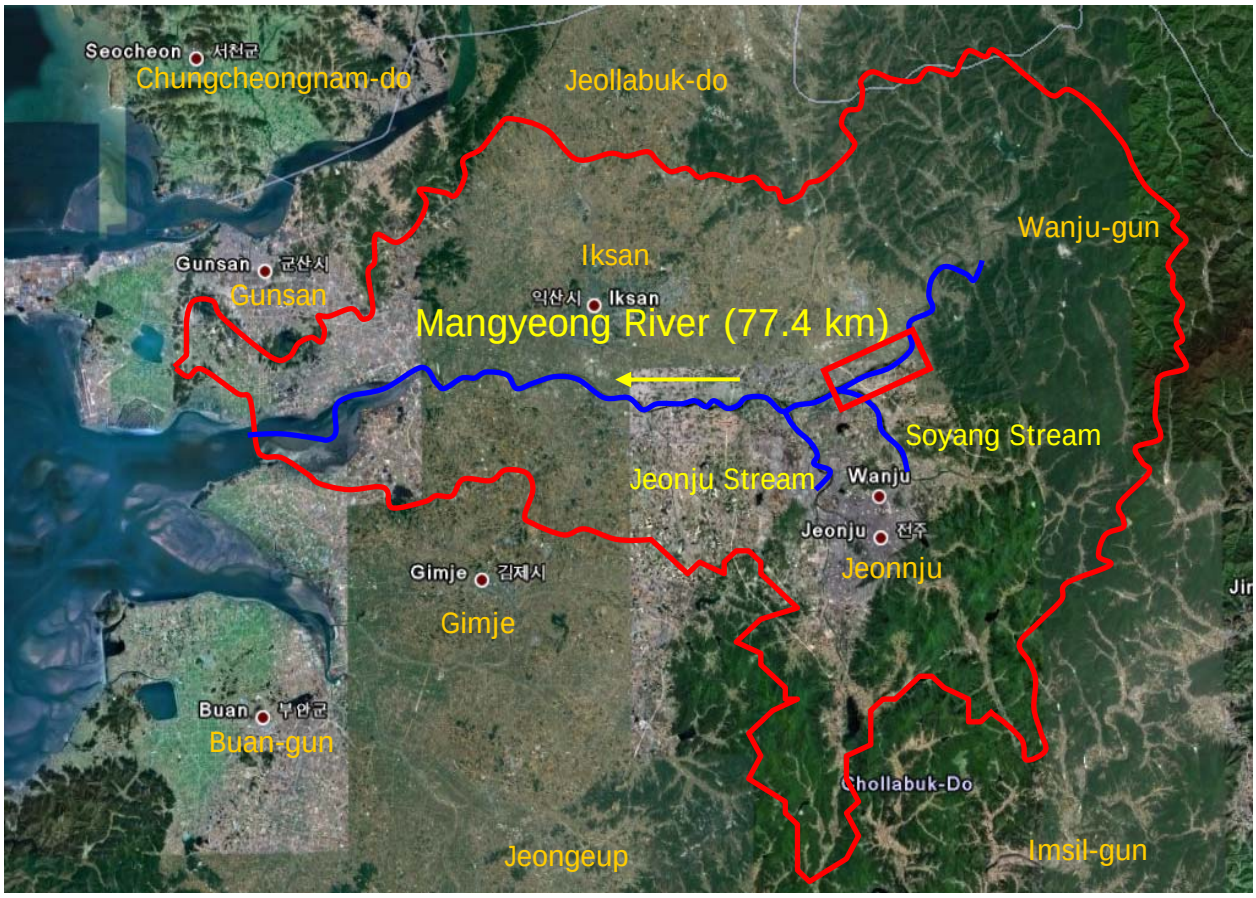

Figure 1-2: Location of Mangyeong River

Within the study site area about 67% of the land is devoted to agriculture and forest. In May of 2005 the estimated population within this region was 6,144 people. The population density of this region is approximately 377.1 people per 1 km^2.

1.2 STUDY REACH

An abandoned channel was located within the study reach from station 95+000 to 91+000. Thus, for analysis purpose, the study reach was extended from Bongdong Bridge (104+000) to upstream of Soyang Stream tributary (87+000) and its length is 4.25 km. Three sills which are Sill A (Gumanri-bo), Sill B (Sae-bo), Sill C (Jangja-bo) were constructed in 1969, 1966, and 1976 respectively. Figure 1-3 is an image of study reach.

Figure 1-3: Study Reach on Mangyeong River

Figure 1-4 shows the field site photos numbering A to C. No. A is the Sill A (Gumanri-bo). No. B is the Sill B (Sae-bo). No C. is the Sill C (Jangja-bo). In the downstream of each sill, vegetations were observed and it has been well developed for a long time judging from its length and areas.

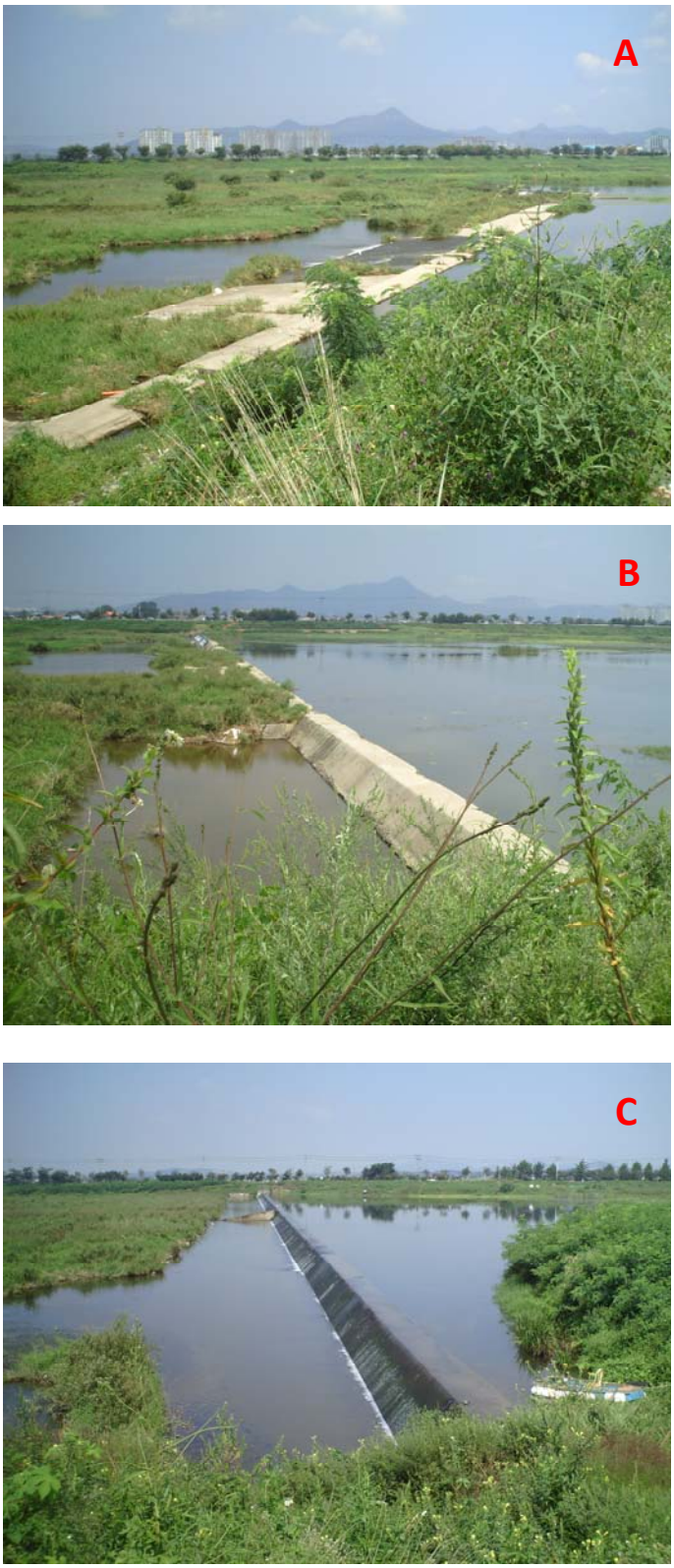

Figure 1-4: Field Site Photos

1.3 OBJECTIVES

The objectives of this project are to analyze the morphological changes and equilibrium conditions along Mangyeong River for future abandoned channel restoration. To accomplish this study, the following analyses will be performed:

- Hydrologic analysis using flow duration analysis.
- Hydraulic analysis based on HEC-RAS data.
- Bed material classification and sediment transport capacity analysis.
- Equilibrium analysis using downstream hydraulic geometry.
- Geomorphic characterizations of the study reach using survey data and aerial photos.

The results of this study will be used to analyze existing and future channel changes.

Chapter 2 AVAILABLE DATA

The data used in this project were provided by the Korea Institute of Construction Technology (KICT). The entire analysis has been performed and reported in SI units.

2.1 HYDROLOGY DATA

Based on three reports, MOCT (1976), IRCMA (1993), Wanju-Gun (2009), discharge values which will be using for hydrology analysis were different from each report. Thus, flood discharge with respect to return interval along Mangyeong River was obtained from HEC-RAS file. There are 4 distinct discharges and summarized in Table 2-1.

Table 2-1: Flood Discharge with Return Intervals

Return Interval (years)	Discharge (m^3/s)
30	1513
50	1695
80	1864
100	1943

2.2 SEDIMENT

2.2.1 Suspended Sediment Measurements

Sediment measurements were taken in July 2009 at Bongdong Station (Yongbong Bridge) in Mangyeong River from KICT (2009). This station is located in 2 km upstream of study reach. Suspended load was measured by D-74, one of depth-integrating samples. In practice, the transit time must be adjusted so that the container is not completely filled. Suspended load was taken at three points with equal width increment method on the Yongbong Bridge and was measured 19 times totally. Total load was determined by KICT using the Modified Einstein Procedure. Table 2-2 summarizes the calculated total sediment load based at Bongdong Station. Figure 2-1 shows the location of Bongdong Station.

Table 2-2: Sediment Measurement

No.	Date Measured	Water Depth	Discharge	Concentration of Wash Load	Wash Load	Total Load
		(m)	(m^3/s)	(mg/L)	(tons/day)	(tons/day)
1	7/09/09	0.85	36.0	16.0	49.8	49.7
2	7/10/09	0.70	22.7	8.7	17.0	17.0
3	7/12/09	0.50	8.3	4.0	2.9	2.9
4	7/12/09	1.02	57.5	63.7	316.0	315.7
5	7/12/09	1.29	98.6	90.7	772.2	772.2
6	7/12/09	1.63	165.4	174.0	2,486.0	2,486.0
7	7/12/09	1.89	234.6	200.0	4,054.0	6836.9
8	7/12/09	1.89	234.6	209.0	4,236.3	5314.7
9	7/12/09	1.72	187.5	99.3	1,609.0	28696.4
10	7/12/09	1.85	154.5	76.7	1,203.4	1,203.4
11	7/13/09	1.48	133.9	43.7	505.0	505.0
12	7/13/09	1.38	114.6	29.3	290.5	290.5
13	7/13/09	0.84	36.0	8.7	27.0	26.9
14	7/15/09	3.15	784.0	1,413.7	95,762.1	95,666.4
15	7/15/09	3.30	874.6	1,251.3	94,555.4	95,914.2
16	7/15/09	3.33	893.4	1,642.0	126,740.8	128,545.2
17	7/15/09	2.95	672.0	1,332.3	77,351.0	77,273.7
18	7/15/09	2.62	508.2	1,231.7	54,074.9	54,020.8
19	7/15/09	2.37	401.0	421.0	14,587.6	14,573.0

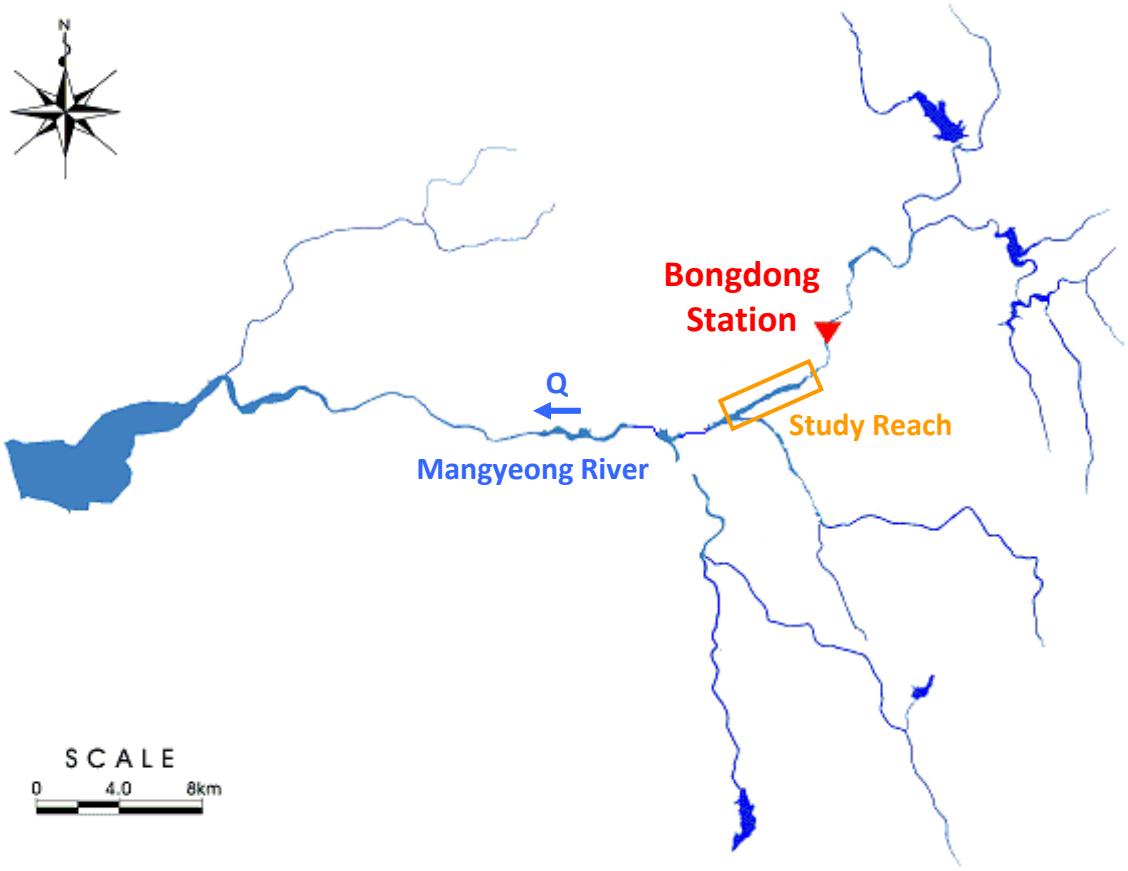

Figure 2-1: Sediment Measurement Location

2.2.2 Bed Material

Bed material was also measured at Bongdong Station (Yongbong Bridge) with BM-54 in December 2009. 15 samples of bed material were taken with respect to 10m of equal increment at the cross section on Yongbong Bridge and 13 samples were selected for analysis. The measured particles were analyzed with sieves in a laboratory. In general, the samples indicated that the bed is composed of gravel. Figure 2-2 shows the 13 particle size distributions at Bongdong Station.

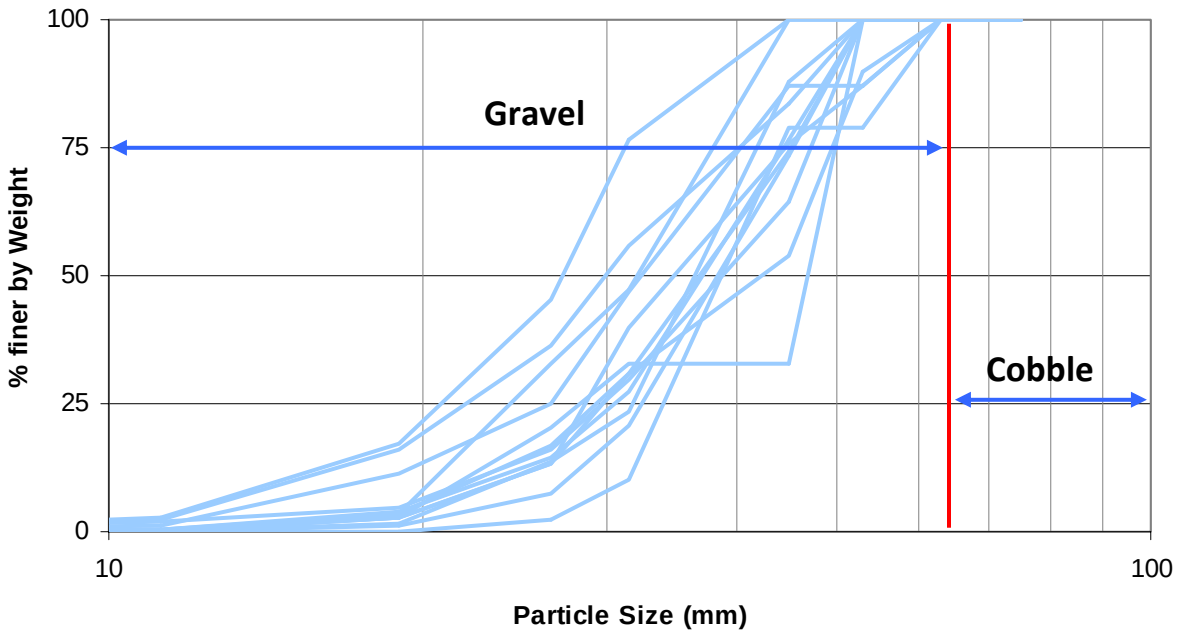

Figure 2-2: Particle Size Distribution at Bongdong Station

2.3 HYDRAULIC DATA

Hydraulic data was provided by KICT for Mangyeong River. The study reach extends from station 104+000 (Bongdong Bridge) to station 87+000 (just upstream of Soyang Stream). Figure 2-3 provides a cross section location map of the study reach.

Figure 2-3: Cross Section Map for Study Reach

Detailed survey files from 2009 were provided by KICT. The files included cross section survey, longitudinal survey, and CAD file. In addition, thalweg profile and mean bed elevation were provided by the Master Plan reports of MOCT (1976), IRCMA (1993), and Wanju-Gun(2009).

The hydraulic roughness coefficient was estimated based on the classification developed by (Chow 1959). For natural streams the Manning's n value ranges from 0.025 to 0.06. Based on the judgment of survey team, the n value of Mangyeong River was determined to be 0.03.

2.4 AERIAL PHOTOS

Seven aerial photos were provided by KICT. Aerial photos were provided for the following years: 1967, 1973, 1978, 1989, and 2003, refer to Appendix A. Planform analysis was conducted using these images.

Chapter 3 FLOW DURATION ANALYSIS

3.1 FLOW DURATION CURVE

From the 2009 survey CAD file and the Aerial photographs, it is really hard to determine the bankfull discharge because the Mangyeong River has been channelized and it is difficult to select the representative cross section due to three sills. The effective discharge analysis is also unavailable because the discharge which transports the largest fraction of the annual sediment load over a period of years was 1250 m^3/s and the discharge which transports the second largest sediment load was also high of 600 m^3/s. Therefore, a flow duration analysis was used to find the channel forming discharge.

The flow duration curve is a plot that shows the percentage of time that flow in a stream is likely to equal or exceed some specified value of interest. The flow duration curves do not represent the actual sequence of flows, but they are useful in predicting the availability and variability of sustained flows. Figure 3-1 shows the flow duration curve for Mangyeong River at Bondong station which is 2km upstream of study reach. Data were available from 2004 to 2009.

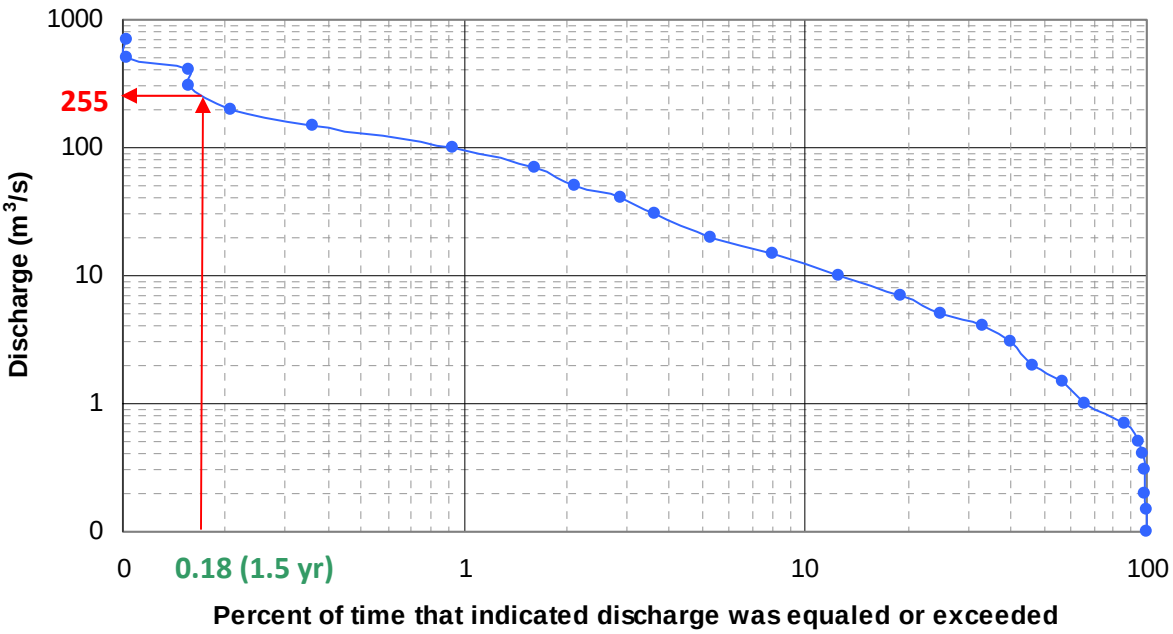

Figure 3-1: Flow Duration Curve for Mangyeong River at Bongdong Station (2004-2009)

The discharge with return interval of 1.5 year from flow duration curve was acquired to 255 m^3/s. This discharge will be used for all analysis including hydraulic modeling, sediment analysis, equilibrium, and channel classification.

Chapter 4 HYDRAULICS

4.1 METHODS

The hydraulic analysis was conducted using HEC-RAS. The Manning's n value of 0.03 is assumed based on initial observations by the surveying team. The hydraulic analysis was conducted on Mangyeong River for 5 distinct flow rates. Discharge with a return interval of 1.5 year was acquired from flow duration analysis and other discharges with respect to return interval were obtained from KICT. The input data of discharges for this analysis were shown in Table 4-1

Table 4-1: The input data of discharges with return interval

Return Interval (year)	Discharge (m^3/s)
1.5	255
30	1513
50	1695
80	1864
100	1943

The following channel geometry parameters were calculated using HEC-RAS: minimum channel elevation, water surface elevation, energy grade line slope, velocity, cross sectional area, top width, Froude number, hydraulic radius, shear stress, stream power, wetted perimeter, and mean flow depth. Three additional channel geometry properties were determined:

Maximum flow depth = Water Surface Elevation - Minimum Channel Elevation

Width/Depth Ratio, W/D = Top width / Mean Flow Depth

Water surface slope = Water surface elevation / distance between cross sections

These hydraulic parameters were analyzed for each discharge. Two distinct analyses were performed. The first analysis is based on spatial trends for all 5 discharges. The second analysis is based on a reach-averaged value.

4.2 RESULTS

Figure 4-1 shows the spatial trends in the top width, wetted perimeter, maximum flow depth, cross-sectional area, mean flow depth, width/depth ratio, channel velocity, Froude number for the study reach with channel forming discharge of 255 m^3/s. A, B, and C in each graph represent three sills from upstream to downstream within study reach.

The horizontal line indicates the average value on each graph and these values are as follows; The top width is 244 m, the wetted perimeter is 240 m, the maximum flow depth is 1.90 m, the cross sectional area is 265 m^2, the mean flow depth is 1.11 m, the width/depth ratio is 277, the channel velocity is 1.18 m/s, and Froude number is 0.42.

All results showed that there was sudden change in the location of sills. At the distance of 43 km, geometry results including top width, wetted perimeter, and cross sectional area had decreased values because there are agriculture area on floodplain at the left bank of Mangyeong River. The area of the floodplain is around 0.1 km^2 and a levee was constructed to protect agriculture area.

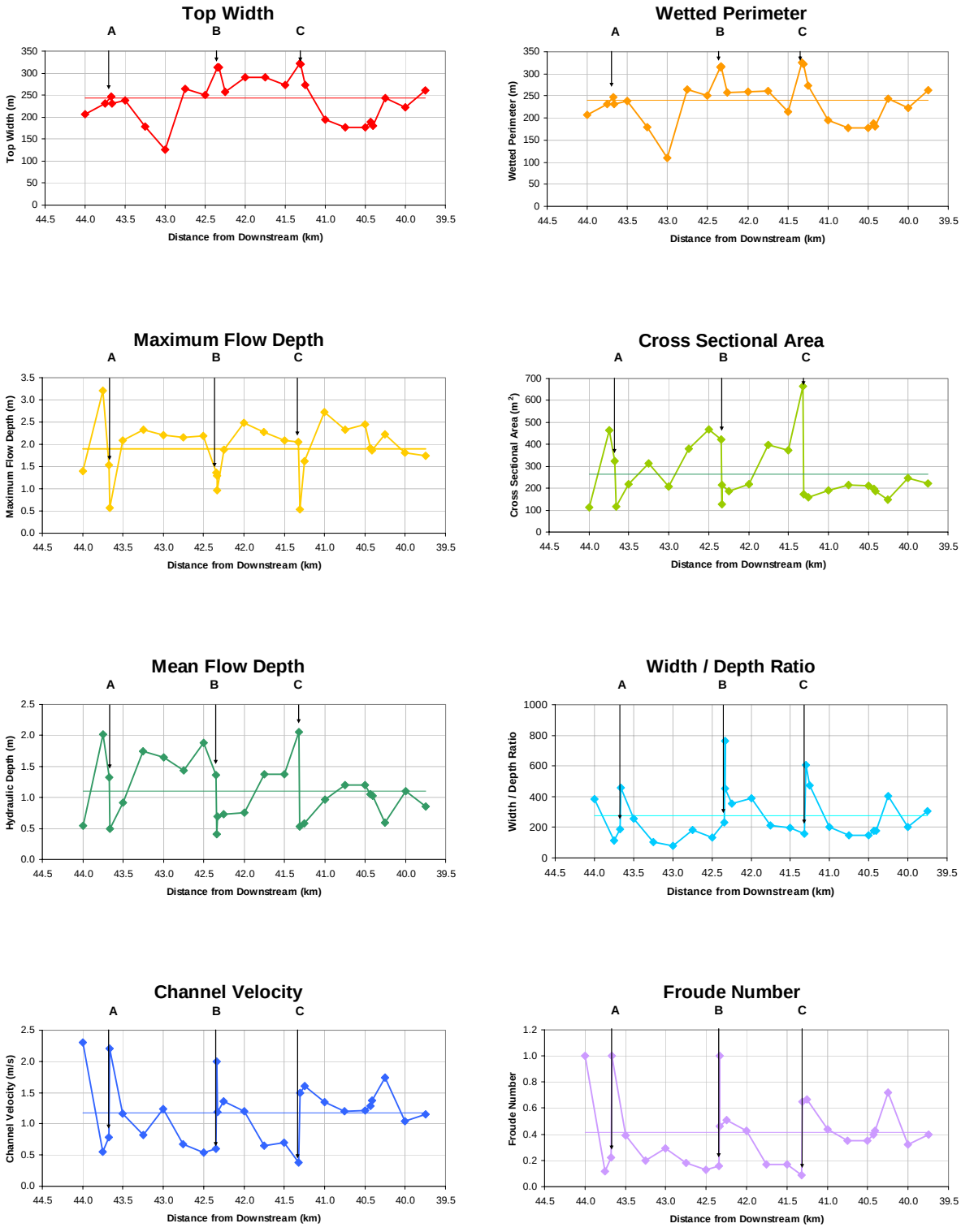

Figure 4-1: Spatial Trends based on channel forming discharge of 255 m^3/s

Reach-averaged hydraulic parameters for each return interval were computed and summarized in Figure 3-2. The reach averaged hydraulic parameters increased as discharge increase. The width / depth ratio decreased because the top width did not change significantly.

The rate at which the hydraulic geometry parameters change with discharge is quite important in defining at-a-station hydraulic geometry relationships. The cross sectional area was changed most as a result of change in discharge. The cross section area is 265 m^2 at the return interval of 1.5 year but it is increased from 720 m^2 to 839 m^2 in the return interval of 30 to 100 year respectively. The change rate was increased with 2.7 to 3.2 when it compared with that of 1.5 year of return interval.

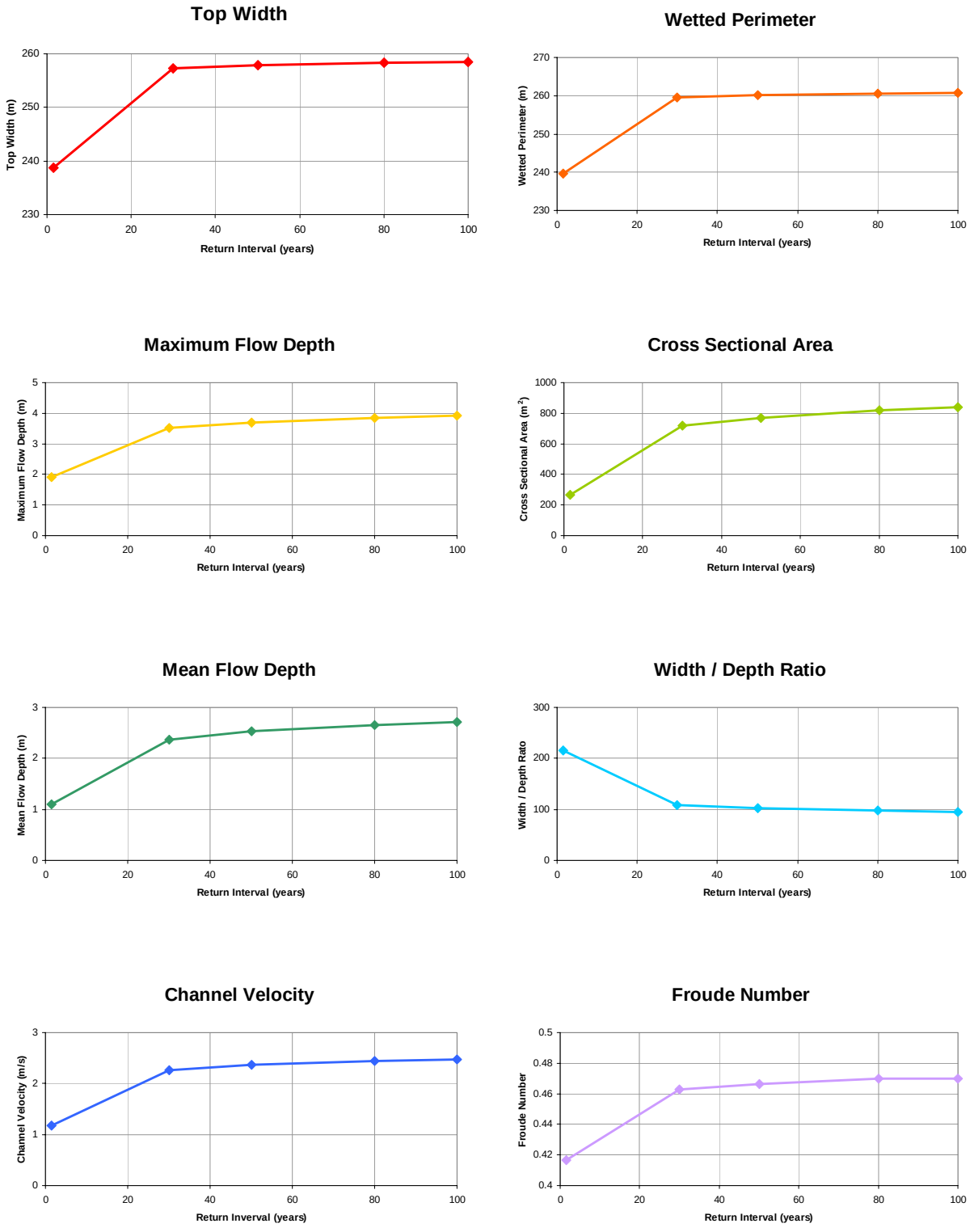

Figure 4-2: Reach Averaged Spatial Trends on Each Return Interval

Chapter 5 BED MATERIAL AND SEDIMENT ANALYSIS

5.1 BED MATERIAL

5.1.1 Methods

Samples of the bed material were taken on July 2009 and spaced 10 m apart on the one cross section of Bongdong Station. The data provided by KICT included the percent finer by weight for all 13 measurements. Table 5-1 is the classification for the bed material (Julien 1998).

Table 5-1: Bed Material Classification (Julien 1998)

Class name	Size range	
	mm	in.
Boulder		
Very large	4,096-2,048	160-80
Large	2,048-1,025	80-40
Medium	1,024-512	40-20
Small	512-256	20-10
Cobble		
Large	256-128	10-5
Small	128-64	5-2.5
Gravel		
Very coarse	64-32	2.5-1.3
Coarse	32-16	1.3-0.6
Medium	16-8	0.6-0.3
Fine	8-4	0.3-0.16
Very fine	4-2	0.16-0.08
Sand		
Very coarse	2.000-1.000	
Coarse	1.000-0.500	
Medium	0.500-0.250	
Fine	0.250-0.125	
Very fine	0.125-0.062	
Silt		
Coarse	0.062-0.031	
Medium	0.031-0.016	
Fine	0.016-0.008	
Very fine	0.008-0.004	
Clay		
Coarse	0.004-0.0020	
Medium	0.0020-0.0010	
Fine	0.0010-0.0005	
Very fine	0.0005-0.00024	

5.1.2 Results

Figure 5-1 shows the averaged bed material particle size distribution for all 13 samples.

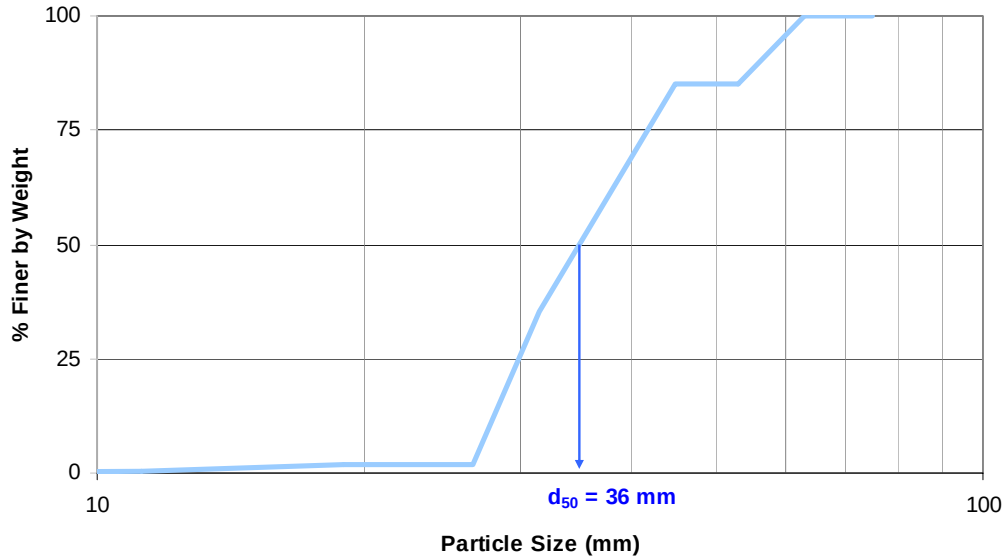

Figure 5-1: Average Bed Material Distribution for Mangyeong River

Mangyeong River at the study reach is composed of coarse gravel and very coarse gravel. The median grain size is 36 mm which is very coarse gravel. Bed material would be coarser due to the place where the samples were taken near bridge but this can be acceptable because study reach is located in the upstream of Mangyeong River and the bed elevation has degraded up to 2 m since 1976. In addition, as three sills have been constructed since 1966, the bed material would be coarser. Table 5-2 summarizes the median grain size of the study reach in Mangyeong River.

Table 5-2: Median Grain Size

Grain Size	Particle Diameter [mm]
d_{16}	20
d_{35}	31
d_{50}	36
d_{65}	41
d_{90}	51

5.2 MAXIMUM MOVABLE GRAIN SIZE

5.2.1 Methods

From the sediment grain size, the shear stress analysis on particle size was performed to obtain particle size at incipient motion. The dimensionless shear stress is the ratio of hydrodynamic forces to the submerged weight, which is called the Shields parameter (τ_*) and expressed as follows;

$$\tau_* = \frac{\tau_0}{(\gamma_s - \gamma_m) d_s}$$

Where, τ_* is Shields parameter, τ_0 is boundary shear stress, γ_s is specific weight of a sediment particle, γ_m is specific weight of the fluid mixture, and d_s is particle size.

When the Shields parameter is assumed to be critical (τ_{*_c}), the maximum movable particle size can be attained from the following equation.

$$d_s = \frac{R\ S_f}{(G-1)\tau_{*_c}}$$

Where, R is hydraulic radius and S_f is friction slope. Based on the critical Shields parameter equation, the maximum movable particle size can be computed iteratively. Table 5-3 contains threshold values for granular material at 20°C (Julien 1998).

Table 5-3: Approximate Threshold Conditions for Granular Material at 20°C (Julien 1998)

Class name	d_s (mm)	d_*	ϕ (deg)	τ_{*c}	τ_c (Pa)	u_{*c} (m/s)
Boulder						
Very large	> 2,048	51,800	42	0.054	1,790	1.33
Large	> 1,024	25,900	42	0.054	895	0.94
Medium	> 512	12,950	42	0.054	447	0.67
Small	> 256	6,475	42	0.054	223	0.47
Cobble						
Large	> 128	3,235	42	0.054	111	0.33
Small	> 64	1,620	41	0.052	53	0.23
Gravel						
Very coarse	> 32	810	40	0.05	26	0.16
Coarse	> 16	404	38	0.047	12	0.11
Medium	> 8	202	36	0.044	5.7	0.074
Fine	> 4	101	35	0.042	2.71	0.052
Very fine	> 2	50	33	0.039	1.26	0.036
Sand						
Very coarse	> 1	25	32	0.029	0.47	0.0216
Coarse	> 0.5	12.5	31	0.033	0.27	0.0164
Medium	> 0.25	6.3	30	0.048	0.194	0.0139
Fine	> 0.125	3.2	30	0.072	0.145	0.0120
Very fine	> 0.0625	1.6	30	0.109	0.110	0.0105
Silt						
Coarse	> 0.031	0.8	30	0.165	0.083	0.0091
Medium	> 0.016	0.4	30	0.25	0.065	0.0080

Since the median grain size of the study reach is approximately 36 mm, the initial assumed value of d_s is 40 mm, and τ_{*_c} is 0.05. The discharge with the return interval of 1.5 year was selected to get hydraulic radius (R) from HEC-RAS and the slope (S) of 0.00230 m/m from survey data. This critical Shields parameter (τ_{*_c}) is identified from Table 5-3 and then an iteration is performed until the particle size is the same as the assumed particle size.

5.2.2 Results

The results of the maximum movable particle size are summarized in Table 5-4.

Table 5-4: Maximum Movable Particle Size

Return Interval (year)	Discharge (m^3/s)	R (m)	S (m/m)	τ_{*c}	d_s (mm)
1.5	255	1.11	0.00230	0.047	33

The maximum movable particle size is around 33 mm (very coarse gravel). This result indicates that the sediment currently at study reach in Mangyeong River will not move until the discharge is greater than 255 m^3/s. Based on the study reach location and three sills, only fractions finer than 33 mm will move at a discharge of 255 m^3/s and the bed material will stay on the river bed.

5.3 SEDIMENT TRANSPORT CAPACITY

5.3.1 Methods

The sediment transport capacity was calculated using HEC-RAS. The program has the capability to predict transport capacity for non-cohesive sediment at multiple cross sections based on the hydraulic parameters and known bed material properties for a given river. It does not take into account sediment inflow, erosion, or deposition in its computations. Typically, the sediment transport capacity is comprised of both bed load and suspended load, both of which can be accounted for in the various sediment transport predictors available in HEC-RAS. Results can be used to develop sediment discharge rating curves, which help to understand and predict the fluvial processes found in natural rivers and streams.

HEC-RAS calculates sediment transport capacity using several different methods including those developed by Ackers & White, Engelund & Hansen, Laursen, Meyer-Peter & Müller, Toffaleti, and Yang (gravel). All methods except Meyer-Peter & Müller provide an estimate of the total bed material load. The Meyer-Peter & Müller formula estimates bed load only. HEC-RAS results were compared with the results of sediment measurements in Bongdong Station. For a list of the limitations of each method refer to Appendix E.

5.3.2 Results

Sediment measurements were taken in July 2009 at Bongdong Station (Yongbong Bridge) in Mangyeong River from KICT (2009). From the data of Table 2-2, the relationship between discharge and total load was made and is shown in Figure 5-2. When the discharge of 255 m^3/s at a return interval of 1.5 year is applied, the total load is 6.54 thousand tons per day. The equivalent sediment concentration at 255 m^3/s is 240 mg/l.

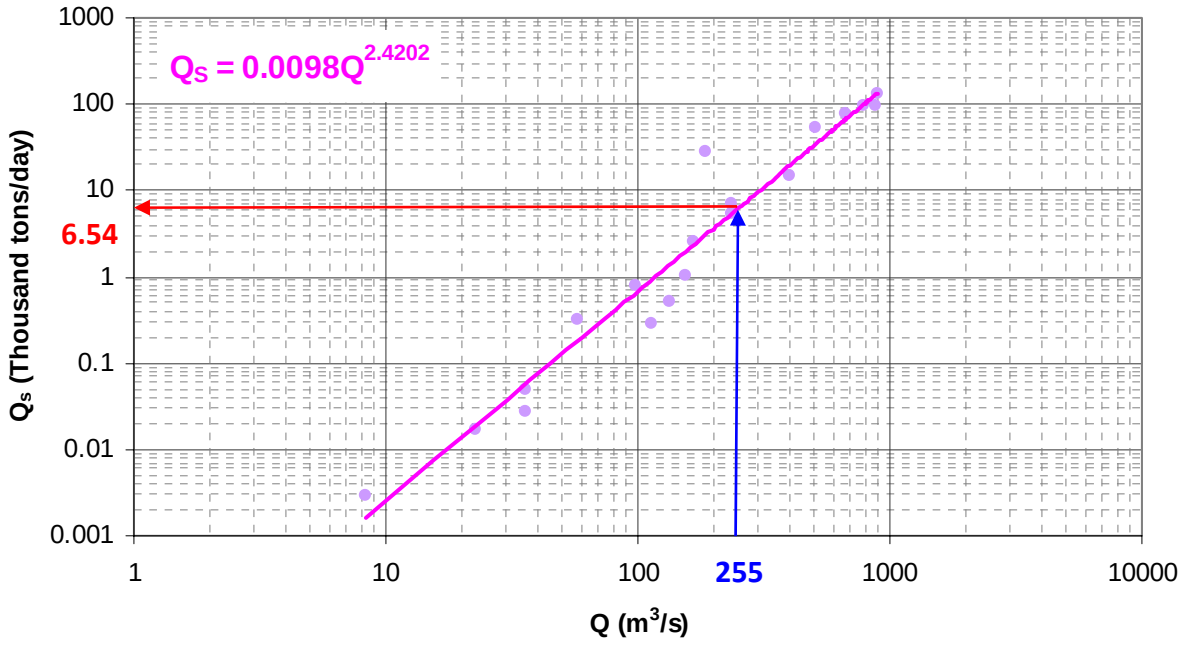

Figure 5-2: The relationship between Discharge and Total Load

With the relationship above, HEC-RAS was used to calculate the sediment transport capacity for all six methods at all five discharges. The water temperature was assumed to be 15°C and the bed material particle size for the reach was determined to be 36 mm. Ackers & White method and Meyer-Peter & Müller method were removed because the results were close to zero. Meyer-Peter & Müller is a bed load transport function. The results for sediment measurement and HEC-RAS modeling are shown in Figure 5-3.

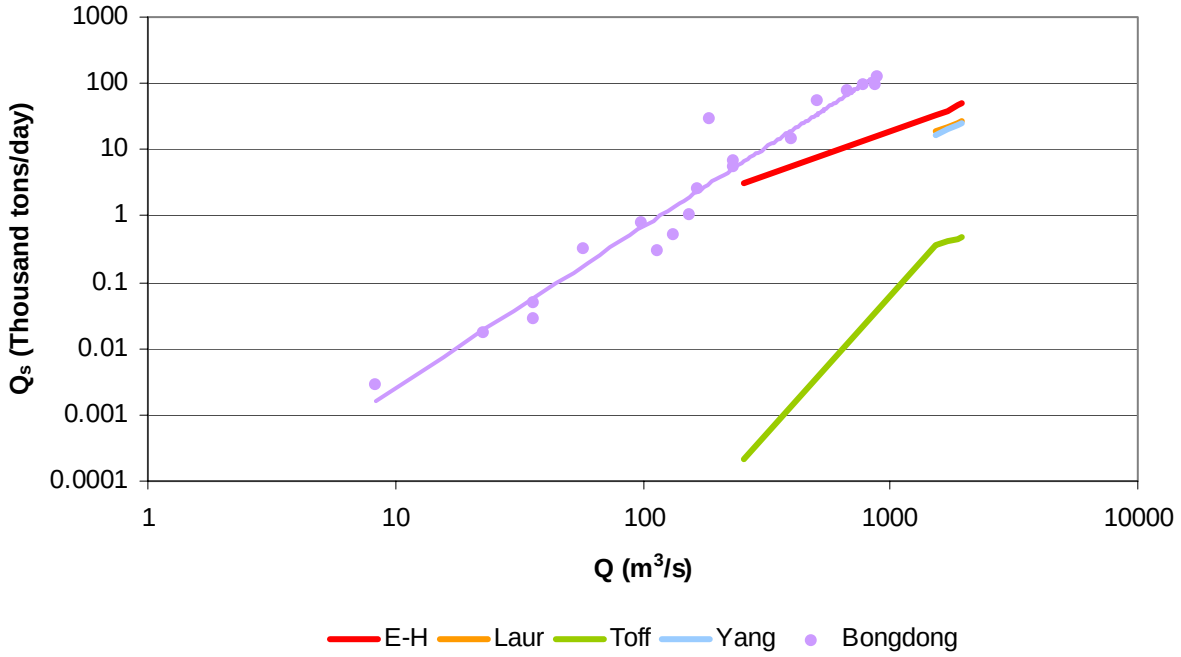

Figure 5-3: Sediment Rating Curve at the Cross Section 96

The measurement result is based on suspended load so total load from the measurement result is closer to the field measurements than any other methods. But at high flows the measured sediment load is about 10 times larger than calculation from Engelund-Hansen method. Therefore, the calculations should be based on the field measurement.

Chapter 6 EQUILIBRIUM

6.1 METHODS

Several hydraulic geometry equations were used to determine the equilibrium channel width. These methods use channel characteristics such as channel width and slope, sediment concentration, and discharge. All of the equilibrium width equations were developed in simplified conditions such as man-made channels.

Julien and Wargadalam (1995) used the concepts of resistance, sediment transport, continuity, and secondary flow to develop semi-theoretical hydraulic geometry equations.

$$h = 0.2\,Q^{\frac{2}{5+6m}}\,d_s^{\frac{6m}{5+6m}}\,S^{\frac{-1}{5+6m}}$$

$$W = 1.33\,Q^{\frac{2+4m}{5+6m}}\,d_s^{\frac{-4m}{5+6m}}\,S^{\frac{-1-2m}{5+6m}}$$

$$V = 3.76\,Q^{\frac{1+2m}{5+6m}}\,d_s^{\frac{-2m}{5+6m}}\,S^{\frac{2+2m}{5+6m}}$$

$$\tau_* = 0.121\,Q^{\frac{2}{5+6m}}\,d_s^{\frac{-5}{5+6m}}\,S^{\frac{4+6m}{5+6m}}$$

$$S = 12.4\,Q^{\frac{-1}{3m+2}}\,d_s^{\frac{5}{6m+4}}\,\tau_*^{\frac{6m+5}{6m+4}} \quad \left(Where, \quad \tau_* = \frac{\gamma\, h\, S}{(\gamma_s - \gamma) d_{50}} \right)$$

$$m = \frac{1}{\ln\left(\frac{12.2\ h}{d_{50}}\right)}$$

Where h (m) is the average depth, W (m) is the average width, V (m/s) is the average one-dimensional velocity, and τ_* is the Shields parameter, and d_{50} (m) is the median grain size diameter.

Simons and Albertson (1963) used five sets of data from canals in India and America to develop equations to determine equilibrium channel width. Simons and Bender collected data from irrigation canals in Wyoming, Colorado and Nebraska. These canals had both cohesive and non

cohesive bank material. Data were collected on the Punjab and Sind canals in India. The average bed material diameter found in the Indian canals varied from 0.43 mm in the Punjab canals to between 0.0346 mm and 0.1642 mm in the Sind canals. The USBR data was collected in the San Luis Valley in Colorado and consisted of coarse non-cohesive material. The final data set was collected in the Imperial Valley canal system, which have conditions similar to those seen in the Indian canals and the Simons and Bender canals.

Two figures were developed by Simons and Albertson to obtain the equilibrium width. Figure 6-1 and Figure 6-2 show the relationships between wetted perimeter and discharge and average width and wetted perimeter, respectively.

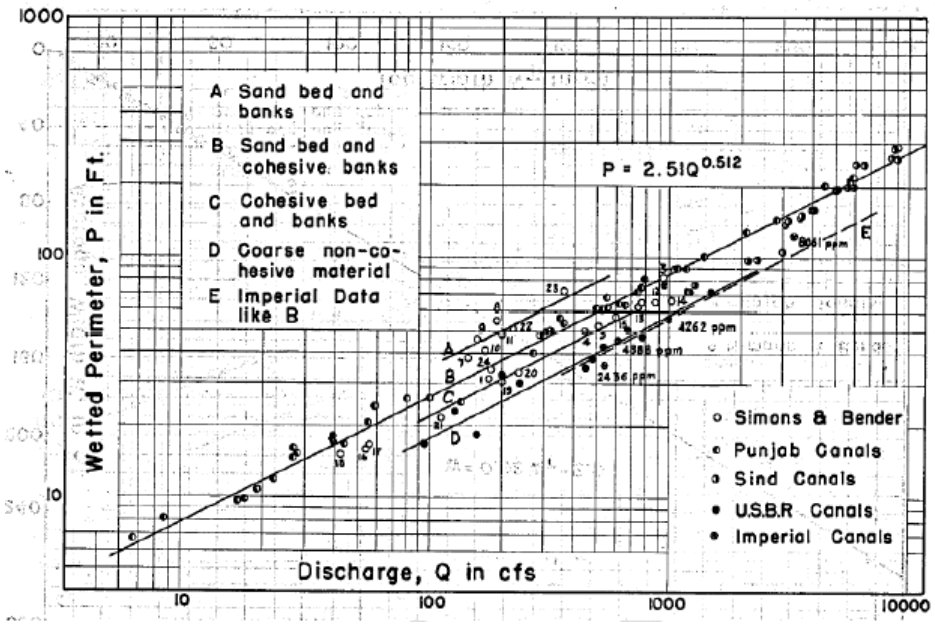

Figure 6-1: Variation of Wetted Perimeter P with Discharge Q and Type of Channel (after Simons and Albertson 1963)

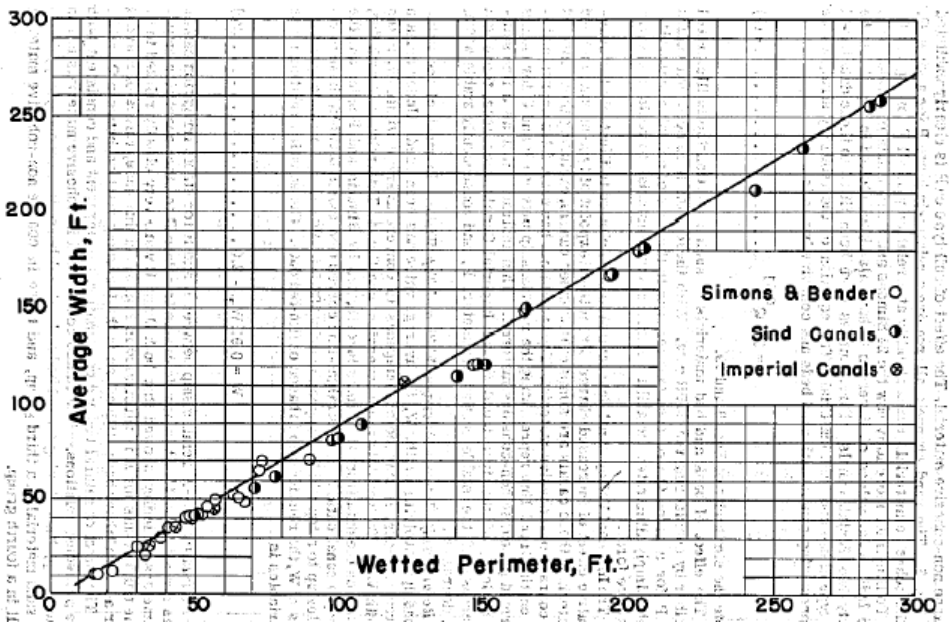

Figure 6-2: Variation of Average Width W with Wetted Perimeter P (Simons and Albertson 1963)

Blench (1957) used flume data to develop regime equations. A bed and a side factor (F_s) were developed to account for differences in bed and bank material.

$$W = \left(\frac{9.6\ (1 + 0.012\ c)}{F_s} \right)^{1/2}\ d^{1/4}\ Q^{1/2}$$

Where, W (ft) is channel width, c (ppm) is the sediment load concentration, d (mm) is the median grain diameter, and Q (ft^3/s) is the discharge. The side factor, F_s =0.1 for slight bank cohesiveness.

Lacey (from Wargadalam 1993)) developed a power relationship for determining wetted perimeter based on discharge.

$$P = 2.667\, Q^{0.5}$$

Where P (ft) is wetted perimeter and Q (ft^3/s) is discharge. For wide, shallow channels, the wetted perimeter is approximately equal to the width.

Klaassen and Vermeer (1988) used data from the Jamuna River in Bangladesh to develop a width relationship for braided rivers.

$$W = 16.1\, Q^{0.53}$$

Where W (m) is width, and Q (m^3/s) is discharge.

Nouh (1988) developed regime equations based on data collected in extremely arid regions of south and southwest Saudi Arabia.

$$W = 2.83\left(\frac{Q_{50}}{Q}\right)^{0.83} + 0.018\ (1+d)^{0.93}\ c^{1.25}$$

Where W (m) is channel width, Q_{50} (m^3/s) is the peak discharge for a 50 year return period, Q (m^3/s) is annual mean discharge, d (mm) is mean grain diameter, and c (kg/m^3) is mean suspended sediment concentration.

6.2 RESULTS

The input data used to calculate equilibrium widths are summarized in Table 6-1.

Table 6-1: Hydraulic Geometry Calculation Input

Return Interval (years)	Q (m^3/s)	d_{50} (mm)	Channel Slope (m/m)
1.5	255	36	0.00230
30	1513	36	0.00230
50	1695	36	0.00230
80	1864	36	0.00230
100	1943	36	0.00230

Table 6-2 summarizes the equilibrium channel widths predicted by the hydraulic geometry equations.

Table 6-2: Predicted Equilibrium Widths from Hydraulic Geometry Equations

Return Interval (year)	Discharge (m^3/s)	d_{50} (mm)	Channel slope (m/m)	Reach Averaged Channel Width (m)	Predicted Width (m)			
					Julien and Wargadalam	Lacey	Simons and Albertson	Klaassen and Vermeer
1.5	255	36	0.00230	239	83	77	113	304
30	1513	36	0.00230	257	183	188	281	780
50	1695	36	0.00230	258	192	199	298	828
80	1864	36	0.00230	258	200	209	313	871
100	1943	36	0.00230	258	204	213	319	891

Julien and Wargadalam method and Lacey method tend to under predict the channel width compared to main channel width. This suggests that the channel most likely was designed for the higher flow events. The Simons and Albertson method tends to predict the channel widths determined from HEC-RAS at lower flows. Klaassen and Vermeer method tends to completely overestimate channel width. The equations of method of Julien-Wargadalam and Lacey predict similar equilibrium channel widths. The comparison between predicted and measured width are shown in Figure 6-3.

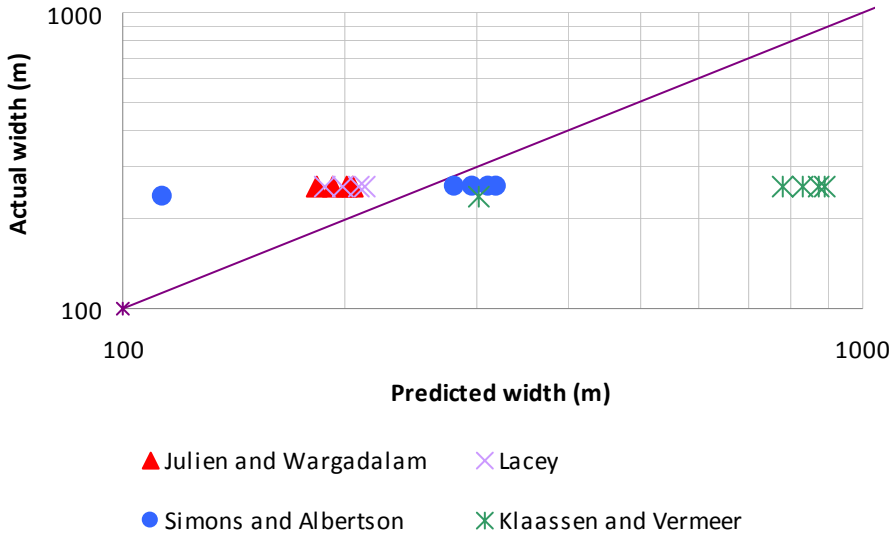

Figure 6-3: Predicted Width and Actual Width

Julien-Wargadalam's method was also used to predict the equilibrium slope. Input data came from reach averaged values and were analyzed with respect to return interval. The Shields parameter (τ_*) is needed for prediction of equilibrium slope. Table 6-3 shows the predicted equilibrium slope.

Table 6-3: Equilibrium Slope Prediction

Return Interval (year)	Discharge (m^3/s)	τ_*	Reach Averaged HEC-RAS Main Channel Slope (m)	Predicted Slope Julien and Wargadalam (m/m)
1.5	255	0.04	0.00230	0.00111
30	1513	0.09	0.00230	0.00136
50	1695	0.10	0.00230	0.00140
80	1864	0.10	0.00230	0.00142
100	1943	0.10	0.00230	0.00144

The results of the equilibrium slope calculations indicate that the channel had a steeper slope than the predicted slope for each return interval. Thus, due to the levees the channel cannot meander to create a flatter slope.

6.3 STABLE CHANNEL DESIGN ANALYSIS

6.3.1 Methods

The stable channel design functions are based on the methods used in the SAM Hydraulic Design Package for channels, developed by the U.S. Army Corps of Engineers Waterways Experiment Station. In this study only the Copeland method was used. It is based on an analytical approach to solve stable channel design based on the depth, width, and slope. This approach is primarily analytical on a foundation of empirically-derived equations and uses the sediment discharge and flow depth prediction methods of Brownlie (1981) to ultimately solve for stable depth and slope for a given channel. The model uses idealized trapezoidal cross sections to determine the stable channel design. This method assumes bed load movement above the bed, and separates hydraulic roughness into bed and bank components.

Sound judgment must be used when selecting the appropriate design discharge for performing a stability analysis. Suggested design discharges that may represent the channel forming discharge are a 2 year to frequency flood, 10 year frequency flood, bankfull discharge, and effective discharge.

6.3.2 Results

For this study 5 distinct return intervals were selected: 1.5 year, 30 year, 50 year, 80 year, and 100 year. The two main input variables for SAM are side slope and bottom width. To estimate a starting point for the analysis, the reach averaged side slope and bottom width were determined based on the existing cross sections within the reach. Other input data came from the hydraulic analysis using HEC-RAS. Input data for this analysis are summarized in Table 6-4. The stable channel design results using SAM are shown in Figure 6-4 and Figure 6-5.

Table 6-4: Important Input Data

Return Interval (year)	Discharge (m^3/s)	Reach averaged Side slope		Bottom width (m)	Bank Height (m)
		Left	Right		
1.5	255	2	2	303	1.06
30	1513	2	2	303	2.61
50	1695	2	2	303	2.80
80	1864	2	2	303	2.95
100	1943	2	2	303	3.02

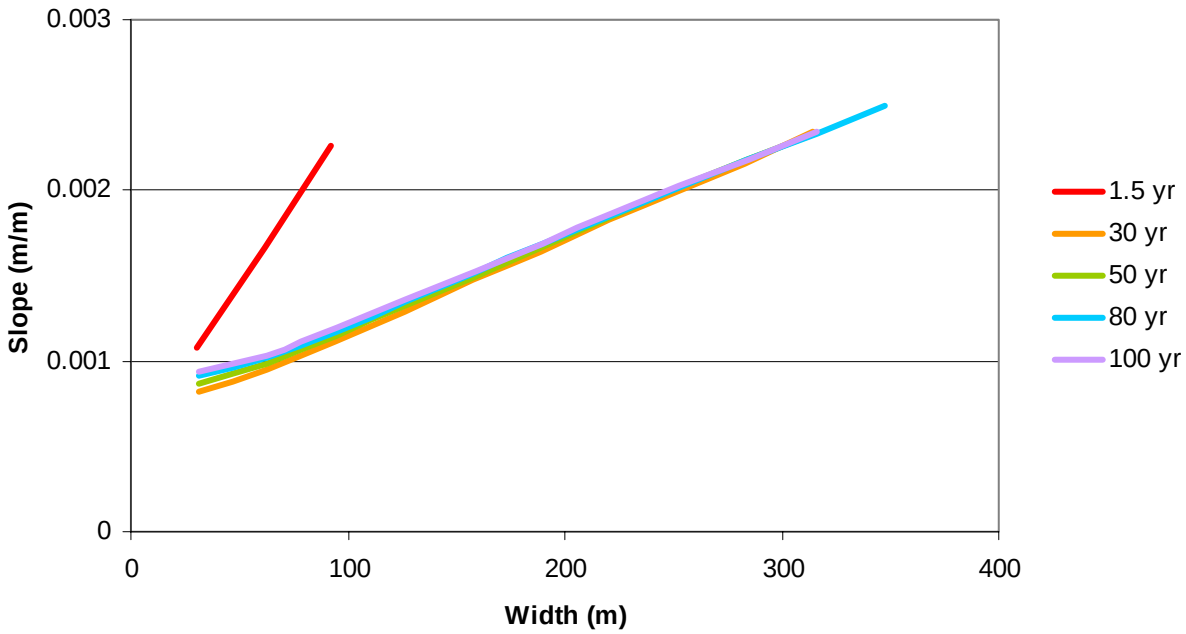

Figure 6-4: Stable Channel Slope and Width from SAM

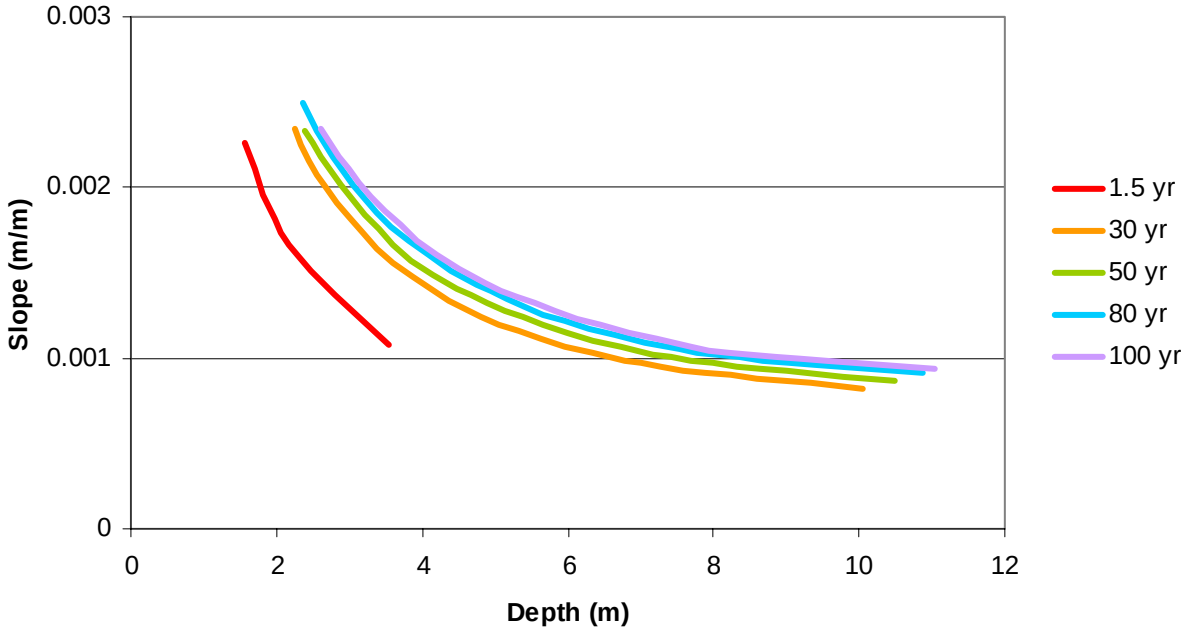

Figure 6-5: Stable Channel Slope and Depth from SAM

In summary, the sills of Mangyeong River force the river to be a lot wider and shallower than predicted with downstream hydraulic geometry relationship. Also, the fact that the riverbed is armored makes the comparisons with methods developed for alluvial rivers difficult to apply.

.

Chapter 7 GEOMORPHOLOGY

7.1 CHANNEL PLANFORM

7.1.1 Methods

A number of channel classification methods were investigated to determine which method was most applicable for Mangyeong River. A qualitative classification of the channel was made, based on observations of aerial photographs (1967 to 2003) and AutoCAD survey file from 2009. The channel was classified based on slope-discharge relationships including Leopold and Wolman (1957), Lane (from Richardson et al. 2001), Henderson (1966), Ackers and Charlton(1982), and Schumm and Khan (1972). Channel morphology methods by Rosgen (1996) and Parker (1976) were also used, along with stream power relationships developed by Nanson and Croke (1992) and Chang (1979). An additional method was also investigated, but found to be inapplicable for Mangyeong River. That method was van den Berg (1995) which was developed for channels with a sinuosity greater than 1.3 were not used.

7.1.1.1 *Aerial Photo*

The visual planform was analyzed using aerial photos in the years of 1967, 1973, 1978, 1989, and 2003. AutoCAD survey file from 2009 was also investigated to analyze planform.

7.1.1.2 *Slope-Discharge Methods*

Leopold and Wolman (1957) determined a critical slope value, based on discharge, which classifies a stream as either braided or meandering. The following equation shows the slope-discharge relationship:

$$S = 0.6\,Q^{-0.44}$$

Where, S is the critical slope and Q is the channel discharge (ft^3/s). Channels with slopes greater than the critical slope will have a braided planform, while channels with slopes less than the critical slope will have a meandering planform. Straight channels may fall on either side of the critical slope. Leopold and Wolman identified channels with a sinuosity greater than 1.5 as meandering and channels with a sinuosity less than 1.5 as straight. Using the slope-discharge relationship and the critical sinuosity value, channels can be divided into straight, meandering, braided, or straight/braided channels.

Lane (1955) developed a slope-discharge threshold value, k, calculated by this equation:

$$k = S\,Q^{0.25}$$

Where, S is the channel slope and Q is the channel discharge (ft^3/s). The classification of the stream is based on the value of k as shown below:

Meandering: $k \leq 0.0017$

Intermediate: $0.010 > k > 0.0017$

Braided: $k \geq 0.010$

These threshold values are based on English units. Values of k are also available for SI units.

Henderson (1966) developed a slope-discharge method that also accounts for the median bed size by plotting the critical slope as defined by Leopold and Wolman against the median bed size. The following equation resulted:

$$S = 0.64\ d_s^{1.14}\ Q^{-0.44}$$

Where, S is the critical slope, d_s is the median grain size (ft), and Q is the discharge (ft^3/s). For slope values that plot close to this line, the channel planform is expected to be straight or meandering. Braided channels plot well above this line.

Ackers (1982) developed the threshold between slope and discharge by adding field data with existing laboratory data.

$$S_{VC} = 0.0008\,Q^{-0.21}$$

Where, S_{VC} is critical slope and Q is the channel discharge (m^3/s). This equation classifies the channel planform as meandering when valley slope is bigger than critical slope.

Schumm and Khan (1972) developed empirical relationships between valley slope (S_v) and channel planform based on flume experiments. Thresholds were determined for each channel classification as follows:

Straight: S_v < 0.0026

Meandering Thalweg: 0.0026 < S_v < 0.016

Braided: 0.016 < S_v

7.1.1.3 *Channel Morphology Methods*

Rosgen (1996) developed a channel classification method based on entrenchment ratio, width/depth ratio, sinuosity, slope, and bed material. Using these channel characteristics, Rosgen developed eight major classifications and a number of sub-classifications. Figure 7-1 shows Rosgen's method for stream classification.

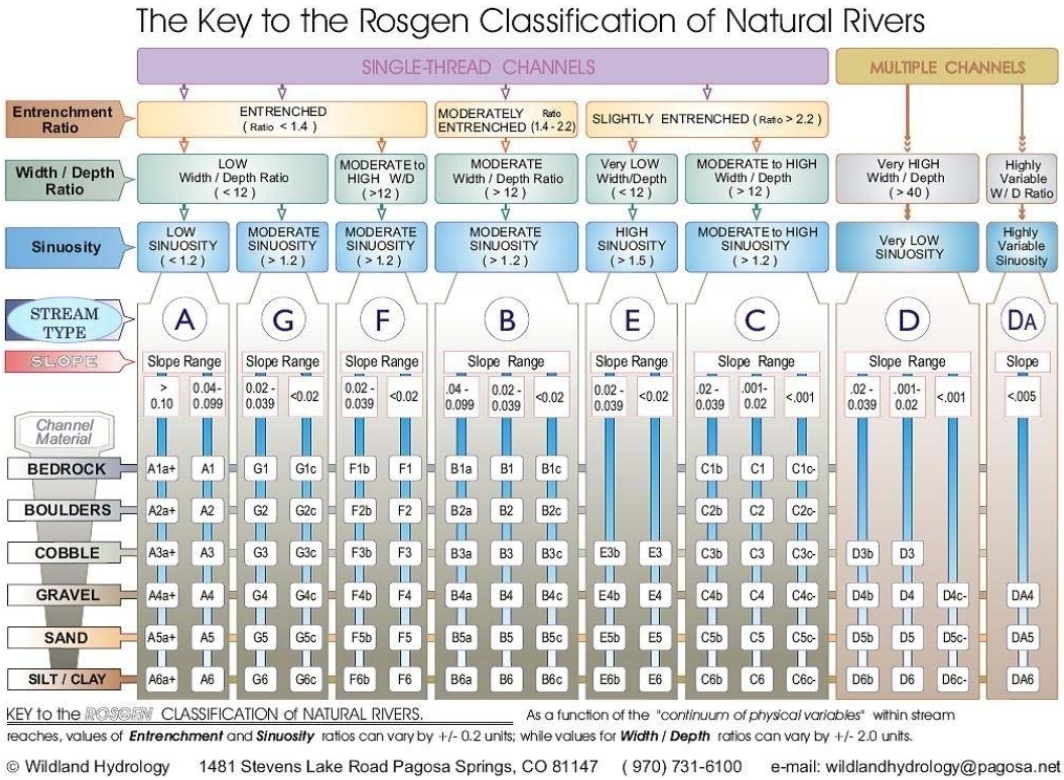

Figure 7-1: Rosgen Channel Classification Key (Rosgen 1996)

Parker (1976) considered the relationship between slope, Froude number, and width to depth ratio. Experiments in laboratory flumes and observations of natural channels lead to the following channel planform classifications:

Meandering: $S/Fr << h/W$

Transitional: $S/Fr \sim h/W$

Braided: $S/Fr >> h/W$

Where S is the channel slope, Fr is the Froude number, and W/h represents the width to depth ratio.

7.1.1.4 *Stream Power Methods*

Nanson and Croke (1992) made use of specific stream power and sediment characteristics to distinguish between types of channel planforms. The equation to determine specific stream power is as follows:

$$\omega = \gamma Q S / W$$

Where, ω is specific stream power (W/m^2), γ is the specific weight of water (N/m^3), S is channel slope, and W is channel width (m).

Specific stream power and expected sediment type are shown below:

Braided-river floodplains (braided):
ω = 50-300
gravels, sand, and occasional silt

Meandering river, lateral migration floodplains (meandering):
ω = 10-60
gravels, sands, and silts

Laterally stable, single-channel floodplains (straight):
ω <10
silts and clays

Chang (1979) used data from numerous rivers and canals to build channel classifications based on stream power. The classifications show in terms of valley slope and discharge. Figure 6.2 present the four classification regions defined by Chang for sand streams.

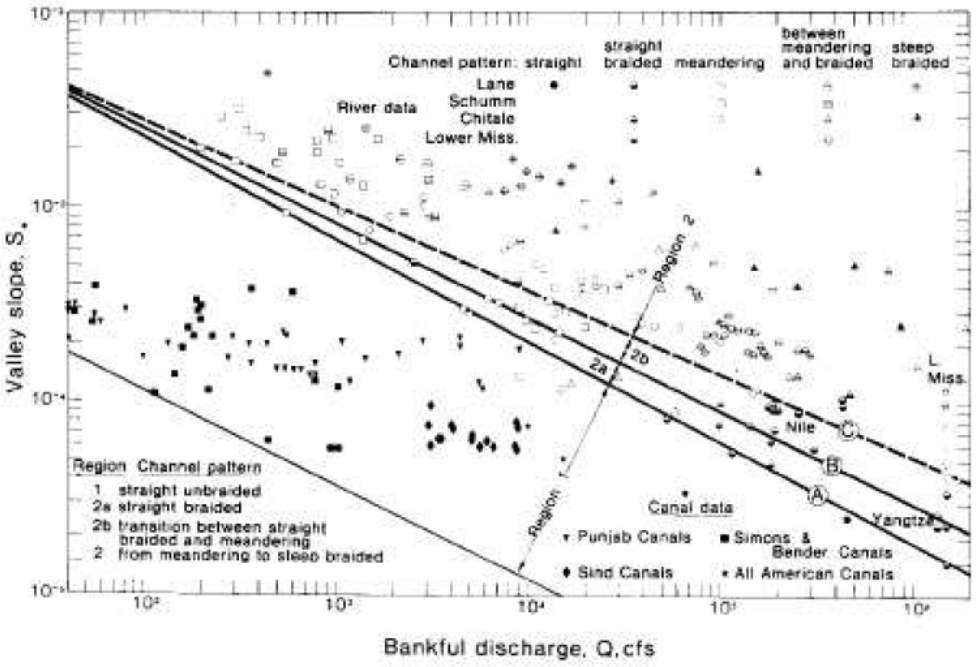

Figure 7-2: Chang's Stream Classification Method Diagram

Chang found that river will have a straight planform at low valley slopes. An increasing valley slope will cause the channel to change to a braided or meandering planform with constant discharge.

7.1.2 Results

Visual characterization of the channel was performed by channel planforms delineated using aerial photographs from 1967 to 2003. Figure 7-3 shows the historical planforms for Mangyeong River.

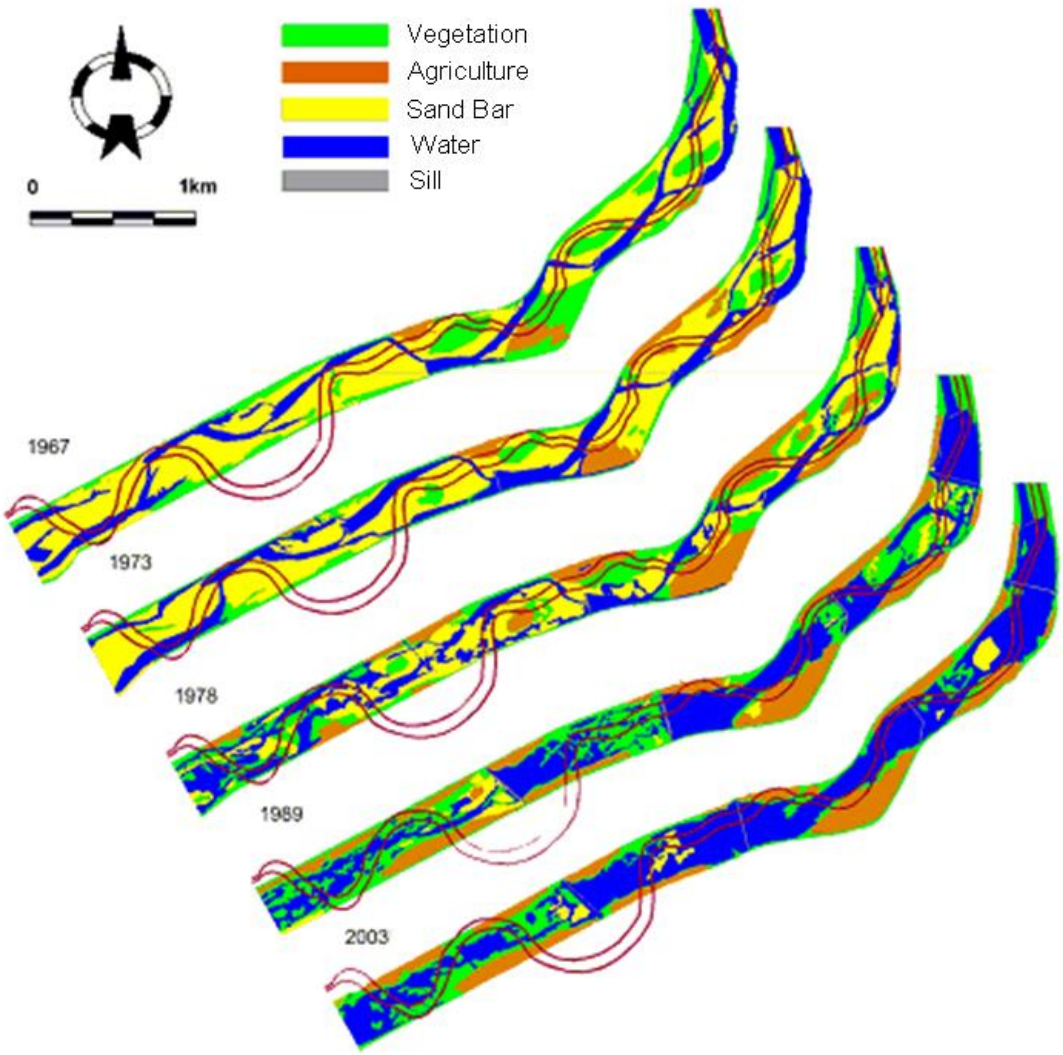

Figure 7-3: Historical Planform

Three sills were started to be constructed in 1966, 1969, and 1976 but there seems to be a sign of complete creation around 1980's. So the effect of each sill was showed after 1989. Due to this, Sand bar just upstream of each sill has disappeared, vegetations just downstream

of each sill have been showed up, and the channel has been changed from sinuous to relatively straight and wide.

To obtain the values needed in the quantitative channel classification methods, a HEC-RAS model of the reach was run at 5 distinct discharges. Table 7-1 shows the input values obtained from HEC-RAS. Channel characteristics were averaged for each cross section.

Table 7-1: Channel Classification Inputs

Return Interval	Q	Channel Slope	Valley Slope	d_{50}	Bankfull Width	Flood Prone Width	Depth	Fr	EG Slope
(year)	(m^3/s)	(m/m)	(m/m)	(mm)	(m)	(m)	(m)		(m/m)
1.5	255	0.00230	0.00237	36	239	309	1.11	0.42	0.00254
30	1513	0.00230	0.00237	36	257	329	2.38	0.46	0.00165
50	1695	0.00230	0.00237	36	258	333	2.53	0.47	0.00162
80	1864	0.00230	0.00237	36	258	336	2.65	0.47	0.00159
100	1943	0.00230	0.00237	36	258	338	2.71	0.47	0.00158

The channel classification for each return flow for the study reach is summarized in Table 7-2. The table shows that none of the methods indicates a distinct change in the channel planform over return interval.

Table 7-2: Channel Classification Results

Return Interval (yrs)	D_{50} Type	Slope - Discharge					Channel Morphology		Stream Power	
		Leopold and Wolman	Lane	Henderson	Ackers	Schumm and Khan	Rosgen	Parker	Nanson and Croke	Chang
1.5	Very Coarse Gravel	Braided/Straight	Braided	Meandering or Straight	Meandering	Straight	F4b	Braiding / Transitional	Meandering	Meandering to Steep Braided
30	Very Coarse Gravel	Braided/Straight	Braided	Meandering or Straight	Meandering	Straight	F4b	Meandering / Transitional	Braided	Meandering to Steep Braided
50	Very Coarse Gravel	Braided/Straight	Braided	Meandering or Straight	Meandering	Straight	F4b	Meandering / Transitional	Braided	Meandering to Steep Braided
80	Very Coarse Gravel	Braided/Straight	Braided	Meandering or Straight	Meandering	Straight	F4b	Meandering / Transitional	Braided	Meandering to Steep Braided
100	Very Coarse Gravel	Braided/Straight	Braided	Meandering or Straight	Meandering	Straight	F4b	Meandering / Transitional	Braided	Meandering to Steep Braided

In slope-discharge analysis, Leopold and Wolman method had braided/straight result. Lane method had braided planform. Henderson, Ackers, and Schumm and Khan methods had constant results of meandering or straight, meandering, and straight planform respectively.

In channel morphology analysis, Rosgen method indicated that the channel is an F4b planform at all flow conditions, but since the river has been channelized Rosgen's classification may not be appropriate. Parker method had results from braiding/transitional to meandering/transitional planform.

In stream power analysis, the Nanson and Croke method had meandering result at low flow and braided result at high flow conditions, whereas Chang method had the same result of meandering to steep braided planform at all flow conditions.

When compared with the observations from the aerial photographs, the methods that indicate a straight or meandering channel classification provide the best representation of the current channel characteristics. Since the construction of sill and levee on both sides of river, the straight classification given by Leopold and Wolman's, Henderson's, and Schumm and Khan's methods are the most accurate for all flow conditions. However, Mangyeong River has been channelized and is not a natural channel. These results may not be as useful as the actual site observation.

7.2 SINUOSITY

7.2.1 Methods

The sinuosity of the Mangyeong River was measured using the AutoCAD survey file from KICT. The valley length was measured for the interested reach as the straight line distance between cross section 104 to 87. The channel length was measured by estimating the location of the river thalweg profile based on the AutoCAD from survey of the reach. The channel

length was divided by the valley length to calculate the sinuosity. The sinuosity was obtained from only one year of 2009 survey data.

7.2.2 Results

The sinuosity for the study reach was 1.03. This reach has relatively short distance and levee was constructed on both sides of bank along the river so the sinuosity is significantly less than 1.5.

7.3 LONGITUDINAL PROFILE

7.3.1 Thalweg Profile

7.3.1.1 *Methods*

The thalweg elevation was calculated as the lowest point in the channel based on MOCT (1976), IRCMA (1993), Wanju-Gun(2009), and 2009 year survey data from KICT. A thalweg comparison is conducted to determine how the channel bed is changing.

7.3.1.2 *Results*

Figure 7-4 shows the historical thalweg elevation profile of the entire reach.

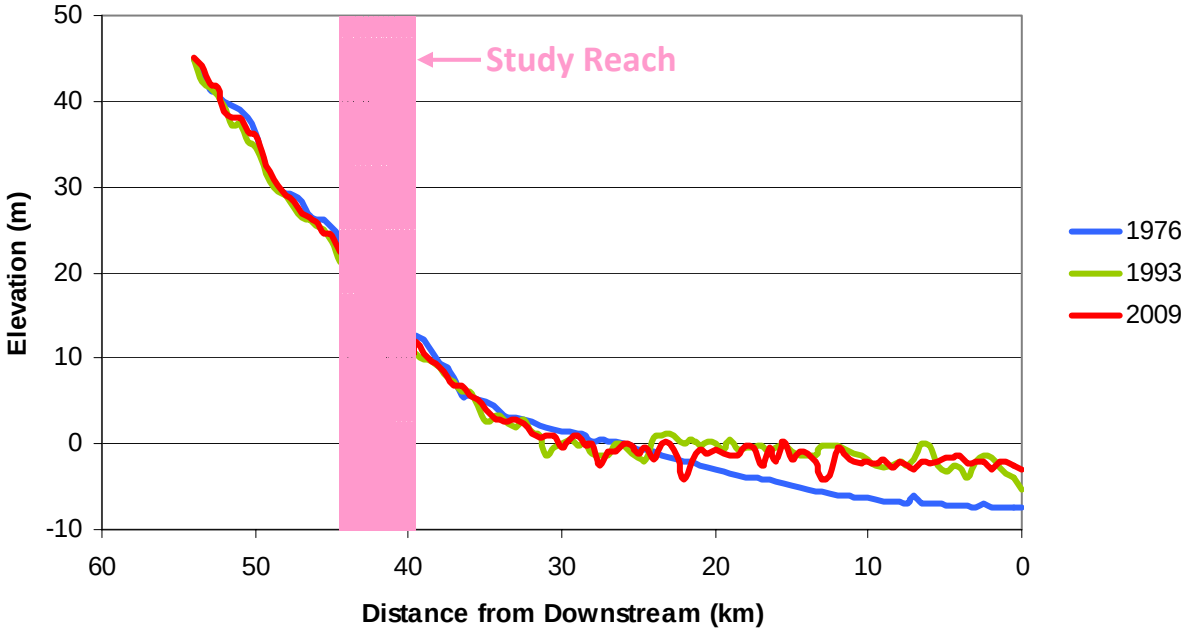

Figure 7-4: Historical Thalweg Profile of Entire Reach

Overall, the results indicate that the downstream reach has aggraded since 1976. The area highlighted shows the study reach.

7.3.2 Mean Bed Elevation

7.3.2.1 *Methods*

Trends in mean bed elevation were evaluated using three years in 1976, 1993, and 2009. The three comparisons can be made as 1976-1993 year, 1993-2009 year, and 1976-2009 year. Each evaluation came from the difference between two years. This tendency shows the changes in mean bed elevation through time.

7.3.2.2 *Results*

The change in mean bed elevation for entire reach is shown in Figure 7-5, Figure 7-6, and Figure 7-7.

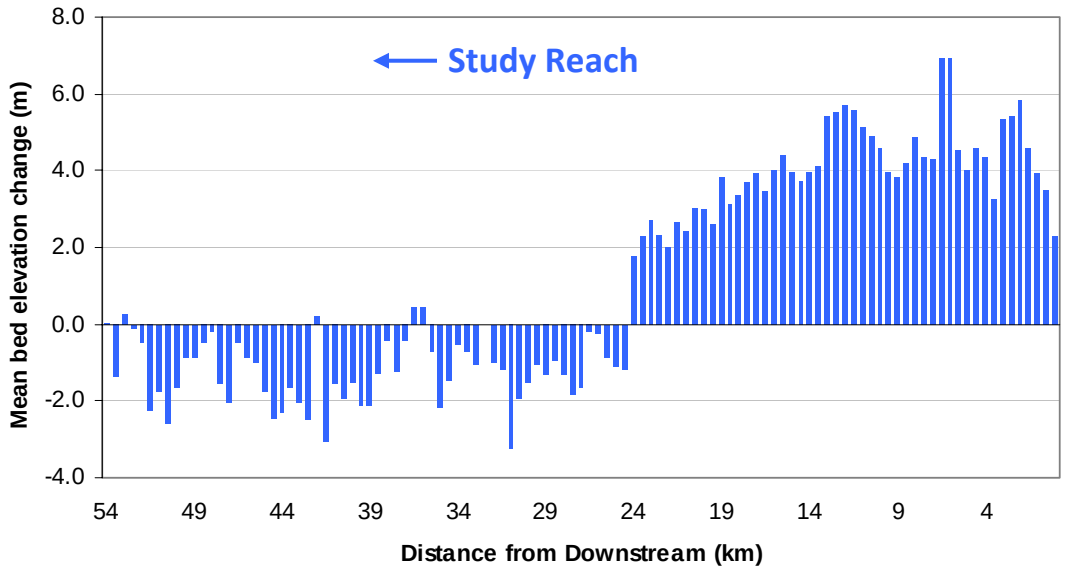

Figure 7-5: Mean Bed Elevation Change between 1976-1993

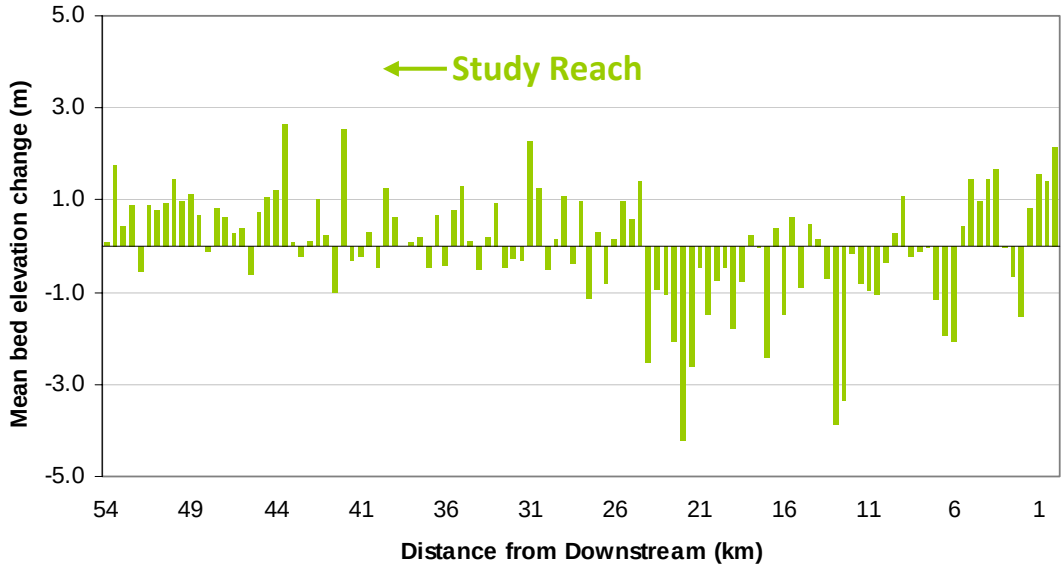

Figure 7-6: Mean Bed Elevation Change between 1993-2009

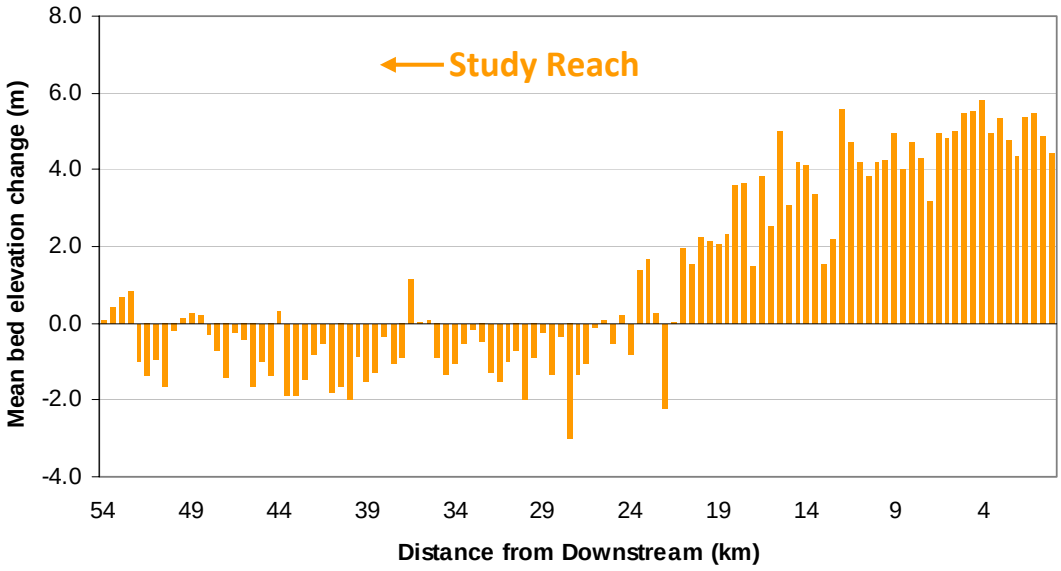

Figure 7-7: Mean Bed Elevation Change between 1976-2009

Overall, the channel has aggraded in the downstream. The river has degraded approximately 2 m along the study reach from 1976 year to 2009 year. The study reach is located in upstream of Mangyeong River. In addition, the construction of levee on the both sides of river confines the river and prevents the banks from eroding.

Chapter 8 SUMMARY

Mangyeong River was analyzed for this study. This stream is 77.4 km long and the reach of interest extends 4.25 km (104+400 to 87+000 m). Due to the interest in reconnecting the abandoned channel to the main channel, the following analysis was performed: changes in hydraulic parameters, sediment, equilibrium, and geomorphology.

Flow Discharge Analysis

Channel forming discharge was not provided. Flow duration analysis was performed to find the discharge with a return interval of 1.5 year and 255 m^3/s was selected for all analysis. Other discharges at different return intervals were also used for HEC-RAS modeling.

Hydraulic Analysis

The input data was obtained from the flow duration analysis and the hydrologic analysis performed by KICT. Fifteen hydraulic parameters were analyzed with respect to discharge.

For the discharge of 255 m^3/s with a return interval of 1.5 year, the average values of the following parameters are obtained. The top width is 244 m, the wetted perimeter is 240 m, the maximum flow depth is 1.90 m, the cross sectional area is 265 m^2, the mean flow depth is 1.11 m, the width/depth ratio is 277, the channel velocity is 1.18 m/s, and Froude number is 0.42. The values near the location of three sills on each graph show sudden change.

When a reach-averaged calculation was performed on each hydraulic parameter at various discharges, the cross sectional area was the most changed hydraulic parameter as a result of discharge changes. The cross sectional area is 265 m^2 at the discharge of a return interval of 1.5 year but it was increased from 720 m^2 to 839 m^2 in the return interval of 30 to

100 year respectively. The change rate is 2.7 to 3.2 compared with a return interval of 1.5 year. All hydraulic parameters increased with respect to discharge except the width/depth ratio. This ratio did not follow the same trend due to a minimal top width change.

Sediment Analysis

The bed material data was available for only one year of 2009. The median bed material size d_{50} for the study reach was 36 mm which is very coarse gravel. The study reach is located in upstream of Mangyeong River and this channel has degraded up to 2 m since 1976.

The maximum movable grain size is 33 mm at the discharge of 255 m^3/s with a return interval of 1.5 year. Since the median particle size is 36 mm, the bed sediment will not move. The river bed is thus armored and the bed material can only move during large floods.

The sediment load was measured from KICT in 2009. The measurement is suspended load and Modified Einstein method was performed to obtain total load. When the discharge of 255 m^3/s is applied, the total load is 6.54 thousand tons per day and the equivalent sediment concentration is 240 mg/l. When the measurement results were compared with HEC-RAS modeling results, total load was closer to the field measurements than any other methods. At high flows, the measurement load is about 10 times larger than the result from Engelund-Hansen method. Therefore, the calculations should be based on the field measurement.

Equilibrium Analysis

Four equations were used to determine the equilibrium width of this channel. These results were compared with the actual width from HEC-RAS modeling result. The method of Julien-Wargadalam and Lacey showed a reasonable predicted channel width of 83 m and 77 m

respectively, compared to measured width of 239 m at the discharge of 255 m^3/s. But at high discharge the results of those two methods were close to the HEC-RAS results. Simons and Albertson was a little more overestimated and Klaassen and Vermeer method is much more overestimated. The method of Julien-Wargadalam was also used to compute the equilibrium slope at different discharges. Based on the equilibrium slope analysis, the measured slope was 0.00230 m/m, which exceeded the predicted slope of 0.00111 m/m at the 255 m^3/s discharge.

It is important to be aware that Mangyeong River is armored and the three sills in the study reach force the river to be a lot wider and shallower.

Geomorphologic Analysis

The channel planform geometry was examined using visual and qualitative methods with data of aerial photos in 1967, 1973, 1978, 1989, and 2003. The 1967 planform geometry showed a sinuous river; however, the construction of three sills since 1966 has resulted in a much straighter channel. The analysis based on slope-discharge, channel morphology, and stream power methods indicated that the methods of Leopold and Wolman, Henderson, and Schumm and Khan are the most accurate for all flow conditions. Those methods showed the channel planform is straight. The channelization in this river prevents Mangyeong River from changing planform geometry.

The sinuosity for the study reach was 1.03. The study reach is relatively short distance of 4.25 km and the levee was constructed on both sides of the river.

Based on the surveyed thalweg for Mangyeong River, the mean bed has degraded about 2 m from 1976 to 2009.

Chapter 9 REFERENCES

Ackers, P. (1982). "Meandering Channels and the Influence of Bed Material." Gravel Bed Rivers: Fluvial Processes, Engineering and Management, R. D. Hey, J. C. Bathurst, and C. R. Thorne, eds., John Wiley & Sons Ltd. , 389-414.

Blench, T. (1957). *Regime Behavior of Canals and Rivers*, Butterworths Scientific Publications, London.

Brownlie, W. R. (1981). "Prediction of Flow Depth and Sediment Discharge in Open channels." California Institute of Technology, Pasadena, CA.

Chang, H. H. (1979). "Stream Power and River Channel Patterns." *Journal of Hydrology*, 41, 303-327.

Chow, V. T. (1959). *Open Channel Hydraulics*, McGraw-Hill.

Henderson, F. M. (1966). *Open Channel Flow*, Macmillan Publishing Co., Inc., New York, NY.

IRCMA. (1993). "Dongjin River, Mangyeong River Restoration Master Plan." Iri Regional Construction and Management Administration.

Julien, P. Y. (1998). *Erosion and Sedimentation.* , Cambridge University Press, New York, NY.

Julien, P. Y., and Wargadalam, J. (1995). "Alluvial Channel Geometry: Theory and Applications." *Journal of Hydraulic Engineering*, 121(4), 312-325.

KICT. (2009). "Sediment Measurement and Analysis Report at Bongdong Station in Mangyeong River." Korea Institute of Construction Technology.

Klaassen, G. J., and Vermeer, K. (1988). "Channel Characteristics of the Braiding Jamuna River, Bangladesh." International Conference on River Regime, 18-20 May 1988, W. R. White, ed., Hydraulics Research Ltd., Wallingford, UK, 173-189.

KRA. (2008). "www.riverlove.or.kr." Korea River Association, Seoul, Republic of Korea.

Lane, E. W. (1955). "The importance of fluvial morphology in hydraulic engineering." *Proc. ASCE*, 81(745), 1-17.

Leopold, L. B., and Wolman, M. G. (1957). "River Channel Patterns: Braided, Meandering, and Straight." *USGS Professional Paper* 282-B, 85.

MOCT. (1976). "Mangyeong River Restoration Master Plan." Ministry of Construction and Transport, Republic of Korea.

Nanson, G. C., and Croke, J. C. (1992). "A genetic classification of floodplains." *Geomorphology*, 4, 459-486.

Nouh, M. (1988). "Regime Channels of an Extremely Arid Zone." International Conference of River Regime, 18-20 May 1988, W. R. White, ed., Hydraulics Research Ltd., Wallingford, UK, 55-66.

Parker, G. (1976). "On the Cause and Characteristic Scales of Meandering and Braiding in Rivers." *Journal of Fluid Mechanics*, 76(Part 3), 457-480.

Richardson, E. V., Simons, D. B., and Lagasse, P. F. (2001). *River Engineering for Highway Encroachments, Highways in the River Environment*, United States Department of the Transportation, Federal Highway Administration.

Rosgen, D. (1996). *Applied River Morphology*, Wildland Hydrology, Pagosa Springs, CO.

Schumm, S. A., and Khan, H. R. (1972). "Experimental Study of Channel Patterns." *Geological Society of America Bulletin*, 83, 1755-1770.

Simons, D. B., and Albertson, M. L. (1963). "Uniform Water Conveyance Channels in Alluvial Material." *Transactions of the American Society of Civil Engineers*, 128, 65-107.

van den Berg, J. H. (1995). "Prediction of Alluvial Channel Pattern of Perennial Rivers." *Geomorphology*, 12, 259-279.

Wanju-Gun. (2009). "Mangyeong River Abandoned Channel and Floodplain Restoration Master Plan." Wanju-Gun.

Wargadalam, J. (1993). "Hydraulic Geometry of Alluvial Channels," Ph.D. Dissertation, Colorado State University, Fort Collins, CO.

APPENDIX A - Aerial Photo Images

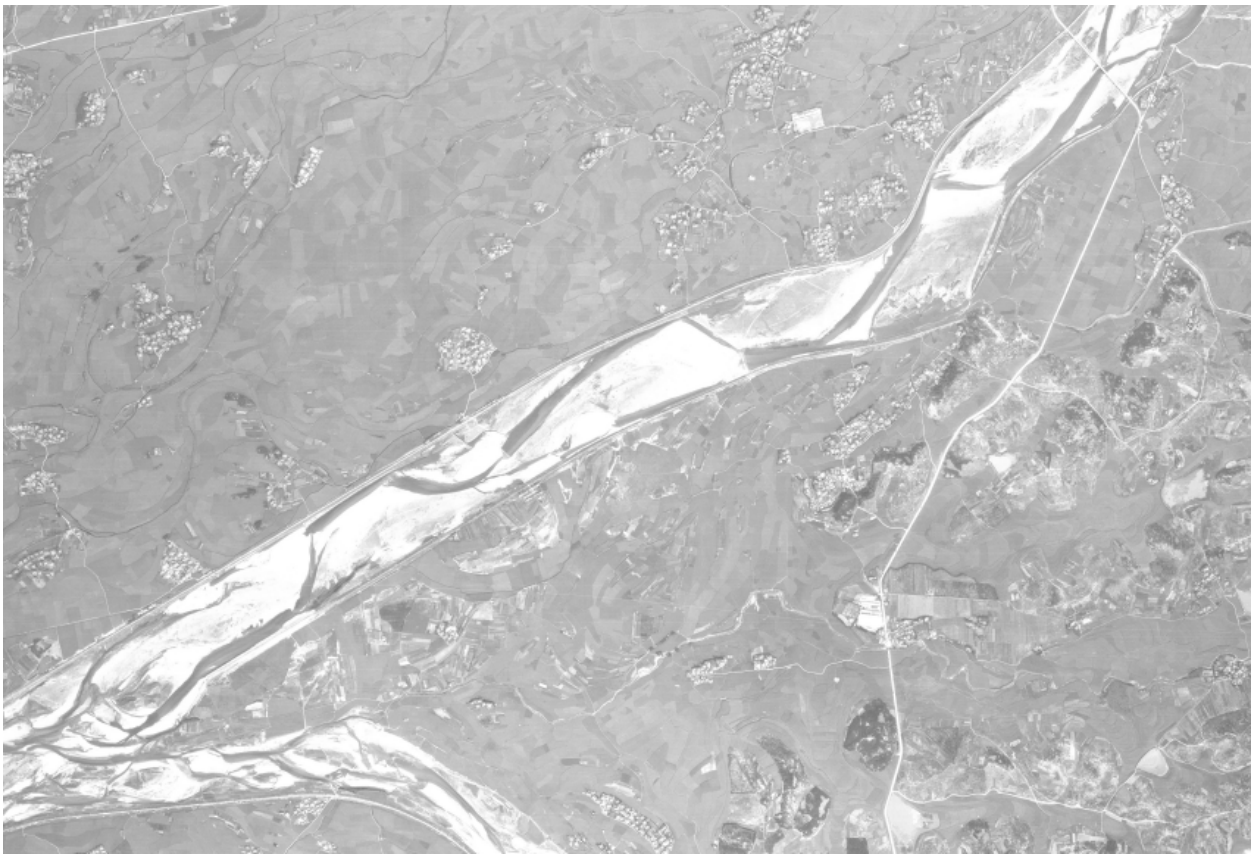

Figure A-1: Aerial Photo Image in 1967

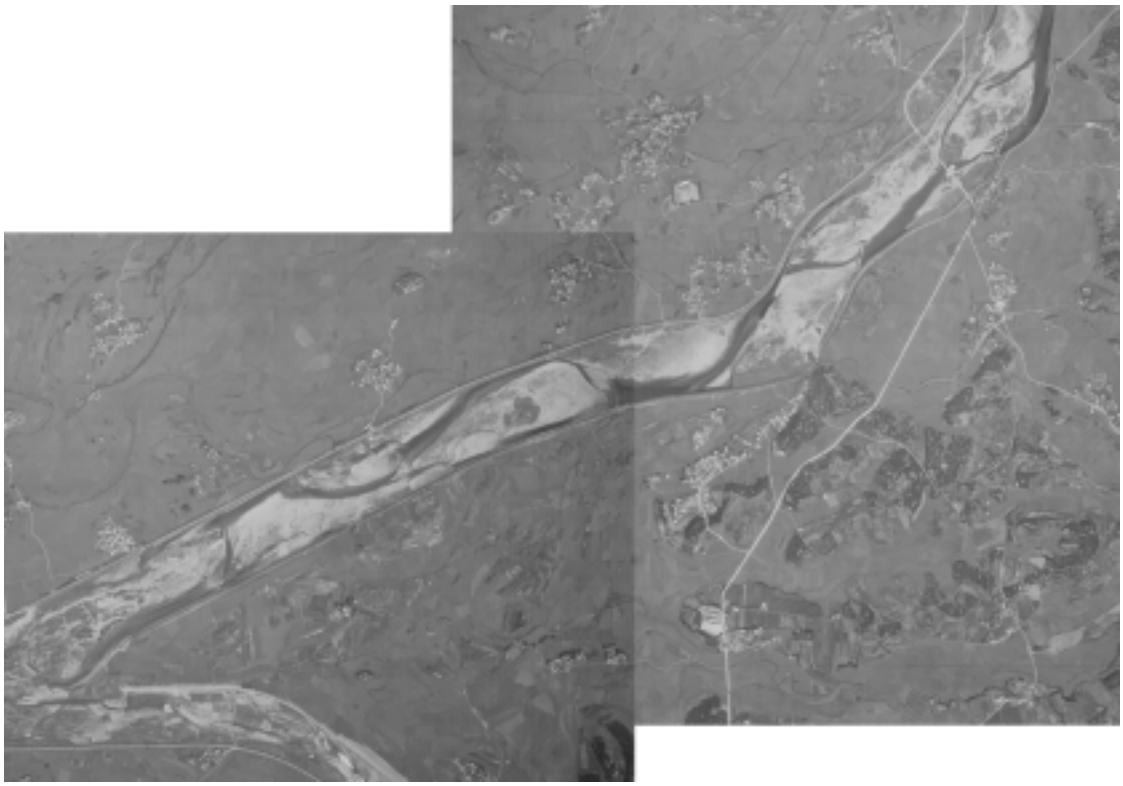

Figure A-2: Aerial Photo Image in 1973

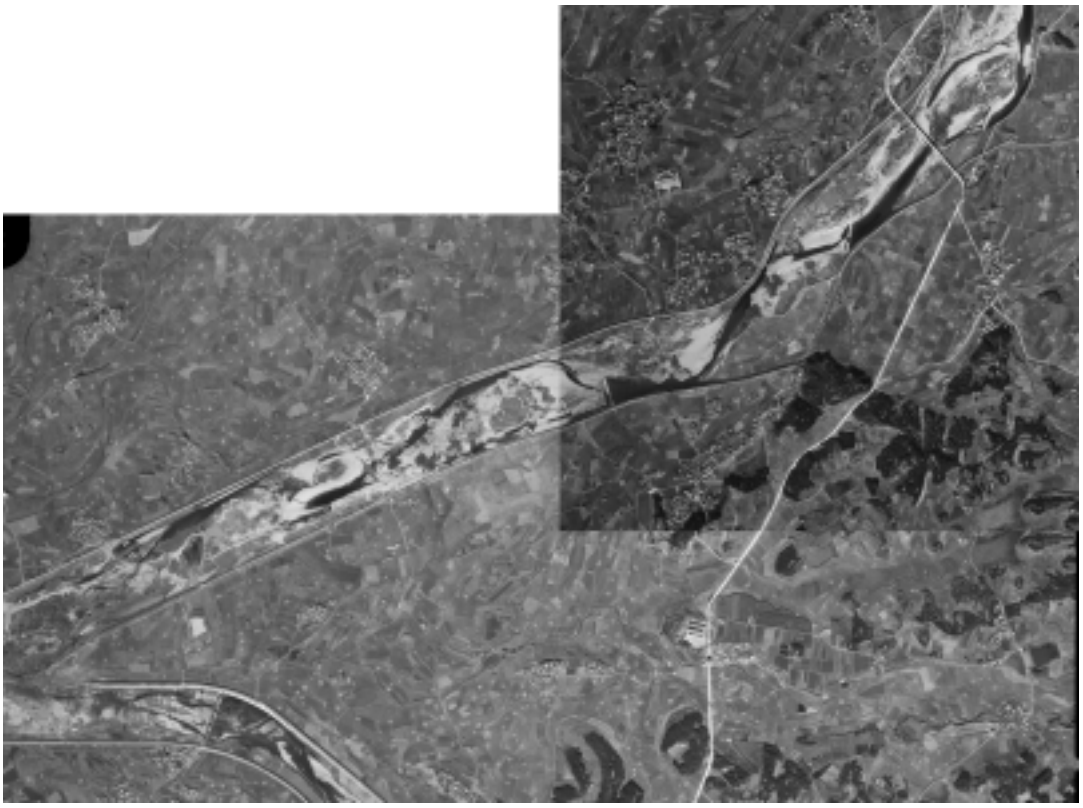

Figure A-3: Aerial Photo Image in 1978

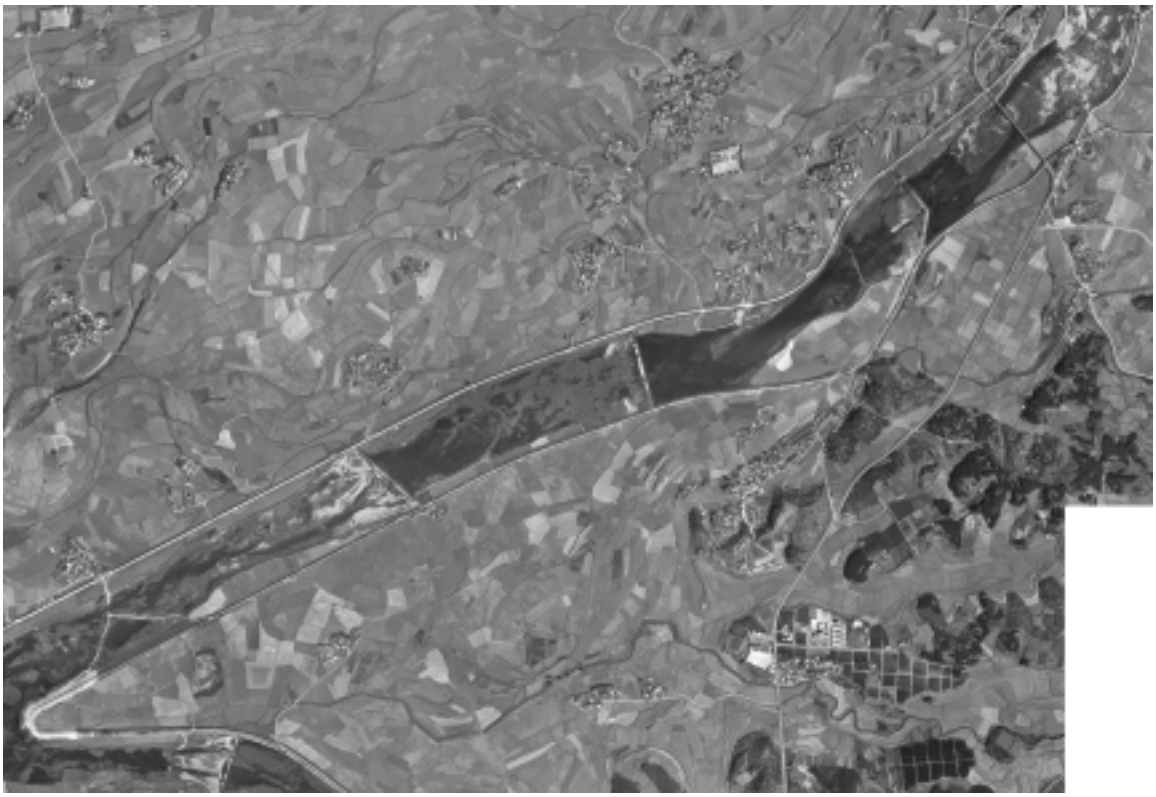

Figure A-4: Aerial Photo Image in 1989

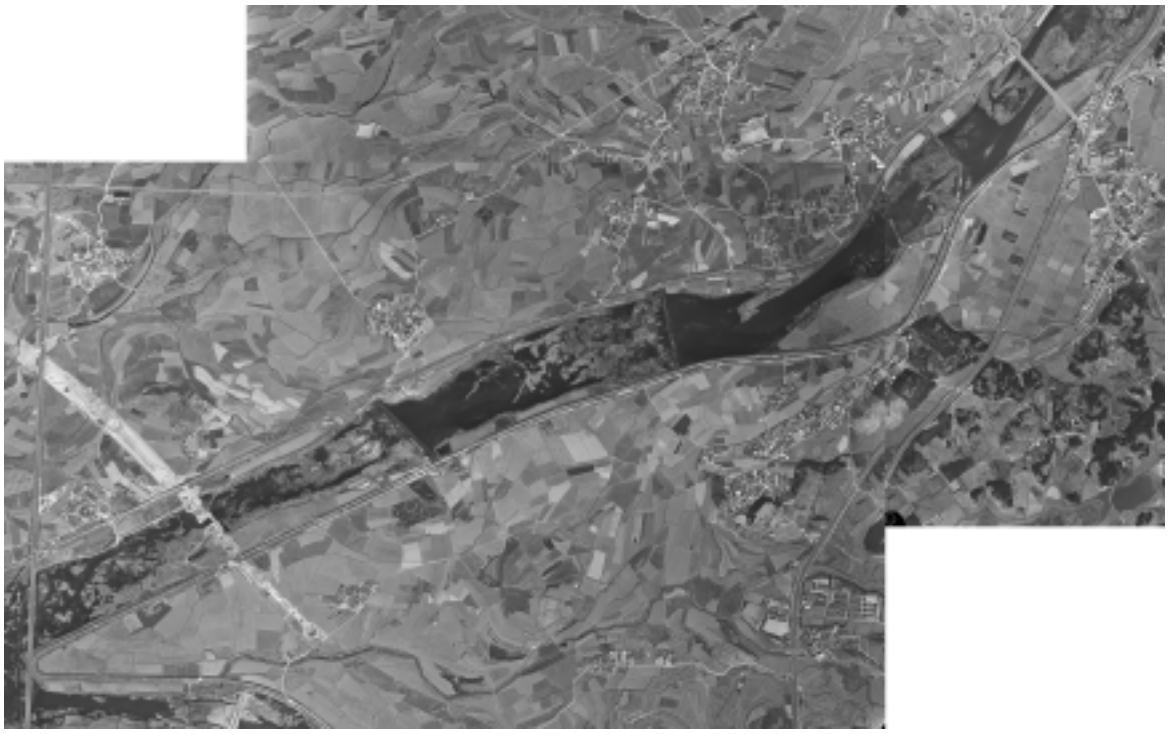

Figure A-5: Aerial Photo Image in 2003

APPENDIX B - Raw Data for HEC-RAS Modeling

Table B-1: Raw Data for HEC-RAS Modeling

River Sta	Profile	Q Total (m3/s)	Top Width (m)	W.Perimeter (m)	Max Chl Dpth (m)	Flow Area (m2)	Hydr Depth (m)	Vel Chnl (m/s)	Froude #	Min Ch El (m)	W.S. Elev (m)	E.G. Slope (m/m)	Hydr Radius (m)	Shear Chan (N/m2)	Power Chan (N/m s)
104	1.5 yr	255	206.18	206.74	1.39	110.85	0.54	2.3	1	21.63	23.02	0.010935	0.54	57.5	132.27
104	30yr	1513	299.1	300.45	2.73	481.53	1.61	3.14	0.79	21.63	24.36	0.004737	1.6	74.46	233.94
104	50yr	1695	299.88	301.32	2.91	536.08	1.79	3.16	0.75	21.63	24.54	0.004174	1.78	72.82	230.24
104	80yr	1864	300.57	302.07	3.07	584.05	1.76	3.19	0.73	21.63	24.7	0.003805	1.75	72.15	230.25
104	100yr	1943	300.88	302.41	3.14	605.6	1.83	3.21	0.72	21.63	24.77	0.003666	1.82	71.99	230.81
103	1.5 yr	255	230.6	231.47	3.21	465.35	2.02	0.55	0.12	19.42	22.63	0.000107	2.01	2.1	1.15
103	30yr	1513	238.47	240.05	4.9	860.36	2.96	1.74	0.29	19.42	24.32	0.000498	2.94	17.49	30.46
103	50yr	1695	239.24	240.9	5.06	900.07	3.08	1.86	0.31	19.42	24.48	0.000535	3.06	19.61	36.4
103	80yr	1864	239.66	241.36	5.21	935.88	3.18	1.96	0.32	19.42	24.63	0.000565	3.16	21.48	41.99
103	100yr	1943	239.79	241.5	5.28	952.04	3.25	2	0.32	19.42	24.7	0.000578	3.23	22.33	44.63
102.176	1.5 yr	255	246.56	247.7	1.53	324.99	1.32	0.78	0.22	21.07	22.6	0.000386	1.31	4.96	3.89
102.176	30yr	1513	252.66	254.24	3.14	727.49	2.5	2.03	0.38	21.07	24.21	0.000916	2.49	25.72	52.3
102.176	50yr	1695	253	254.62	3.3	768.23	2.66	2.15	0.39	21.07	24.37	0.00095	2.64	28.11	60.31
102.176	80yr	1864	253.3	254.96	3.45	805.11	2.8	2.24	0.4	21.07	24.52	0.000975	2.78	30.18	67.59
102.176	100yr	1943	253.44	255.11	3.51	821.72	2.86	2.28	0.4	21.07	24.58	0.000986	2.84	31.13	71.05
102.163	1.5 yr	255	230.18	231.05	0.57	115.25	0.5	2.21	1	20.97	21.54	0.011138	0.5	54.48	120.54
102.163	30yr	1513	249.94	251.87	2.18	507.03	2.03	2.98	0.67	20.97	23.15	0.003153	2.01	62.24	185.74
102.163	50yr	1695	250.8	252.79	2.35	550.58	2.16	3.08	0.66	20.97	23.32	0.003021	2.15	64.53	198.64
102.163	80yr	1864	251.12	253.14	2.51	588.98	1.94	3.16	0.66	20.97	23.48	0.002923	1.93	66.7	211.06
102.163	100yr	1943	251.27	253.3	2.57	606.44	2.01	3.2	0.66	20.97	23.54	0.002879	2	67.6	216.39
102	1.5 yr	255	237.85	238.02	2.08	219.63	0.92	1.16	0.39	19	21.08	0.001351	0.92	12.22	14.19
102	30yr	1513	269.53	270.37	4.08	742.55	2.58	1.98	0.38	19	23.08	0.000914	2.56	24.63	48.68
102	50yr	1695	270.28	271.21	4.26	792.34	2.75	2.07	0.39	19	23.26	0.000921	2.73	26.38	54.53
102	80yr	1864	270.72	271.7	4.42	836.16	2.89	2.15	0.39	19	23.42	0.000928	2.87	28.02	60.21
102	100yr	1943	270.88	271.88	4.5	855.95	2.96	2.18	0.39	19	23.5	0.000931	2.94	28.74	62.79
101	1.5 yr	255	178.49	178.96	2.33	312.14	1.75	0.82	0.2	18.64	20.97	0.000286	1.74	4.89	4
101	30yr	1513	185.94	187.31	4.21	654.53	2.6	2.11	0.36	18.64	22.85	0.000755	2.58	25.88	54.59
101	50yr	1695	186.64	188.1	4.39	687.5	2.76	2.22	0.37	18.64	23.03	0.000785	2.74	28.15	62.4
101	80yr	1864	187.26	188.79	4.55	716.69	2.91	2.31	0.38	18.64	23.19	0.00081	2.89	30.17	69.67
101	100yr	1943	187.54	189.1	4.62	729.88	2.97	2.35	0.38	18.64	23.26	0.000821	2.95	31.09	73.09
100	1.5 yr	255	109.97	110.3	2.21	203.51	1.65	1.24	0.29	18.61	20.82	0.000615	1.64	11.13	13.85
100	30yr	1513	125.42	126.17	3.92	403.6	2.13	2.61	0.47	18.61	22.53	0.001304	2.11	40.91	106.91
100	50yr	1695	127.3	128.1	4.11	426.51	2.29	2.68	0.47	18.61	22.72	0.001296	2.27	42.3	113.17
100	80yr	1864	128.97	129.8	4.27	447.01	2.43	2.73	0.47	18.61	22.88	0.001289	2.42	43.52	118.75
100	100yr	1943	129.72	130.56	4.34	456.32	2.5	2.75	0.47	18.61	22.95	0.001286	2.48	44.08	121.35
99	1.5 yr	255	263.43	263.96	2.15	379.26	1.44	0.67	0.18	18.62	20.77	0.000251	1.44	3.54	2.38
99	30yr	1513	269.76	270.96	3.74	804.9	2.77	1.87	0.35	18.62	22.36	0.000741	2.76	21.57	40.44
99	50yr	1695	270.07	271.31	3.91	850.78	2.91	1.98	0.36	18.62	22.53	0.000771	2.89	23.72	47.04
99	80yr	1864	270.34	271.62	4.06	891.43	3.03	2.08	0.37	18.62	22.68	0.000797	3.01	25.65	53.29
99	100yr	1943	270.46	271.76	4.13	909.77	3.08	2.12	0.37	18.62	22.75	0.000808	3.06	26.53	56.27
98	1.5 yr	255	249.59	249.91	2.19	468.2	1.88	0.54	0.13	18.54	20.73	0.000116	1.87	2.12	1.16
98	30yr	1513	254.01	254.69	3.69	846.89	2.95	1.7	0.3	18.54	22.23	0.000527	2.95	17.18	29.28
98	50yr	1695	254.35	255.06	3.86	888.65	3.11	1.81	0.31	18.54	22.4	0.000558	3.1	19.06	34.5
98	80yr	1864	254.65	255.4	4	925.75	3.25	1.9	0.32	18.54	22.54	0.000584	3.24	20.77	39.49
98	100yr	1943	254.78	255.55	4.07	942.49	3.31	1.94	0.32	18.54	22.61	0.000596	3.3	21.56	41.89
97.093	1.5 yr	255	312.8	315.51	1.36	423.86	1.36	0.6	0.16	19.35	20.7	0.00022	1.34	2.9	1.74
97.093	30yr	1513	316.34	320.84	2.77	869.4	2.75	1.74	0.34	19.35	22.12	0.000721	2.71	19.17	33.37
97.093	50yr	1695	317.03	321.59	2.93	919.47	2.9	1.84	0.35	19.35	22.28	0.000754	2.86	21.13	38.96
97.093	80yr	1864	317.64	322.27	3.07	964.06	3.04	1.93	0.35	19.35	22.42	0.000781	2.99	22.9	44.27
97.093	100yr	1943	317.91	322.57	3.14	984.18	3.1	1.97	0.36	19.35	22.49	0.000793	3.05	23.72	46.82
97.084	1.5 yr	255	312.8	315.39	1.3	127.21	0.41	2	1	19.15	20.45	0.012137	0.4	48	96.23
97.084	30yr	1513	312.8	317.25	2.22	417.44	1.33	3.62	1	19.15	21.37	0.0082	1.32	105.8	383.48
97.084	50yr	1695	313.53	318.14	2.33	450.98	1.44	3.76	1	19.15	21.48	0.007984	1.42	110.99	417.13
97.084	80yr	1864	313.95	318.6	2.43	480.9	1.53	3.88	1	19.15	21.58	0.007809	1.51	115.59	448.04
97.084	100yr	1943	314.13	318.8	2.47	494.08	1.57	3.93	1	19.15	21.62	0.007761	1.55	117.95	463.84
97.081	1.5 yr	255	312.8	316.51	0.96	214.94	0.69	1.19	0.46	18.25	19.21	0.002122	0.68	14.13	16.77
97.081	30yr	1513	312.8	319.54	2.47	689.18	2.2	2.2	0.47	18.25	20.72	0.001557	2.16	32.92	72.28
97.081	50yr	1695	312.8	319.88	2.64	741.58	2.37	2.29	0.47	18.25	20.89	0.001532	2.32	34.84	79.63
97.081	80yr	1864	312.8	320.18	2.79	788.39	2.52	2.36	0.48	18.25	21.04	0.001513	2.46	36.54	86.38
97.081	100yr	1943	312.8	320.31	2.86	809.64	2.59	2.4	0.48	18.25	21.11	0.001505	2.53	37.31	89.55

River Sta	Profile	Q Total (m3/s)	Top Width (m)	W.Perimeter (m)	Max Chl Dpth (m)	Flow Area (m2)	Hydr Depth (m)	Vel Chnl (m/s)	Froude #	Min Ch El (m)	W.S. Elev (m)	E.G. Slope (m/m)	Hydr Radius (m)	Shear Chan (N/m2)	Power Chan (N/m s)
97	1.5 yr	255	257.94	258.37	1.88	188	0.73	1.36	0.51	17.11	18.99	0.00253	0.73	18.05	24.49
97	30yr	1513	277.67	278.59	3.4	603.33	2.11	2.48	0.54	17.11	20.51	0.001969	2.1	41.81	103.51
97	50yr	1695	277.91	278.87	3.57	649.43	2.27	2.57	0.54	17.11	20.68	0.001929	2.26	44.05	113.3
97	80yr	1864	278.12	279.13	3.71	690.57	2.42	2.66	0.54	17.11	20.82	0.001898	2.41	46.04	122.29
97	100yr	1943	278.22	279.25	3.78	709.2	2.48	2.69	0.54	17.11	20.89	0.001885	2.47	46.96	126.52
96	1.5 yr	255	258.93	259.7	2.49	206.53	0.75	1.2	0.43	16	18.49	0.001747	0.75	13.63	16.3
96	30yr	1513	266.17	267.47	4.19	653.82	2.37	2.12	0.43	16	20.19	0.001227	2.36	29.41	62.31
96	50yr	1695	266.68	268.01	4.36	699.99	2.54	2.21	0.44	16	20.36	0.001223	2.52	31.32	69.23
96	80yr	1864	267.14	268.49	4.52	741.1	2.69	2.29	0.44	16	20.52	0.00122	2.67	33.02	75.64
96	100yr	1943	267.34	268.71	4.58	759.63	2.75	2.33	0.44	16	20.58	0.00122	2.73	33.81	78.69
95	1.5 yr	255	261.52	261.91	2.28	382.72	1.37	0.65	0.17	16.12	18.4	0.000232	1.37	3.33	2.18
95	30yr	1513	272.12	273.3	3.9	815.03	2.88	1.75	0.32	16.12	20.02	0.000646	2.86	18.88	33.14
95	50yr	1695	272.36	273.61	4.07	861.22	2.99	1.86	0.33	16.12	20.19	0.000672	2.97	20.75	38.52
95	80yr	1864	272.4	273.67	4.22	902.17	3.11	1.95	0.34	16.12	20.34	0.000697	3.09	22.52	43.88
95	100yr	1943	272.4	273.67	4.29	920.78	3.18	1.99	0.35	16.12	20.41	0.000706	3.15	23.28	46.28
94	1.5 yr	255	214.51	214.79	2.09	363.31	1.37	0.7	0.17	16.25	18.34	0.000218	1.36	3.61	2.52
94	30yr	1513	220.5	221.49	3.53	677.05	2.58	2.05	0.37	16.25	19.78	0.000851	2.56	25.5	52.23
94	50yr	1695	220.73	221.76	3.69	711.59	2.72	2.16	0.38	16.25	19.94	0.00089	2.7	28.02	60.63
94	80yr	1864	220.93	222	3.83	742.4	2.85	2.26	0.39	16.25	20.08	0.000923	2.83	30.26	68.51
94	100yr	1943	221.02	222.11	3.89	756.43	2.91	2.31	0.4	16.25	20.14	0.000936	2.89	31.27	72.21
93.071	1.5 yr	255	321.7	325.83	2.06	664.26	2.06	0.38	0.09	16.27	18.33	0.000051	2.04	1.03	0.39
93.071	30yr	1513	322	327.8	3.5	1126.71	3.41	1.34	0.23	16.27	19.77	0.000312	3.35	10.52	14.11
93.071	50yr	1695	322	327.8	3.66	1177.25	3.56	1.44	0.24	16.27	19.93	0.000338	3.5	11.91	17.11
93.071	80yr	1864	322	327.8	3.8	1222.34	3.69	1.52	0.25	16.27	20.07	0.00036	3.63	13.18	20.05
93.071	100yr	1943	322	327.8	3.86	1242.87	3.75	1.56	0.25	16.27	20.13	0.00037	3.68	13.77	21.47
93.056	1.5 yr	255	320.3	322.43	0.53	170.87	0.53	1.49	0.65	15.87	16.4	0.004674	0.53	24.29	36.25
93.056	30yr	1513	321.7	330.57	2.04	653.14	2.03	2.32	0.52	15.87	17.91	0.001948	1.98	37.74	87.43
93.056	50yr	1695	321.7	330.93	2.21	710.09	2.21	2.39	0.51	15.87	18.08	0.001853	2.15	38.99	93.07
93.056	80yr	1864	321.7	331.24	2.37	761.02	2.37	2.45	0.51	15.87	18.24	0.001781	2.3	40.13	98.29
93.056	100yr	1943	321.7	331.39	2.44	784.23	2.44	2.48	0.51	15.87	18.31	0.001752	2.37	40.65	100.73
93	1.5 yr	255	273.06	273.35	1.62	159.16	0.58	1.6	0.67	14.5	16.12	0.004752	0.58	27.13	43.47
93	30yr	1513	291.31	292.3	3.27	628.06	2.16	2.41	0.52	14.5	17.77	0.001884	2.15	39.69	95.62
93	50yr	1695	292.67	293.73	3.45	679.55	2.32	2.49	0.52	14.5	17.95	0.00183	2.31	41.52	103.56
93	80yr	1864	293.87	295	3.61	725.67	2.47	2.57	0.52	14.5	18.11	0.001788	2.46	43.14	110.81
93	100yr	1943	294.42	295.58	3.68	746.73	2.54	2.6	0.52	14.5	18.18	0.001771	2.53	43.87	114.16
92	1.5 yr	255	194.98	195.8	2.72	188.56	0.97	1.35	0.44	12.75	15.47	0.001731	0.96	16.34	22.1
92	30yr	1513	229.02	230.93	4.58	592.99	2.37	2.49	0.49	12.75	17.33	0.001586	2.35	39.94	99.42
92	50yr	1695	229.53	231.59	4.75	632.71	2.53	2.6	0.5	12.75	17.5	0.001597	2.5	42.78	111.36
92	80yr	1864	229.99	232.17	4.9	668.15	2.66	2.7	0.51	12.75	17.65	0.001604	2.63	45.28	122.32
92	100yr	1943	230.2	232.43	4.97	684.29	2.73	2.75	0.51	12.75	17.72	0.001607	2.69	46.41	127.4
91	1.5 yr	255	177.56	178.36	2.32	213.38	1.2	1.2	0.35	12.84	15.16	0.001012	1.2	11.87	14.19
91	30yr	1513	188.92	190.73	4.13	548.51	2.27	2.48	0.47	12.84	16.97	0.001357	2.24	38.28	95.05
91	50yr	1695	189.57	191.47	4.31	581.49	2.43	2.59	0.47	12.84	17.15	0.001369	2.4	40.77	105.46
91	80yr	1864	190.15	192.13	4.46	611.19	2.57	2.67	0.48	12.84	17.3	0.001375	2.54	42.89	114.65
91	100yr	1943	190.41	192.43	4.54	624.78	2.63	2.71	0.48	12.84	17.38	0.001376	2.6	43.82	118.83
90	1.5 yr	255	176.04	177.33	2.44	211.15	1.2	1.21	0.35	12.47	14.91	0.00104	1.19	12.14	14.67
90	30yr	1513	207.14	210.04	4.05	535.46	2.13	2.67	0.53	12.47	16.52	0.001846	2.11	46.15	123.36
90	50yr	1695	207.24	210.23	4.21	569.93	2.28	2.79	0.54	12.47	16.68	0.001848	2.25	49.12	136.85
90	80yr	1864	207.33	210.41	4.37	601.64	2.41	2.88	0.54	12.47	16.84	0.001836	2.38	51.48	148.11
90	100yr	1943	207.37	210.49	4.44	616.27	2.46	2.92	0.54	12.47	16.91	0.001828	2.43	52.48	153.08
89.182	1.5 yr	255	188.26	188.46	1.92	197.24	1.05	1.29	0.4	12.89	14.81	0.001416	1.05	14.53	18.78
89.182	30yr	1513	254.66	255.36	3.56	604.58	2.08	2.37	0.49	12.89	16.45	0.001606	2.07	37.3	88.52
89.182	50yr	1695	255	255.73	3.73	648.46	2.21	2.47	0.49	12.89	16.62	0.001583	2.2	39.37	97.09
89.182	80yr	1864	255	255.73	3.89	689.57	2.37	2.53	0.49	12.89	16.78	0.001535	2.36	40.6	102.73
89.182	100yr	1943	255	255.73	3.97	708.49	2.44	2.56	0.49	12.89	16.86	0.001514	2.43	41.12	105.2
89.158	1.5 yr	255	180.73	180.92	1.86	186.06	1.03	1.37	0.43	12.89	14.75	0.001628	1.03	16.42	22.51
89.158	30yr	1513	254.39	255.07	3.45	576.01	1.98	2.5	0.53	12.89	16.34	0.001906	1.97	42.2	105.69
89.158	50yr	1695	254.82	255.53	3.63	621.03	2.14	2.58	0.53	12.89	16.52	0.001834	2.13	43.71	112.8
89.158	80yr	1864	255	255.73	3.78	661.27	2.26	2.65	0.53	12.89	16.67	0.001785	2.25	45.25	120.05
89.158	100yr	1943	255	255.73	3.86	680.59	2.34	2.68	0.52	12.89	16.75	0.001749	2.33	45.64	122.16

River Sta	Profile	Q Total (m3/s)	Top Width (m)	W.Perimeter (m)	Max Chl Dpth (m)	Flow Area (m2)	Hydr Depth (m)	Vel Chnl (m/s)	Froude #	Min Ch El (m)	W.S. Elev (m)	E.G. Slope (m/m)	Hydr Radius (m)	Shear Chan (N/m2)	Power Chan (N/m s)
89	1.5 yr	255	243.8	244.46	2.22	146.25	0.6	1.74	0.72	12.04	14.26	0.005428	0.6	31.84	55.52
89	30yr	1513	253.96	255.17	4.03	599.21	2.13	2.41	0.5	12.04	16.07	0.001675	2.12	38.58	93
89	50yr	1695	254.44	255.69	4.22	647.36	2.31	2.48	0.5	12.04	16.26	0.001604	2.3	39.83	98.78
89	80yr	1864	254.86	256.15	4.39	690.07	2.47	2.54	0.49	12.04	16.43	0.001552	2.46	41	104.23
89	100yr	1943	255.07	256.37	4.47	710.74	2.55	2.57	0.49	12.04	16.51	0.001521	2.53	41.35	106.1
88	1.5 yr	255	223.09	223.45	1.81	244.98	1.1	1.04	0.32	12.07	13.89	0.000863	1.1	9.27	9.65
88	30yr	1513	232.65	233.49	3.74	685.25	2.53	2.11	0.39	12.07	15.81	0.000951	2.51	27.37	57.68
88	50yr	1695	233.26	234.13	3.93	730.22	2.71	2.2	0.4	12.07	16	0.000954	2.69	29.18	64.12
88	80yr	1864	233.79	234.69	4.1	770	2.87	2.28	0.4	12.07	16.17	0.000957	2.84	30.79	70.09
88	100yr	1943	234.06	234.97	4.19	789.69	2.94	2.31	0.4	12.07	16.26	0.000951	2.92	31.35	72.31
87	1.5 yr	255	261.49	262.24	1.75	222.27	0.85	1.15	0.4	11.84	13.59	0.001477	0.85	12.28	14.08
87	30yr	1513	269.57	270.79	3.77	758.46	2.65	1.94	0.37	11.84	15.61	0.000858	2.64	23.58	45.75
87	50yr	1695	270.05	271.3	3.96	810.69	2.84	2.03	0.37	11.84	15.8	0.000859	2.82	25.17	51.02
87	80yr	1864	270.46	271.75	4.13	856.75	3	2.1	0.38	11.84	15.97	0.000861	2.98	26.62	55.98
87	100yr	1943	270.67	271.98	4.22	880.05	3.08	2.13	0.38	11.84	16.06	0.000854	3.06	27.1	57.75

APPENDIX C - Hydraulic Geometry Analysis Plots Combined & Averaged

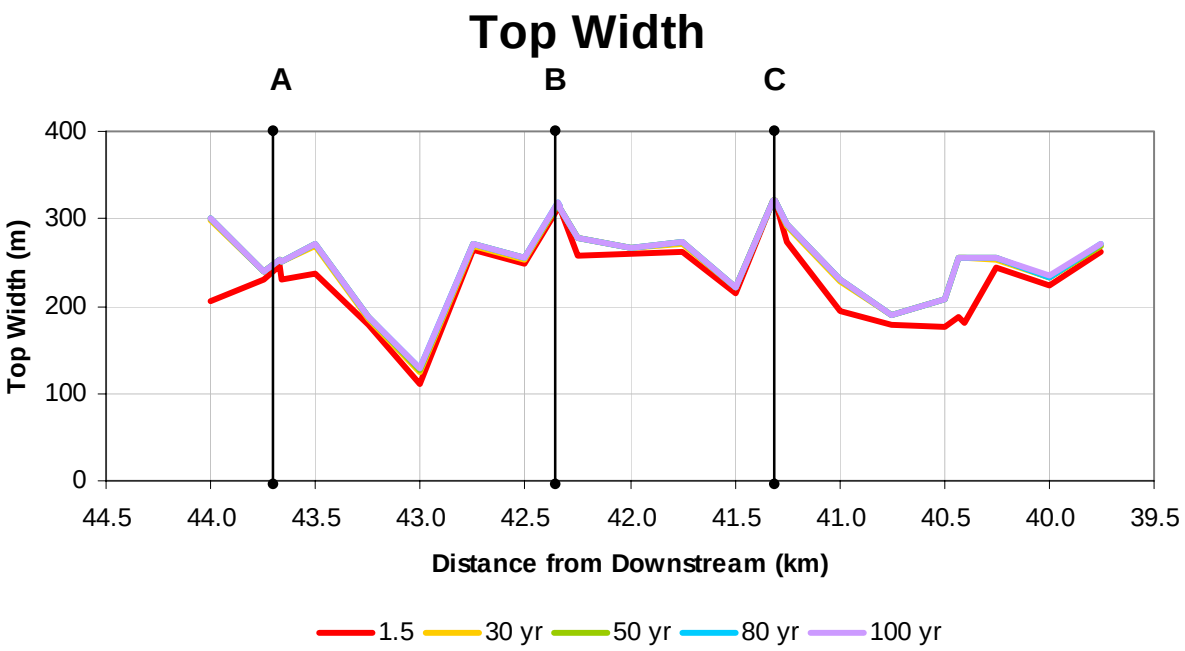

Figure C-1: Combined Top Width due to Discharge

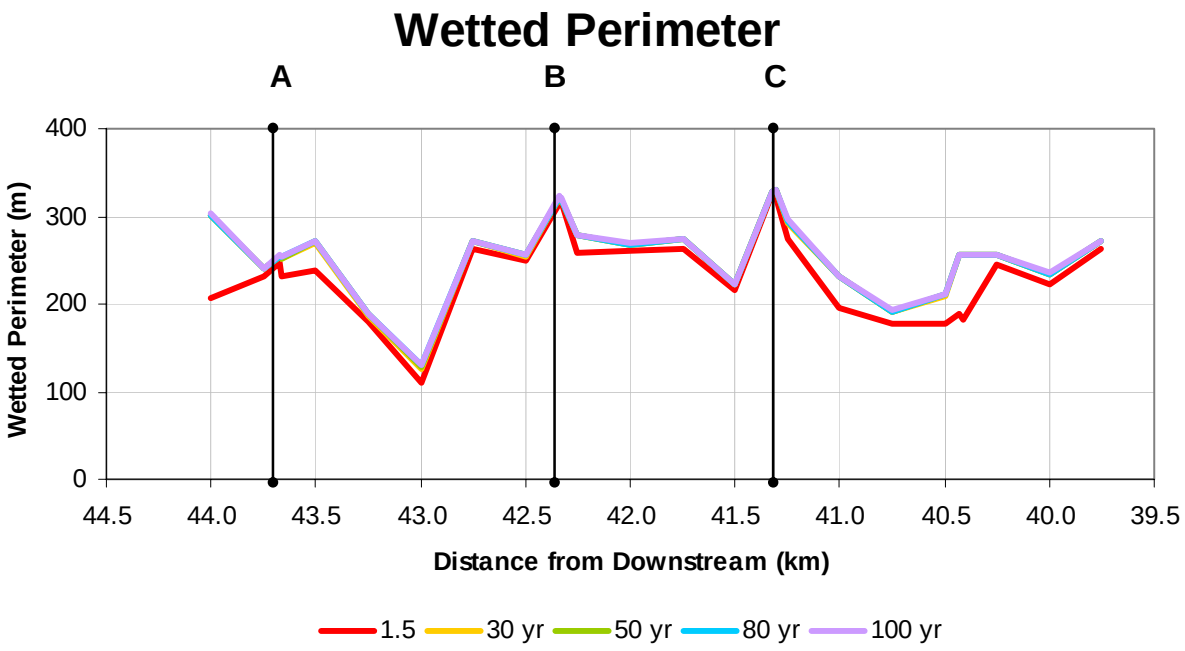

Figure C-2: Combined Wetted Perimeter due to Discharge

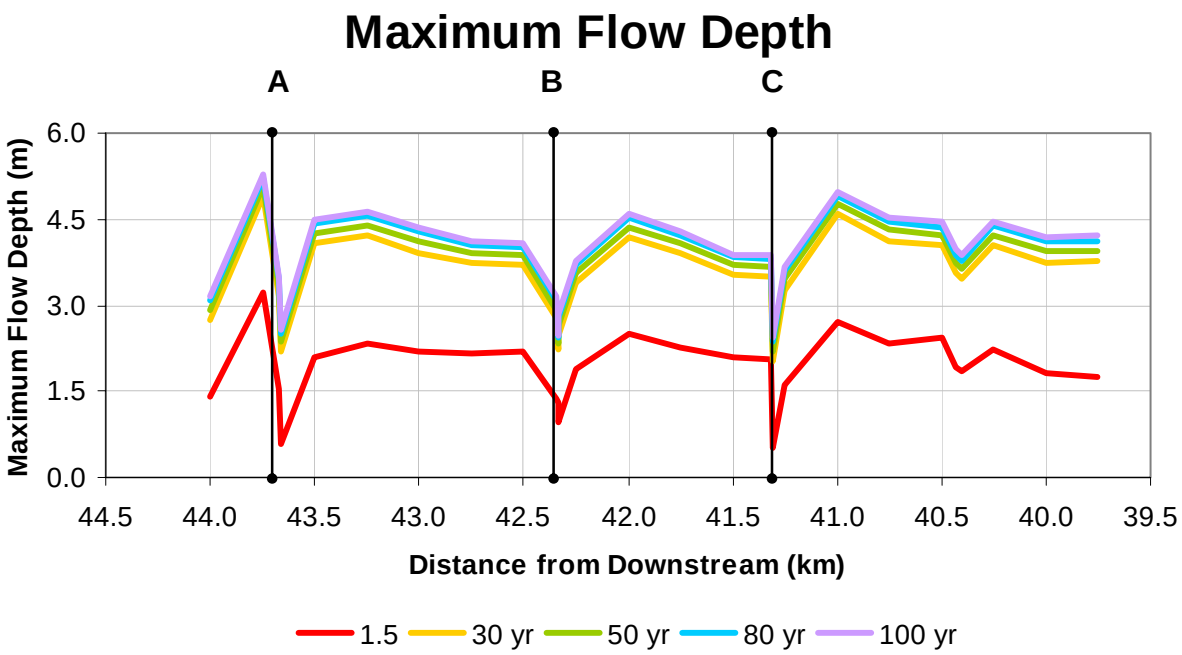

Figure C-3: Combined Maximum Flow Depth due to Discharge

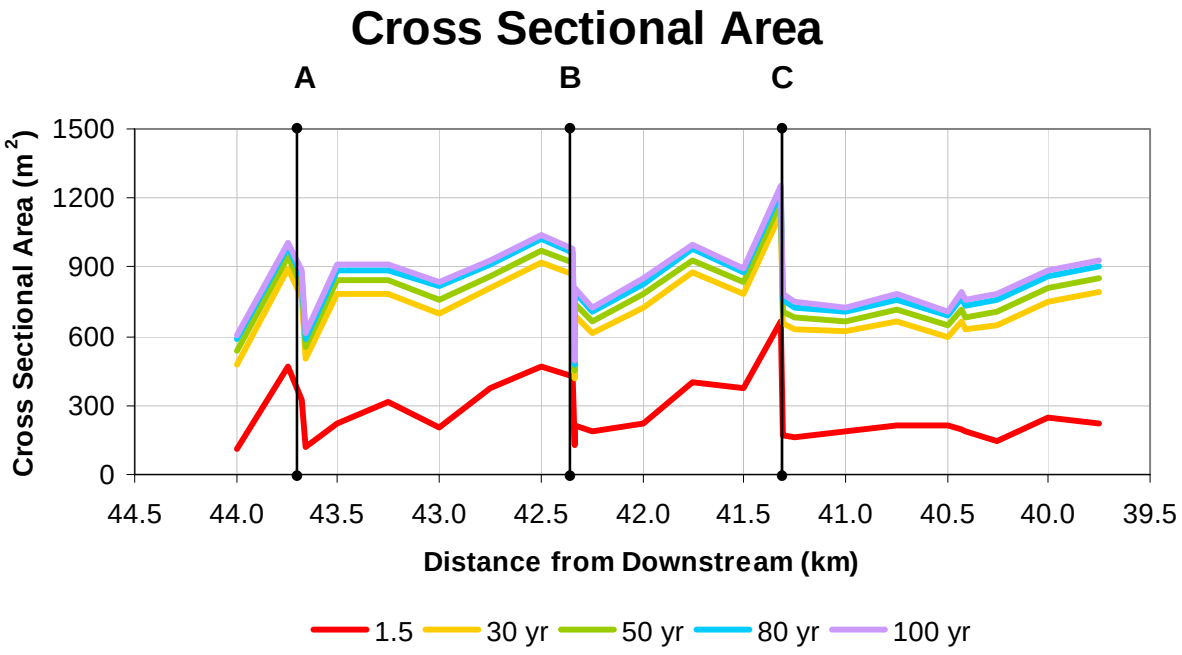

Figure C-4: Combined Cross Sectional Area due to Discharge

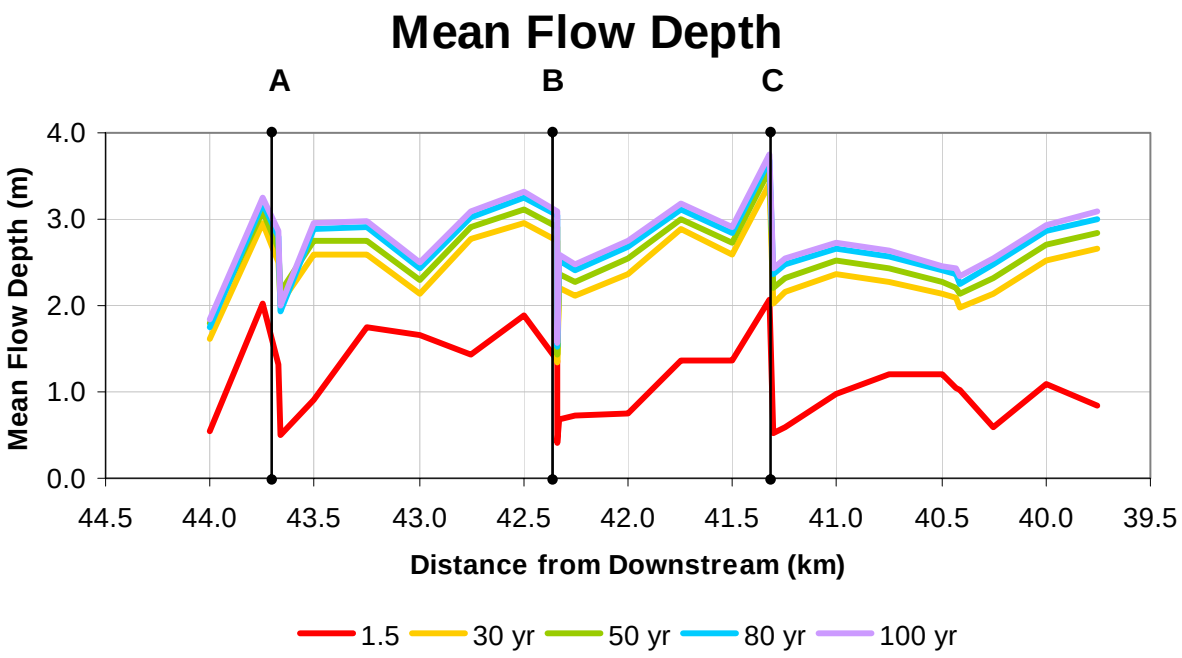

Figure C-5: Combined Mean Flow Depth due to Discharge

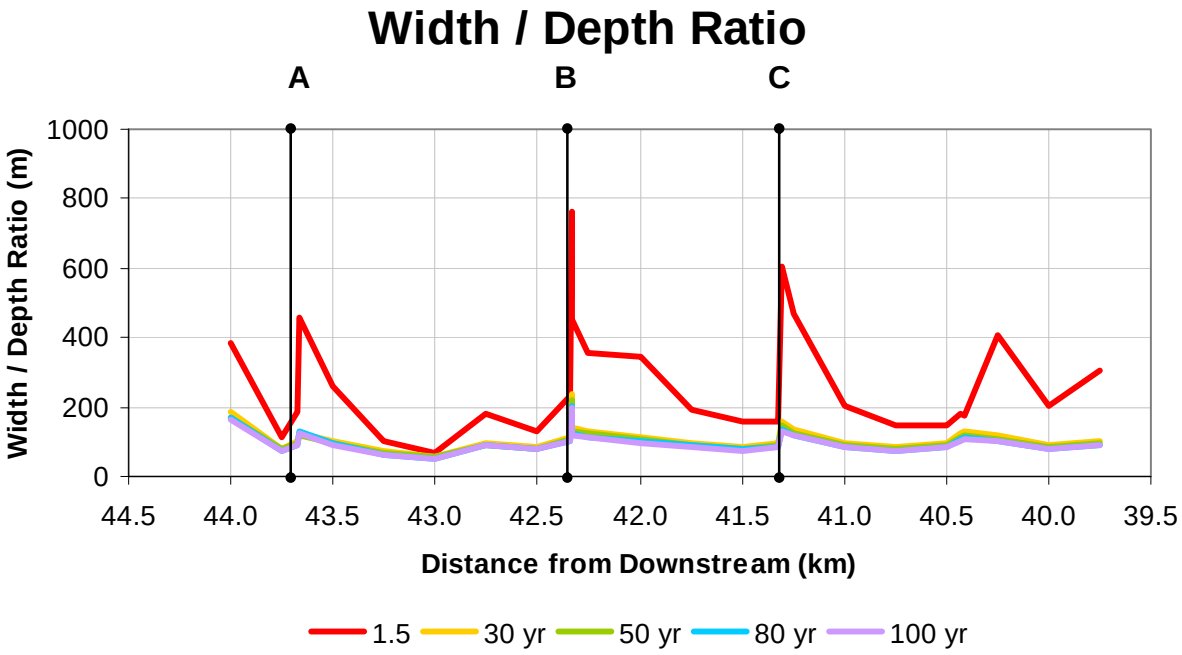

Figure C-6: Combined Width / Depth Ratio due to Discharge

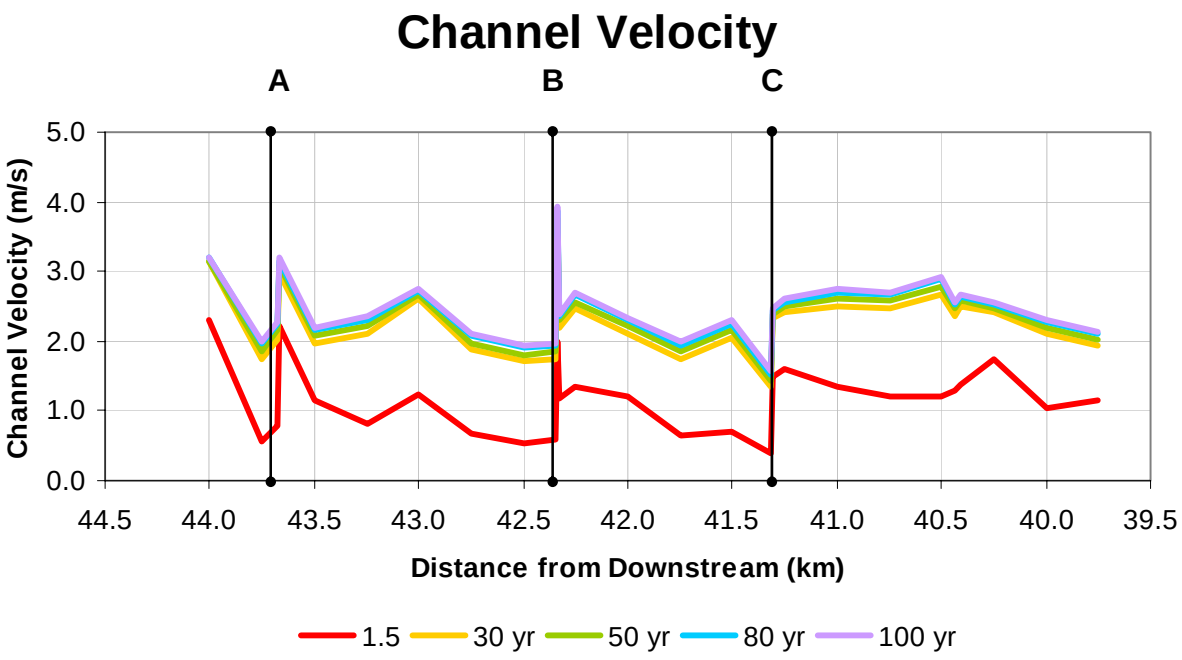

Figure C-7: Combined Channel Velocity due to Discharge

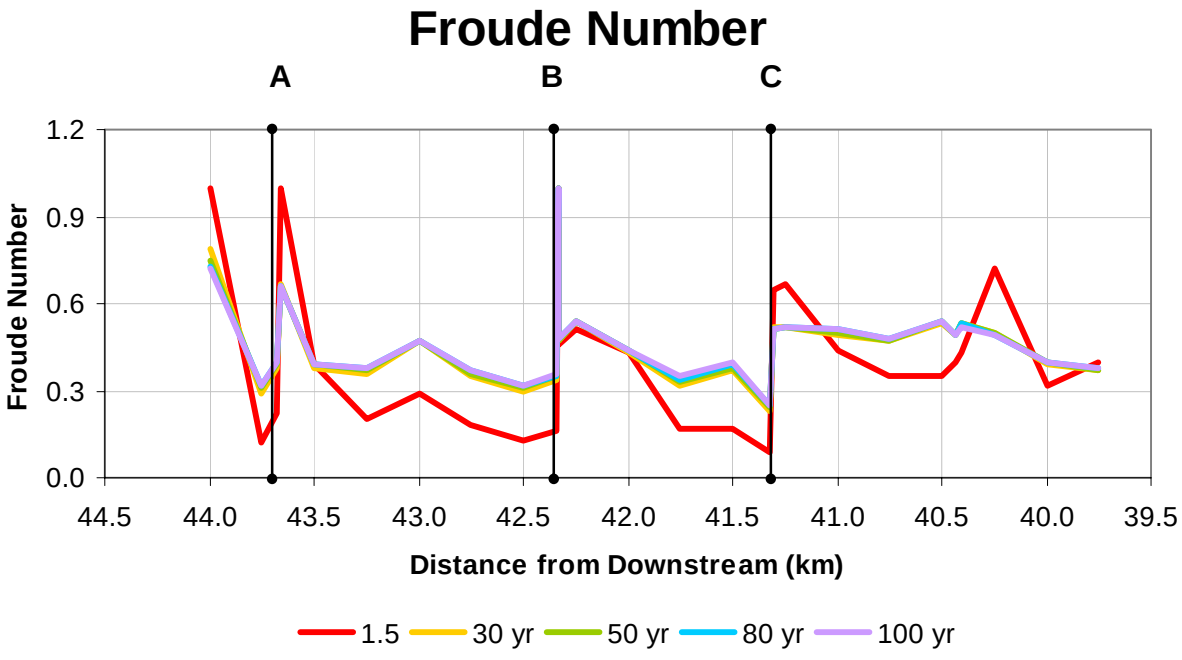

Figure C-8: Combined Froude Number due to Discharge

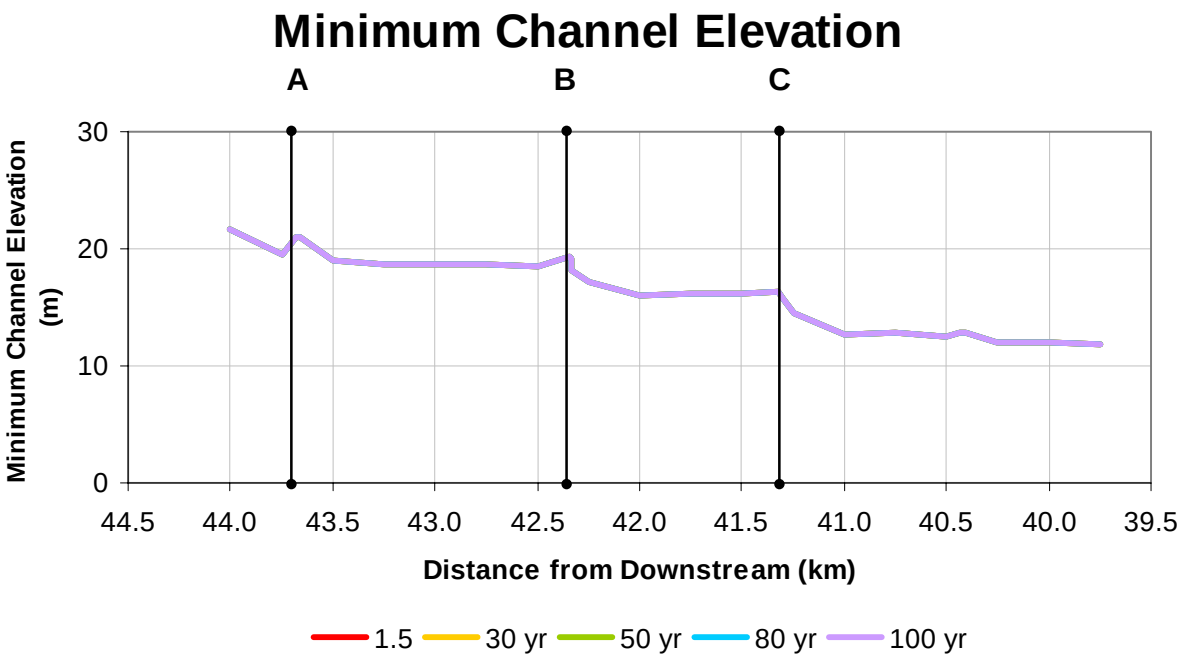

Figure C-9: Combined Minimum Channel Elevation due to Discharge

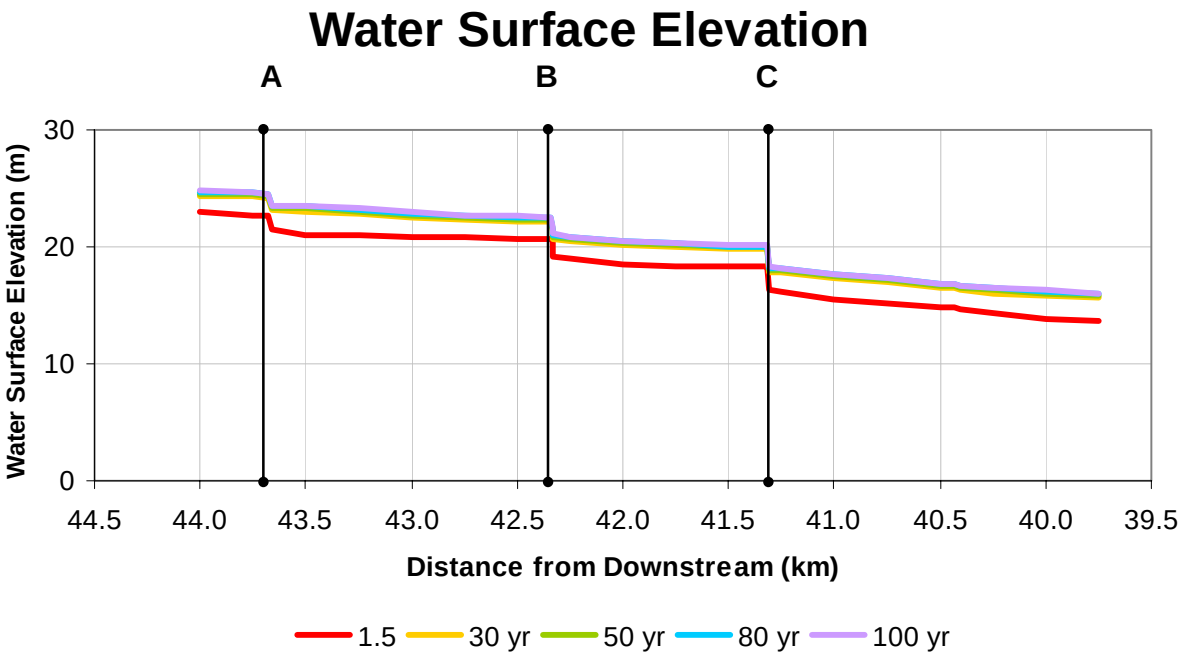

Figure C-10: Combined Water Surface Elevation due to Discharge

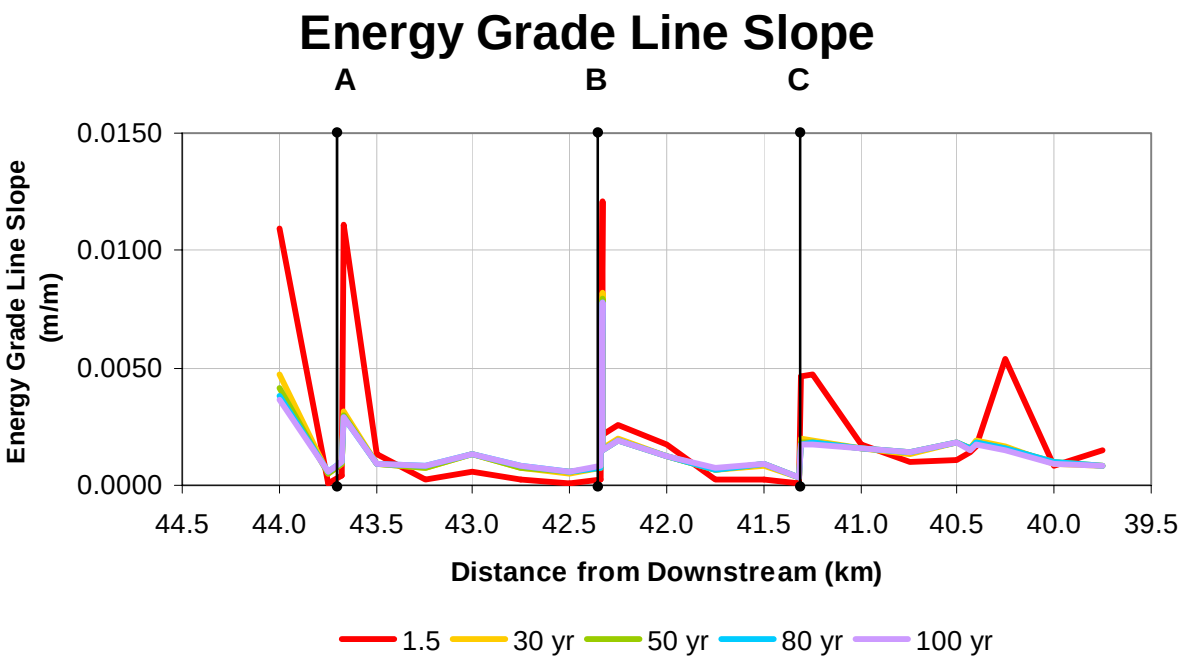

Figure C-11: Combined Energy Grade Line Slope due to Discharge

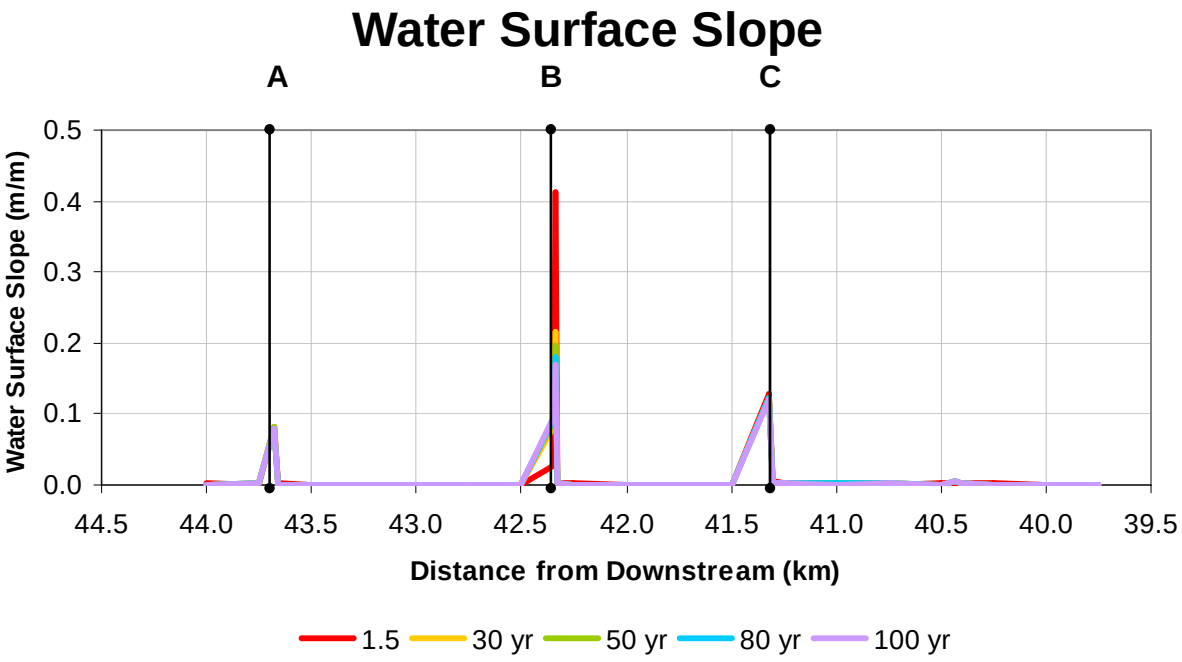

Figure C-12: Combined Water Surface Slope due to Discharge

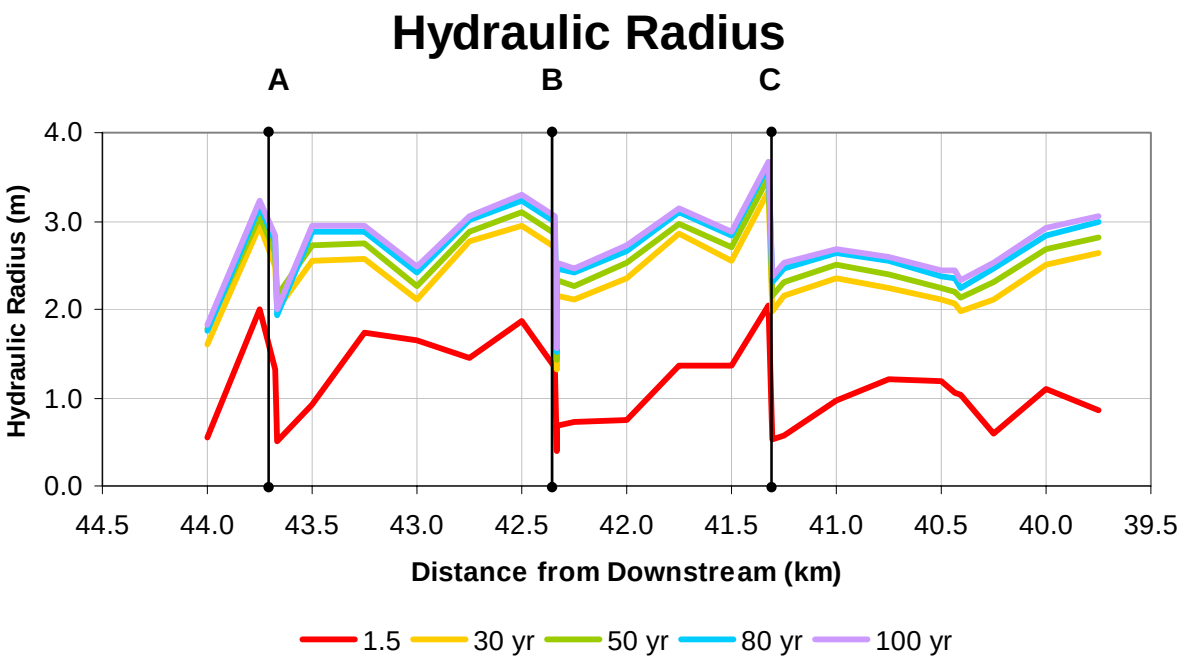

Figure C-13: Combined Hydraulic Radius due to Discharge

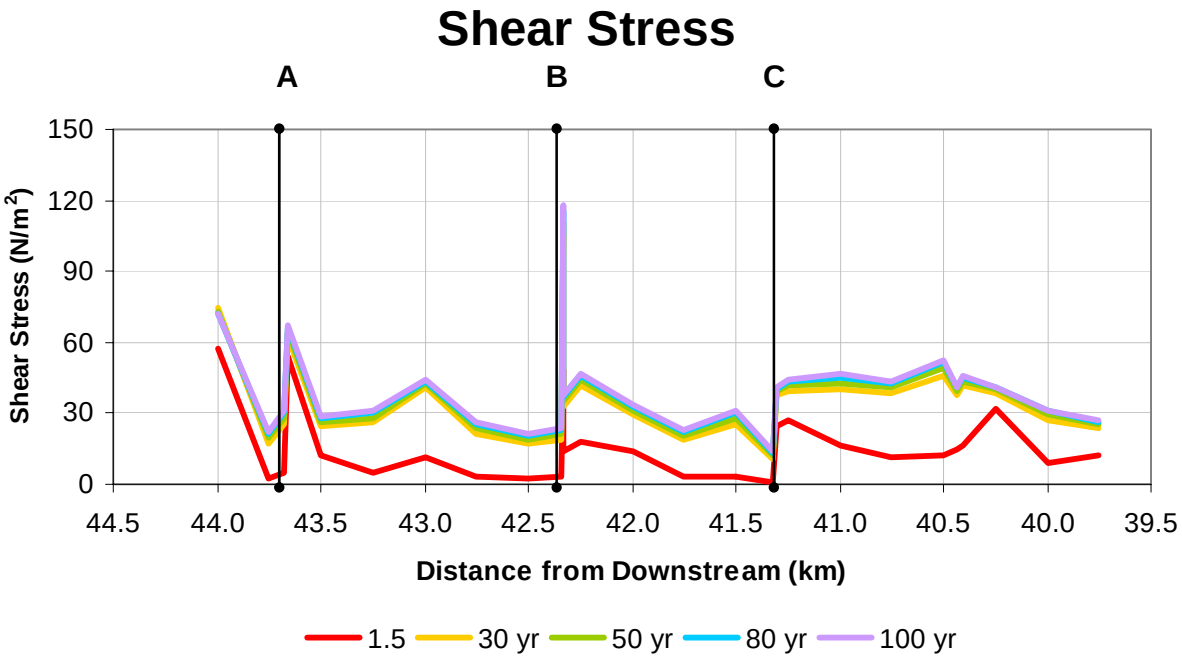

Figure C-14: Combined Shear Stress due to Discharge

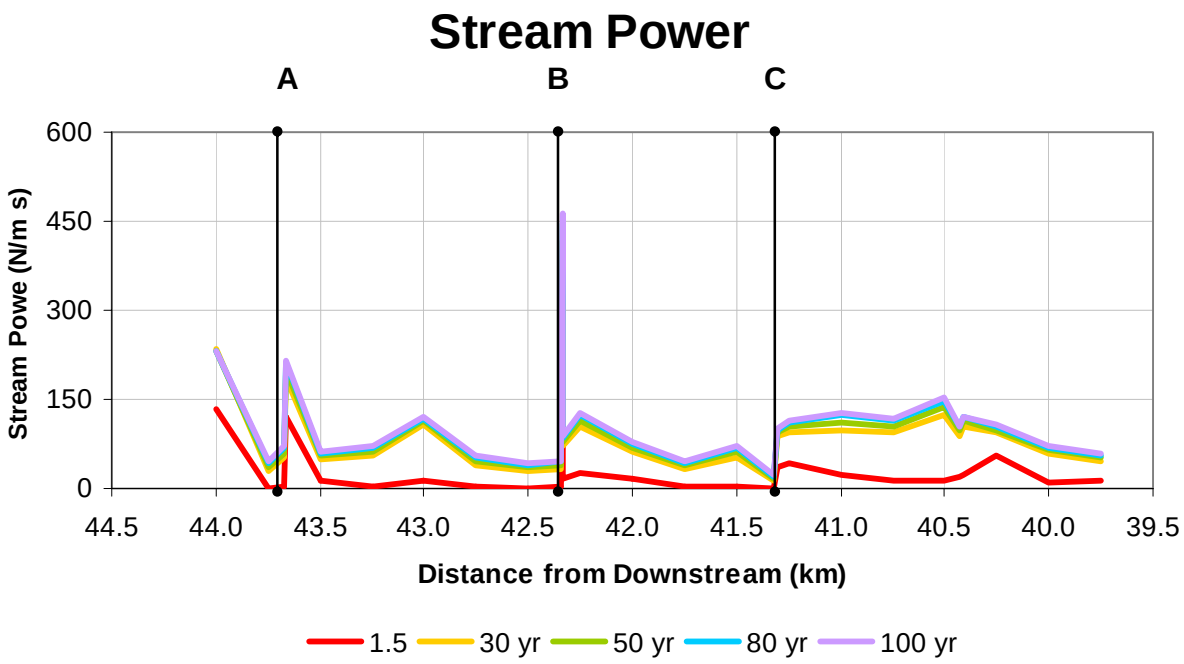

Figure C-15: Combined Stream Power due to Discharge

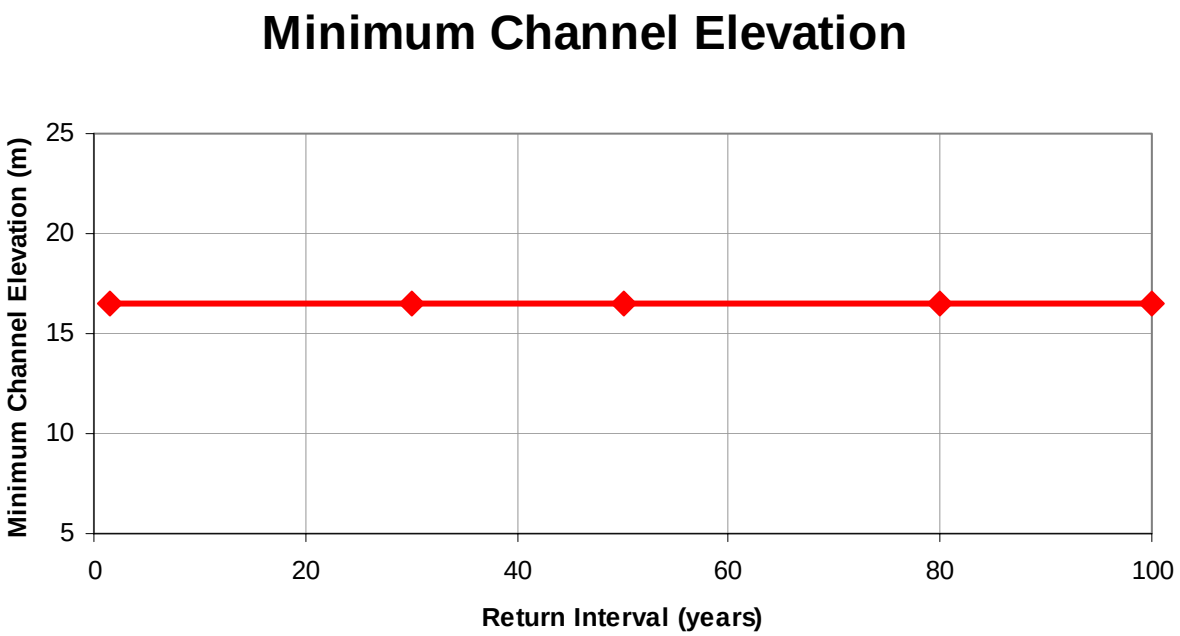

Figure C-16: Averaged Minimum Channel Elevation due to Return Interval

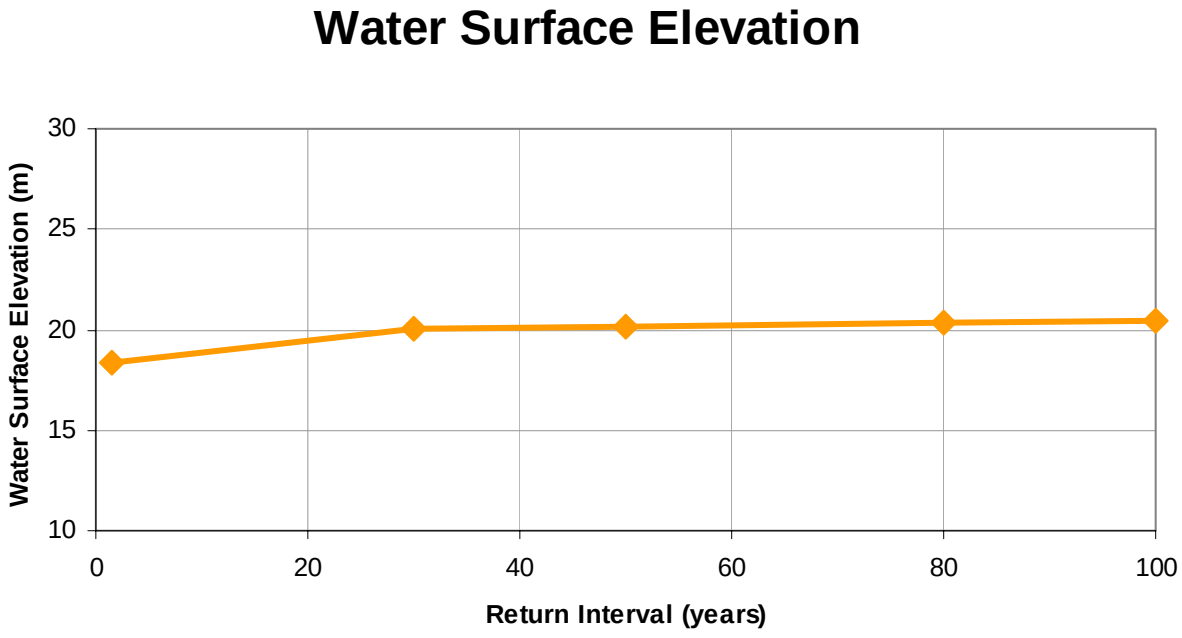

Figure C-17: Averaged Water Surface Elevation due to Return Interval

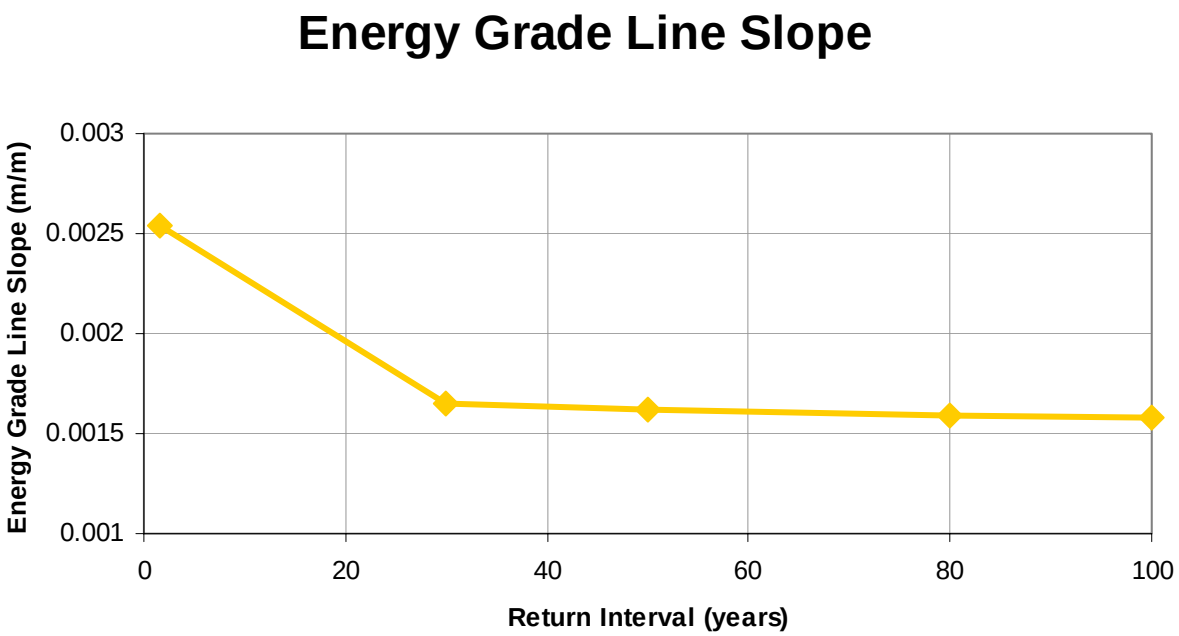

Figure C-18: Averaged Energy Grade Line Slope due to Return Interval

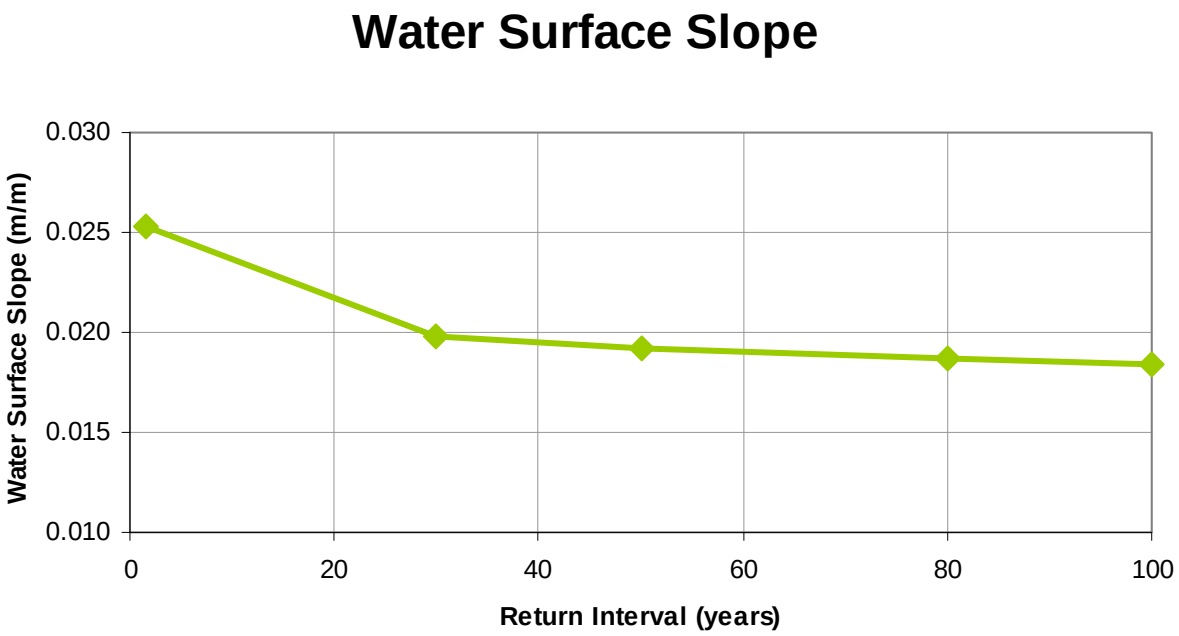

Figure C-19: Averaged Water Surface Slope due to Return Interval

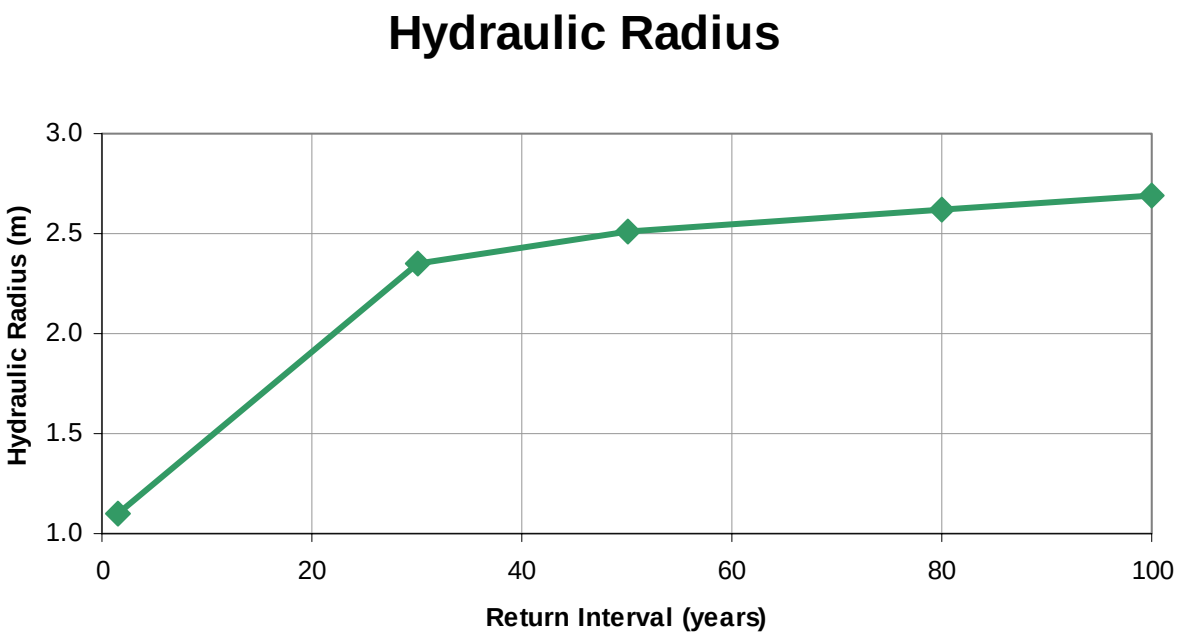

Figure C-20: Averaged Hydraulic Radius due to Return Interval

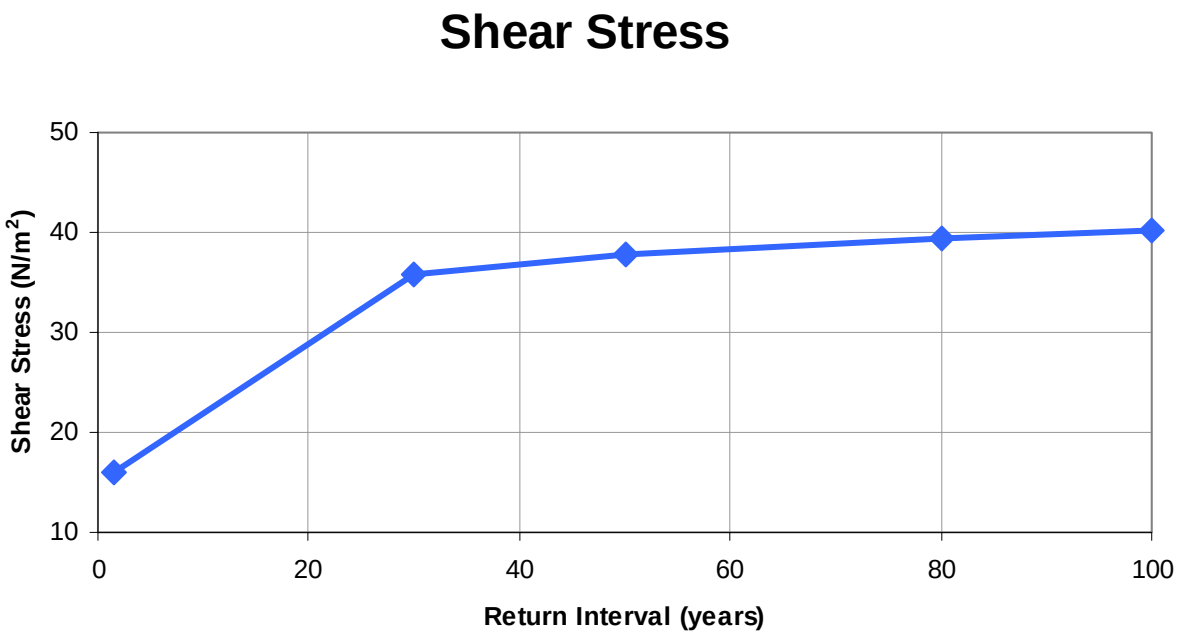

Figure C-21: Averaged Shear Stress due to Return Interval

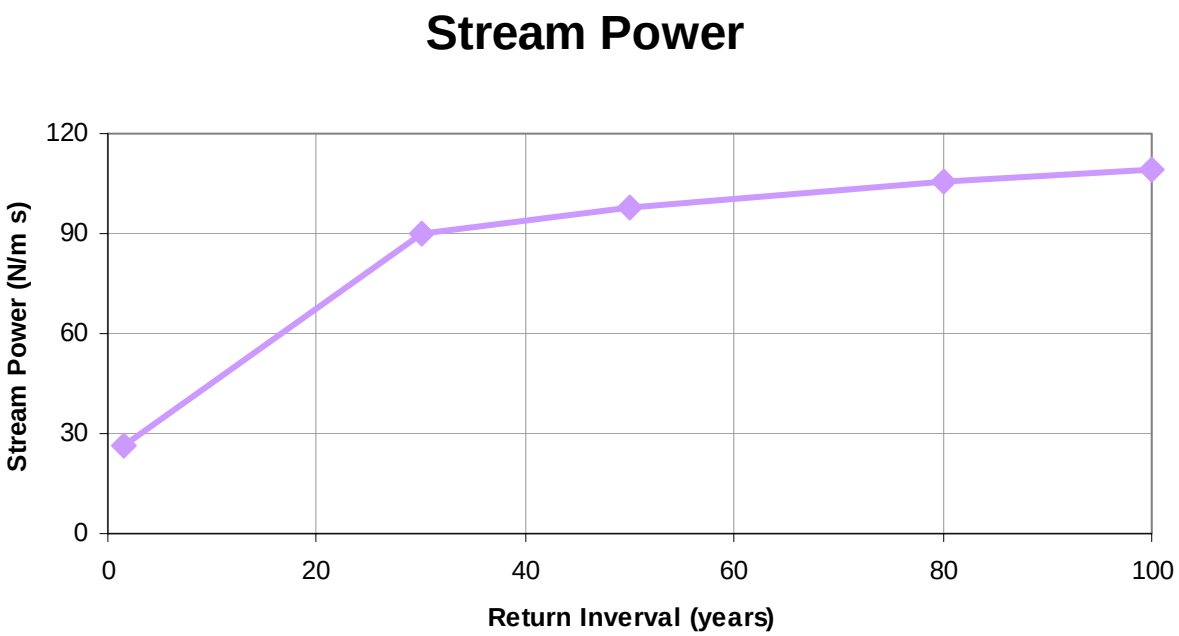

Figure C-22: Averaged Stream Power due to Return Interval

APPENDIX D - Channel Classification Input Data

Table D-1: Channel Classification Raw Data

Return Interval (yrs)	Q (cms)	Channel Slope (m/m)	Valley Slope (m/m)	d_{50} (mm)	Bankfull Width (m)	Flood Prone Width (m)	Depth (m)	Froude Number	E.G. Slope (m/m)	Entrenchment Ratio	Width/Depth Ratio Ratio	Sinuosity	d_{50} Type
1.5	255	0.00230	0.00237	36.36	239	309	1.11	0.42	0.00254	1.30	216	1.03	Very Coarse Gravel
30	1513	0.00230	0.00237	36.36	257	329	2.37	0.46	0.00165	1.28	108	1.03	Very Coarse Gravel
50	1695	0.00230	0.00237	36.36	258	333	2.53	0.47	0.00162	1.29	102	1.03	Very Coarse Gravel
80	1864	0.00230	0.00237	36.36	258	336	2.65	0.47	0.00159	1.30	98	1.03	Very Coarse Gravel
100	1943	0.00230	0.00237	36.36	258	338	2.71	0.47	0.00158	1.31	95	1.03	Very Coarse Gravel

APPENDIX E - HEC-RAS Sediment Transport Application Limits

Sediment transport capacity is analyzed by HEC-RAS 3.1.3. Transported sediment consists of bed load, suspended load and wash load according to Van Rijn(1993). Suspended load is maintained part in suspension in the flowing water. It moves with same velocity as that of the flowing water. Bed load is the sediment in almost continuous contact with the bed, carried forward by rolling, sliding, or hopping. And wash load is a portion of suspended load. However it is comprised of smaller particles than the bed material and it is not contained in transport capacity of the flow.

In HEC-RAS, the sedimentation transport capacity function has the capability of predicting transport capacity for non-cohesive sediment at one or more cross sections based on existing hydraulic parameters and know bed sediment properties [Hydraulic Reference, HEC-RAS 3.1.3]. Following sediment transport functions are available in HEC-RAS:

- Ackers-White
- Engelund-Hansen
- Laursen
- Meyer-Peter Müller
- Toffaleti
- Yang

To estimate sediment transport capacity by these functions, input data is required to HEC-RAS. Table E-1 shows ranges of input parameters required in HEC-RAS to develop each function. Their ranges are taken from SAM package user's manual and based on range stated by developer in their original paper. In the case of Engelund-Hansen function, the ranges are taken from the database (Guy et al, 1966) primarily used in that function's development.

Table E-1: Range of input values for sediment transport functions

Function	d	d_m	s	V	D	S	W	T
Ackers-White *(flume)*	0.04 - 7.0	NA	1.0 - 2.7	0.07 - 7.0	0.01 - 1.4	0.00006 - 0.037	0.23 - 0.4	46 - 89
Englund-Hansen *(flume)*	NA	0.19 - 0.93	NA	0.65 - 6.34	0.19 - 1.33	0.000055 - 0.019	NA	45 - 93
Laursen *(field)*	NA	0.08 - 0.7	NA	0.068 - 7.8	0.67 - 54	0.0000021 - 0.0018	63 - 3640	32 - 93
Laursen *(flume)*	NA	0.011 - 29	NA	0.7 - 9.4	0.03 - 3.6	000025 - 0.025	0.25 - 6.6	46 - 83
Meyer-Peter Müller *(flume)*	0.4 - 29	NA	1.25 – 4	1.2 - 9.4	0.03 - 3.9	0.0004 - 0.02	0.5 - 6.6	NA
Toffaleti *(field)*	0.062 - 4	0.095 - 0.76	NA	0.7 - 7.8	0.07 - 56.7 (R)	0.000002 - 0.0011	63 - 3640	36 - 93
Toffaleti *(flume)*	0.062 - 4	0.45 - 0.91	NA	0.7 - 6.3	0.07 - 1.1 (R)	0.00014 - 0.019	0.8 - 8	40 - 93
Yang *(field-sand)*	0.15 -1.7	NA	NA	0.8 - 6.4	0.04 - 50	0.000043 - 0.028	0.44 - 1750	32 - 94
Yang *(field-gravel)*	2.5 - 7	NA	NA	1.4 - 5.1	0.08 - 0.72	0.0014 - 0.029	0.44 - 1750	32 - 94

Where, d = Overall particle diameter [mm]

d_m = Median particle diameter [mm]

s = Sediment specific gravity

V = Average channel velocity [ft/sec]

D = Channel depth [ft]

S = Energy gradient

W = Channel width [ft]

T = Water temperature [°F]

(R) = Hydraulic Radius [ft]

NA = Data not available

Ackers-White

The Ackers-White transport function is a total load function based on two assumptions. One of these assumptions is that the fine sediment has best relation with turbulent fluctuations in the water column. Another is that the coarse sediment has best relation with mean velocity used as the representative variable. Based on these, the Ackers-White transport function was developed in terms of grain size, mobility and transport.

In Table E-1, the ranges of input values for Ackers-White transport function are shown. It was developed based on over 1000 flume experiments. An equation for Ackers-White function for a single grain is represented by

$$X = \frac{G_{gr}\ s\ d_s}{D\left(\frac{u_*}{V}\right)^n} \qquad \text{and} \qquad G_{gr} = C\left(\frac{F_{gr}}{A} - 1\right)$$

Where: X = Sediment concentration, in parts per part

G_{gr} = Sediment transport parameter

s = Specific gravity of sediments

d_s = Mean particle diameter

D = Effective depth

u_* = Shear velocity

V = Average channel velocity

n = Transition exponent, depending on sediment size

C = Coefficient

F_{gr} = Sediment mobility parameter

A = Critical sediment mobility parameter

Engelund-Hansen

The Engelund-Hansen function is used as a total load predictor which gives adequate results for sand rivers with substantial suspended load. This was developed based on flume data with given sediment size in Table E-1, 0.19 to 0.93mm. General equation for Engelund-Hansen function is represented by

$$g_s = 0.05\gamma_s V^2 \sqrt{\frac{d_{50}}{g\left(\frac{\gamma_s}{\gamma}-1\right)}}\left[\frac{\tau_0}{(\gamma_s-\gamma)d_{50}}\right]^{3/2}$$

Where: g_s = Unit sediment transport

γ = Unit weight of water

γ_s = Unit weight of solid particles

V = Average channel velocity

τ_0 = Bed level shear stress

d_{50} = Particle size of which 50% is smaller

Laursen

The Laursen function is a total sediment load predictor. It is derived from a combination of qualitative analysis, original experiments, and supplementary data. Transport of sediments is primarily defined based on the hydraulic characteristics of mean channel velocity, depth of flow, energy gradient, and on the sediment characteristics of gradation and fall velocity. Contributions by Copeland (Copeland, 1989) extend the range of applicability to gravel-sized sediments. The range of applicability is 0.011 to 29mm, median particle size as shown Table E-1.

The general transport equation for the Laursen function extended by Copeland for a single grain size is represented by

$$C_m = 0.01\gamma\left(\frac{d_s}{D}\right)^{7/6}\left(\frac{\tau_0}{\tau_c}-1\right)f\left(\frac{u_*}{\omega}\right)$$

Where: C_m = Sediment discharge concentration, in weight/volume

G = Unit weight of water

d_s = Mean particle diameter

D = Effective depth of flow

τ_0 = Bed shear stress due to grain resistance

τ_c = Critical bed shear stress

$f\left(\frac{u_*}{\omega}\right)$ = Function of the ratio of shear velocity to fall velocity as defined in Laursen's Figure 14 (Laursen, 1958)

Meyer-Peter Müller

The Meyer-Peter Müller (MPM) is bed load transport function based primarily on experimental data. MPM has been extensively tested and used for rivers with relatively coarse sediment. The transport rate is proportional to the difference between the mean shear stress acting on the grain and the critical shear stress. Applicable particle size is between 0.4 and 2.9mm as mention above Table E-1. The Darcy-Weisbach friction factor is used to define bed resistance.

The general transport equation for the Meyer-Peter Müller (MPM) function is represented by

$$\left(\frac{k_r}{k_r^{'}}\right)^{3/2} \gamma R S = 0.047\left(\gamma_s - \gamma\right) d_m + 0.25\left(\frac{\gamma}{g}\right)^{1/3}\left(\frac{\gamma_s - \gamma}{\gamma_s}\right)^{2/3} g_s^{2/3}$$

Where: g_s = Unit sediment transport rate in weight/time/unit width

k_r = A roughness coefficient

$k_r^{'}$ = A roughness coefficient based on grains

γ = Unit weight of water

γ_s = Unit weight of the sediment

g = Acceleration of gravity

d_m = Median particle diameter

R = Hydraulic radius

S = Energy gradient

Toffaleti

The Toffaleti function is a modified-Einstein total load method. This method divided the suspended load distribution into vertical zones, replicating two-dimensional sediment movement. In the sediment distribution, there are four zones, the upper zone, the middle zone, the lower zone and the bed zone. First, the sediment transport is calculated independently and then they are summed as total sediment transport.

This method was developed using an exhaustive collection of both flume and field data. The flume experiments used sediment particles with mean diameter raging from 0.3 to 0.93 mm. However successful application of the Toffaleti method suggests that mean particle diameter as low as 0.095mm is acceptable.

The general transport equations for the Toffaleti function for a single grain size is represented by

$$g_{ssL} = M \frac{\left(\frac{R}{11.24}\right)^{1+n_v-0.756z} - (2\,d_m)^{1+n_v-0.756z}}{1+n_v-0.756z} \quad \text{(lower zone)}$$

$$g_{ssM} = M \frac{\left(\frac{R}{11.24}\right)^{0.244z}\left[\left(\frac{R}{2.5}\right)^{1+n_v-z} - \left(\frac{R}{11.24}\right)^{1+n_v-z}\right]}{1+n_v-z} \quad \text{(middle zone)}$$

$$g_{ssU} = M \frac{\left(\frac{R}{11.24}\right)^{0.244z}\left(\frac{R}{2.5}\right)^{0.5z}\left[R^{1+n_v-1.5z} - \left(\frac{R}{2.5}\right)^{1+n_v-1.5z}\right]}{1+n_v-1.5z} \quad \text{(upper zone)}$$

$$g_{sb} = M\left(2\,d_m\right)^{1+n_v-0.756z} \text{ (Bed zone)}$$

$$M = 43.2\,C_L\left(1+n_v\right)V\,R^{0.756-n_v}$$

$$g_s = g_{ssL} + g_{ssM} + g_{ssU} + g_{sb}$$

Where: g_{ssL} = Suspended sediment transport in the lower zone, in tons/day/ft

g_{ssM} = Suspended sediment transport in the middle zone, in tons/day/ft

g_{ssU} = Suspended sediment transport in the upper zone, in tons/day/ft

g_{sb} = Bed load sediment transport in tons/day/ft

g_s = Total sediment transport in tons/day/ft

M = Sediment concentration parameter

C_L = Sediment concentration in the lower zone

R = Hydraulic radius

d_m = Median particle diameter

z = Exponent describing the relationship between the sediment and hydraulic characteristics

n_v = Temperature exponent

Yang

Yang's method (1973) is developed under an assumption that unit stream power is the dominant factor in the determination of total sediment concentration. The research is based on data obtained in flume experiments and field data under a wide range conditions found in alluvial channels. Conditions for development and experiments are mentioned in Table E-1.

In 1984, Yang expended the applicability to include gravel sized sediments. The general transport equations for sand and gravel using Yang function for a single grain size is represented by

$$\log C_t = 5.435 - 0.286 \log \frac{\omega d_m}{\nu} - 0.457 \log \frac{u_*}{\omega} + \left(1.799 - 0.409 \log \frac{\omega d_m}{\nu} - 0.314 \log \frac{u_*}{\omega}\right) \log\left(\frac{VS}{\omega} - \frac{V_{cr} S}{\omega}\right)$$

for sand $d_m < 2$ mm

$$\log C_t = 6.681 - 0.633 \log \frac{\omega d_m}{\nu} - 4.816 \log \frac{u_*}{\omega} + \left(2.784 - 0.305 \log \frac{\omega d_m}{\nu} - 0.282 \log \frac{u_*}{\omega}\right) \log\left(\frac{VS}{\omega} - \frac{V_{cr} S}{\omega}\right)$$

for gravel $d_m \geq 2$ mm

Where: C_t = Total sediment concentration

ω = Particle fall velocity

d_m = Median particle diameter

ν = Kinematic viscosity

u_* = Shear velocity

V = Average channel velocity

S = Energy gradient

APPENDIX F - Sediment Transport Capacity Plots

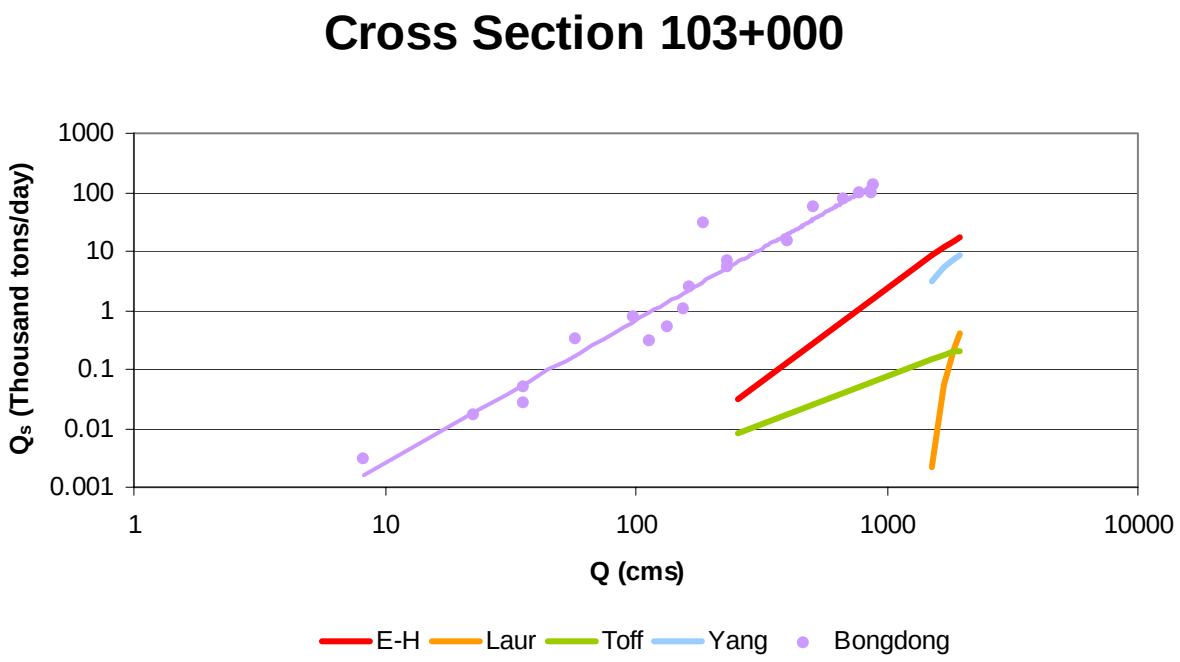

Figure F-1: Sediment Transport Capacity at Cross section 103+000

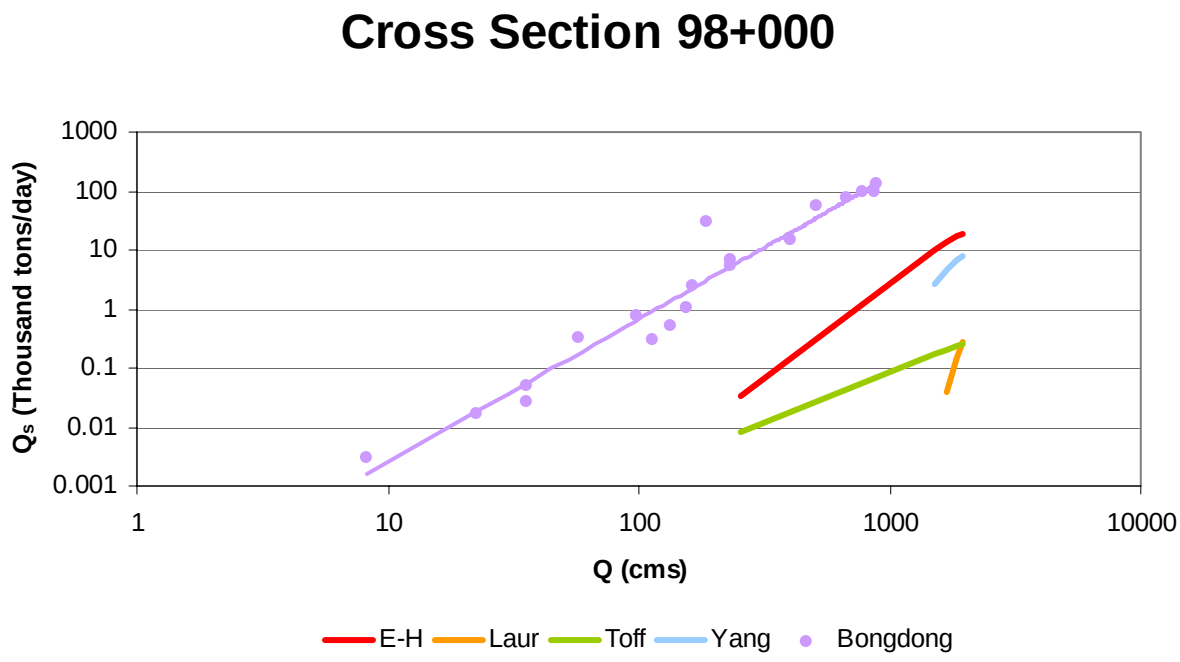

Figure F-2: Sediment Transport Capacity at Cross section 98+800

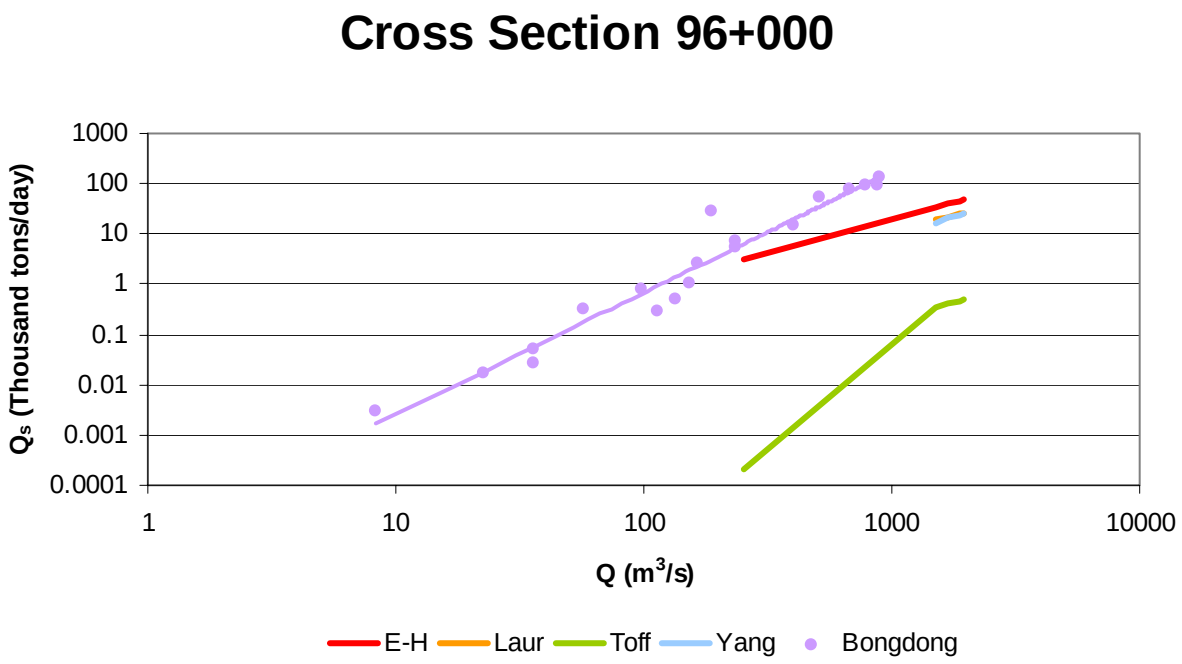

Figure F-3: Sediment Transport Capacity at Cross section 96+000

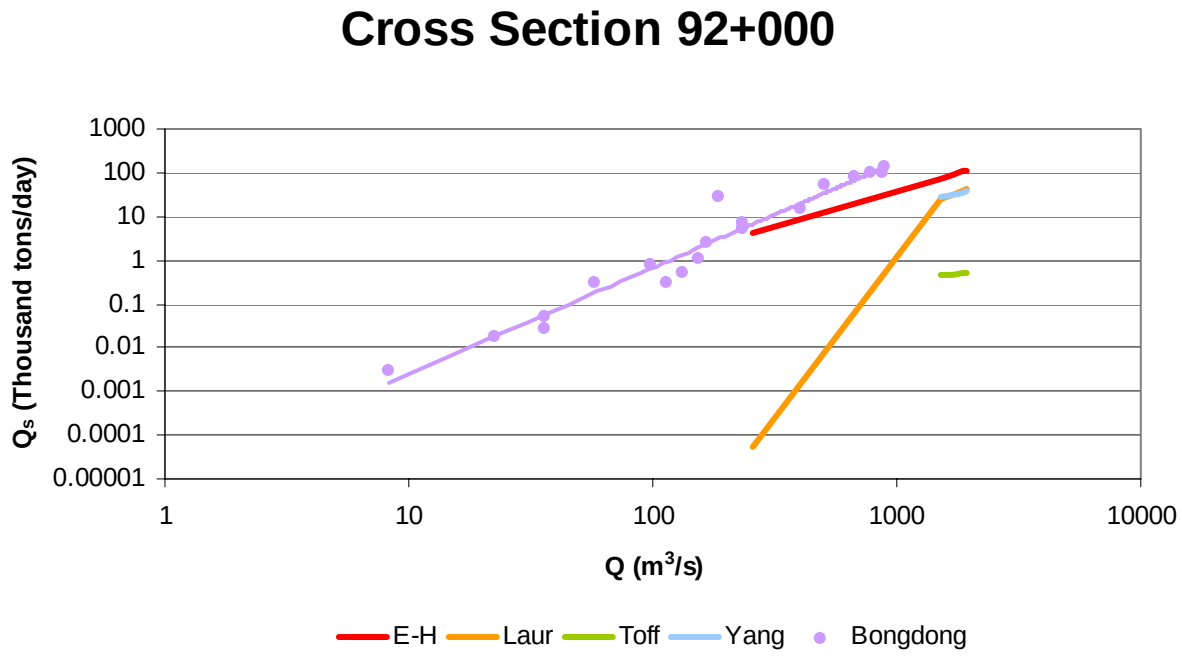

Figure F-4: Sediment Transport Capacity at Cross section 92+000

APPENDIX G - Stable Channel Design Plots

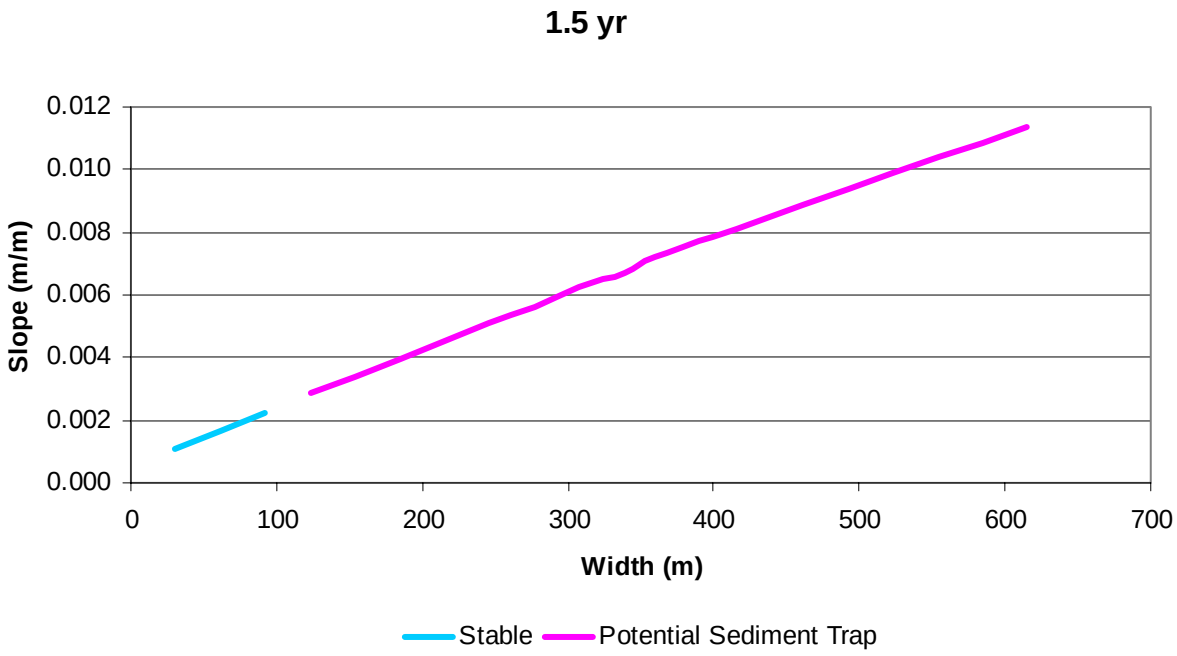

Figure G-1: Stable Channel Slope and Width (1.5 yr)

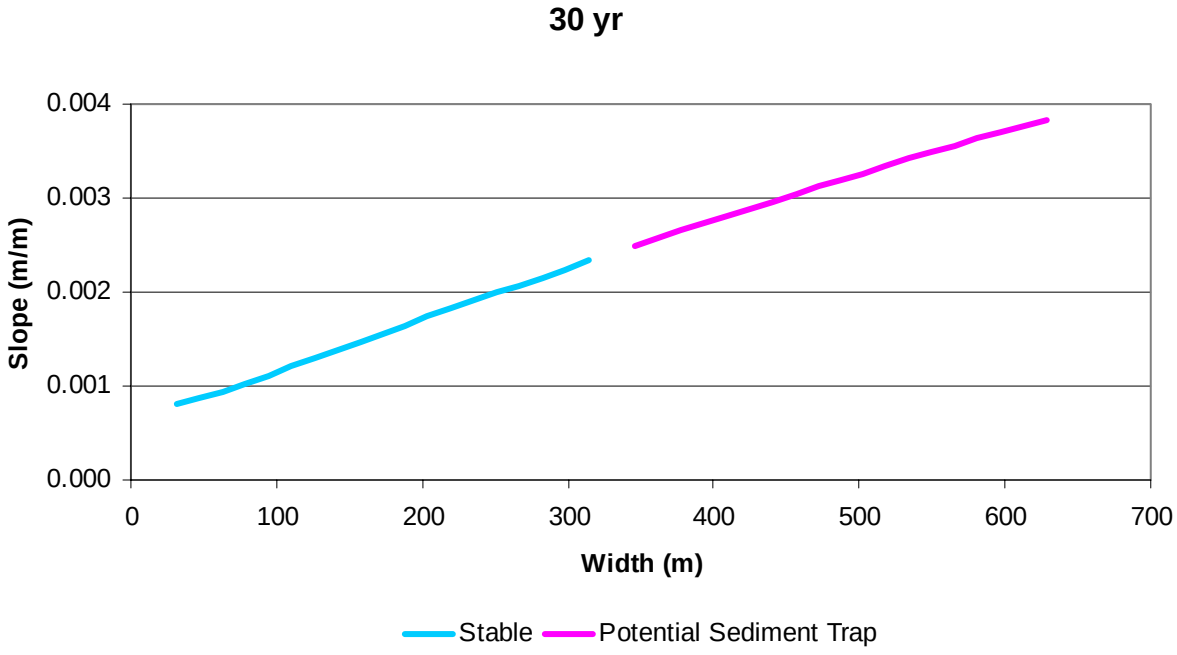

Figure G-2: 2 Stable Channel Slope and Width (30 yr)

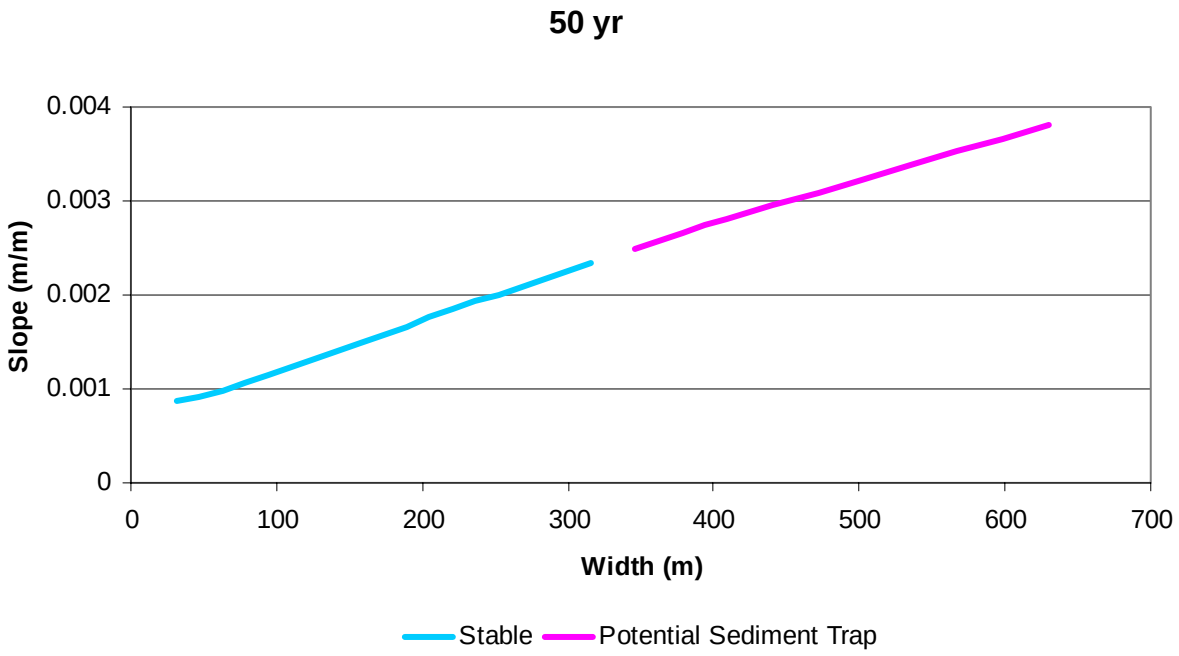

Figure G-3: Stable Channel Slope and Width (50 yr)

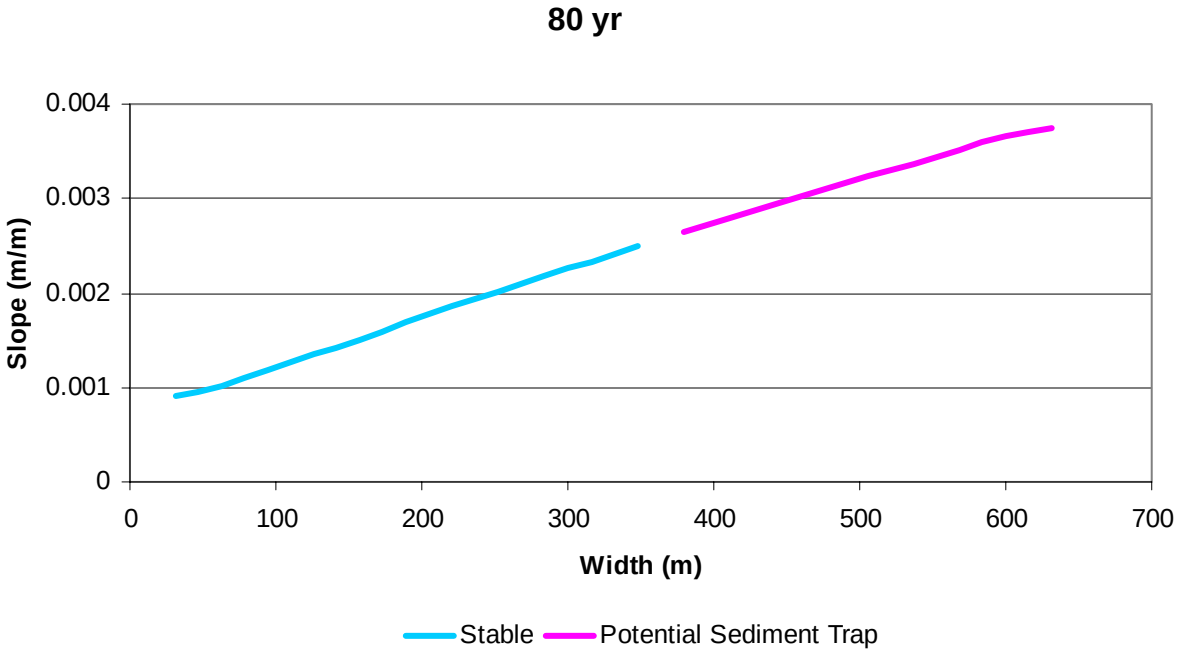

Figure G-4: Stable Channel Slope and Width (80 yr)

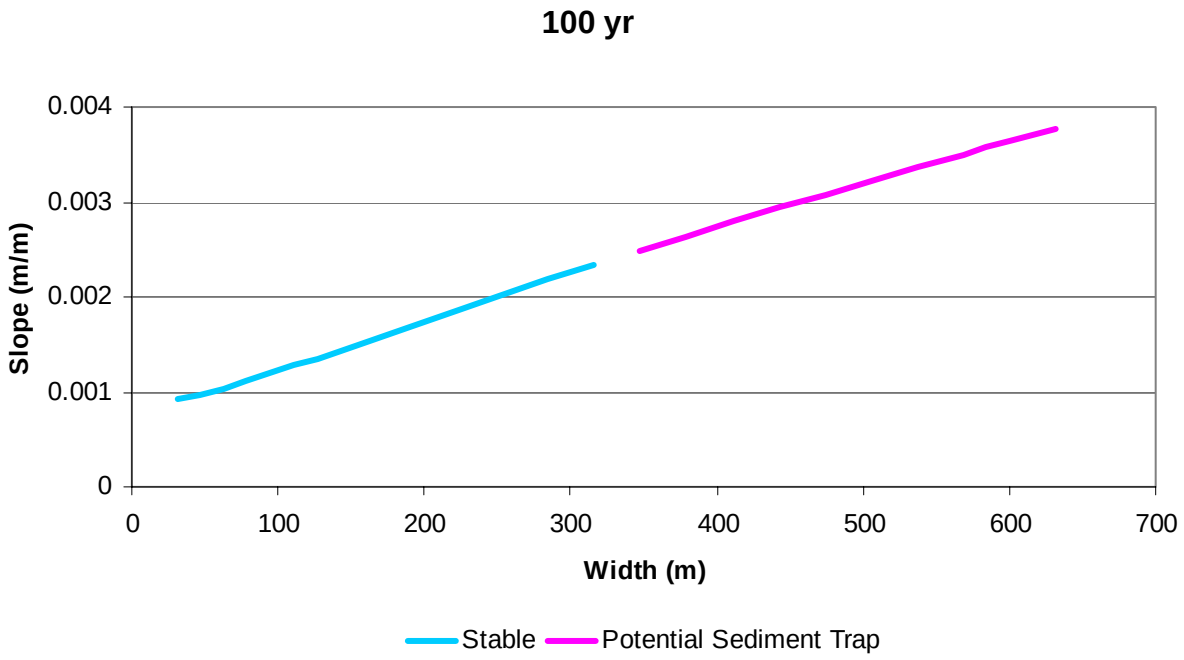

Figure G-5: Stable Channel Slope and Width (100 yr)

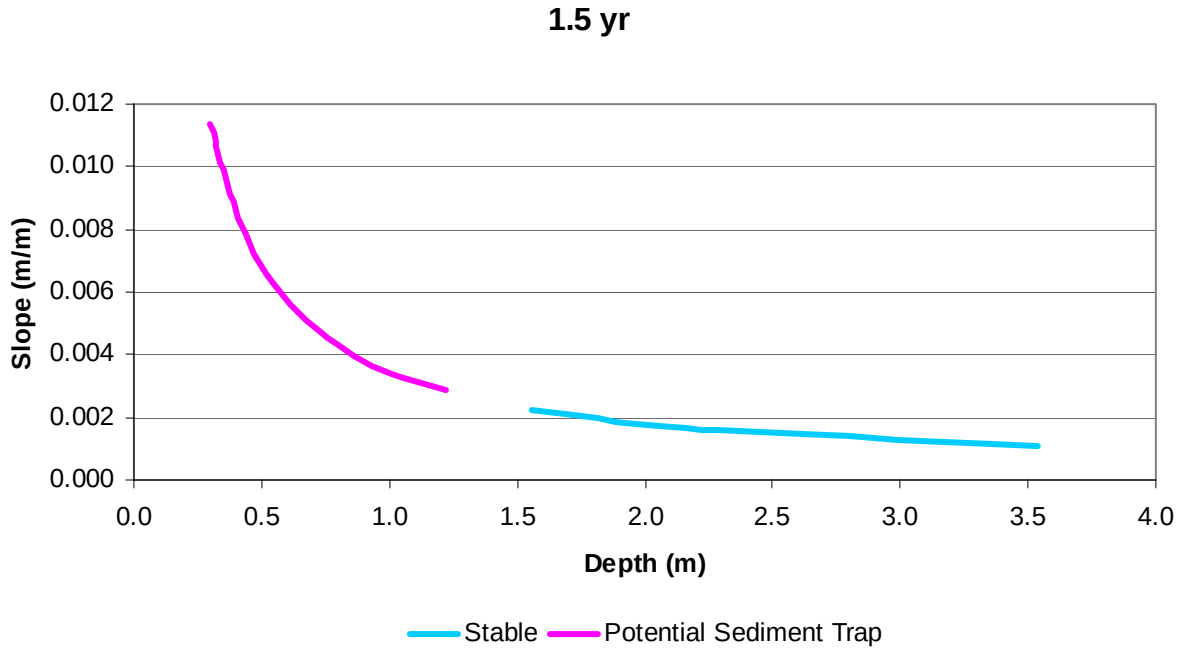

Figure G-6: Stable Channel Slope and Depth (1.5 yr)

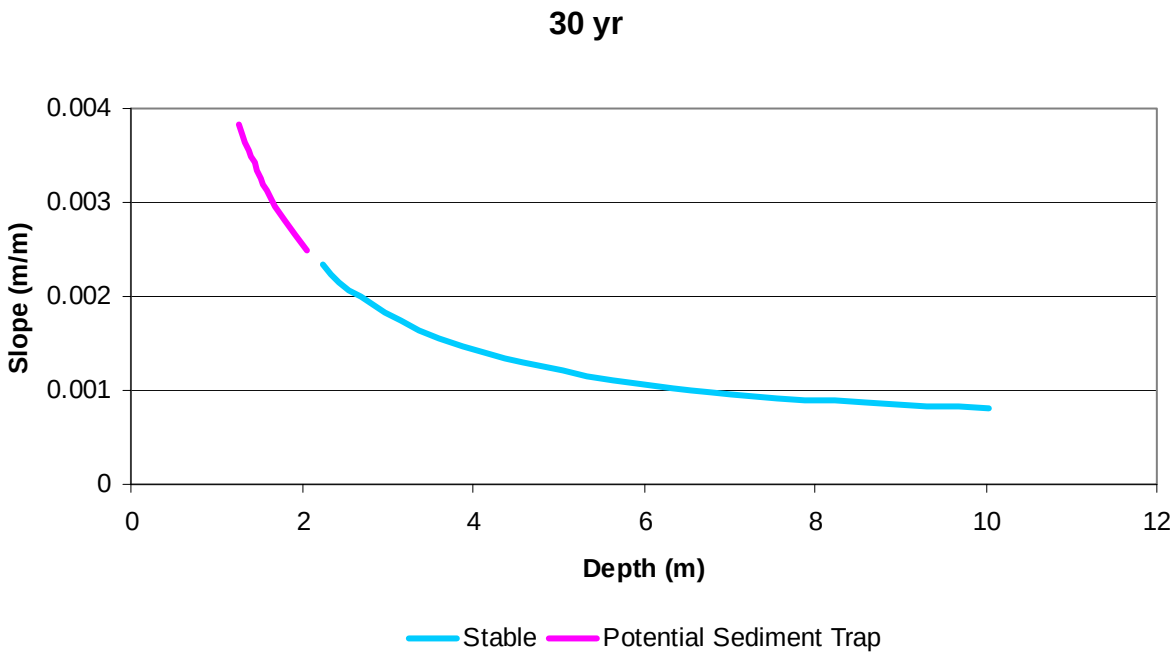

Figure G-7: Stable Channel Slope and Depth (30 yr)

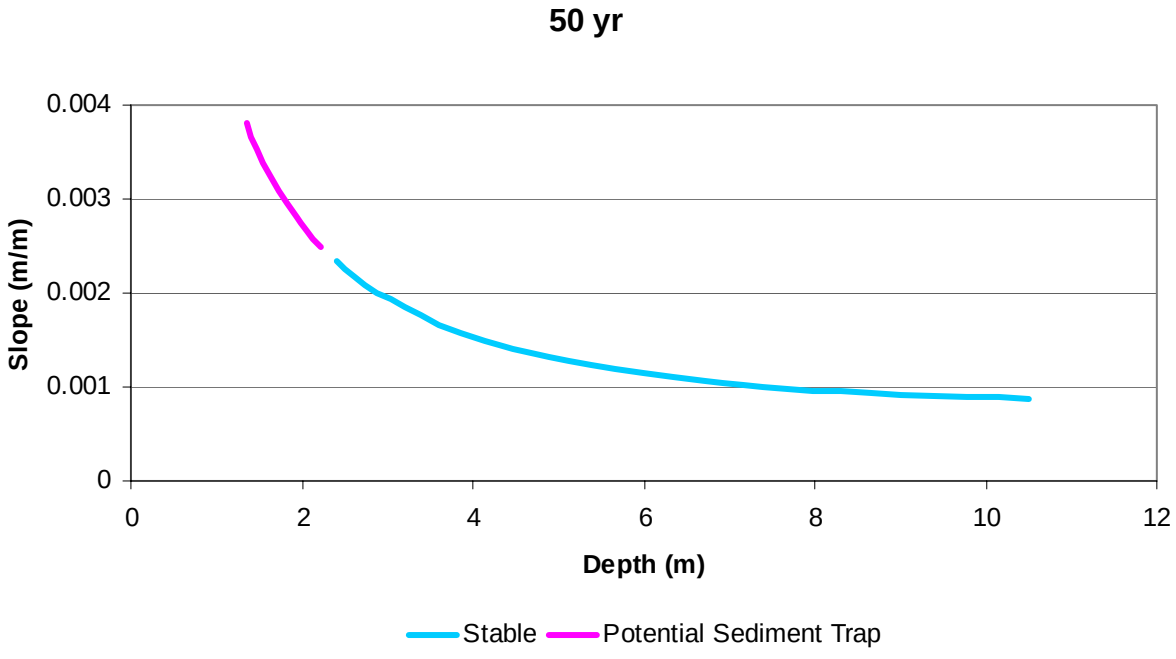

Figure G-8: Stable Channel Slope and Depth (50 yr)

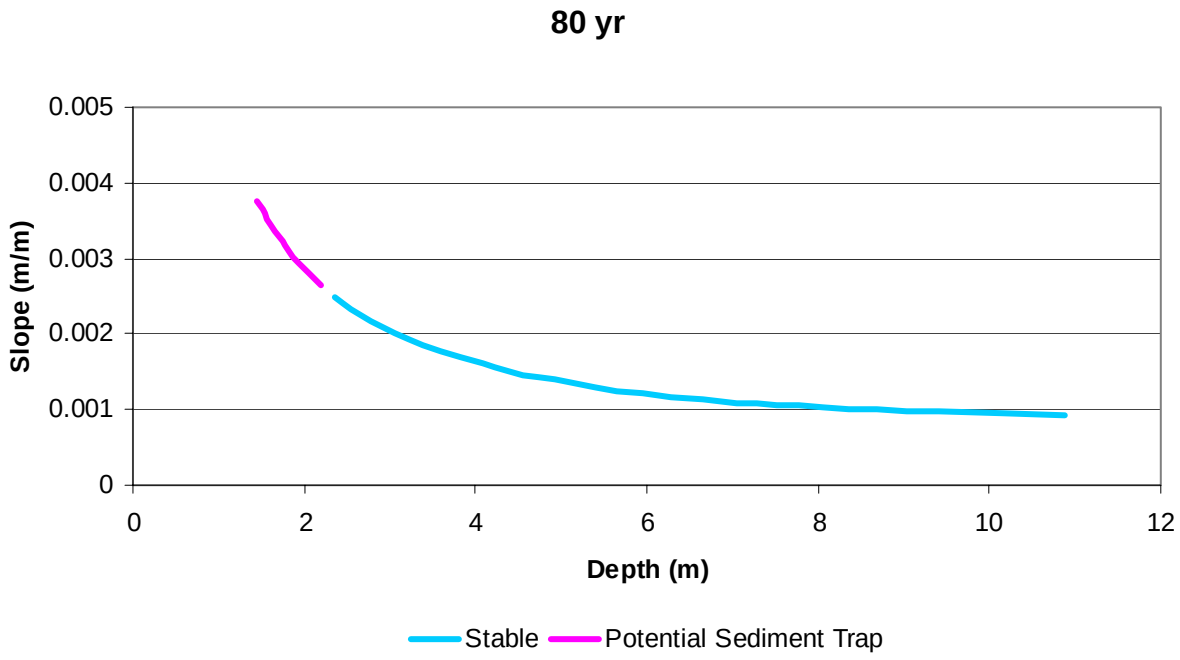

Figure G-9: Stable Channel Slope and Depth (80 yr)

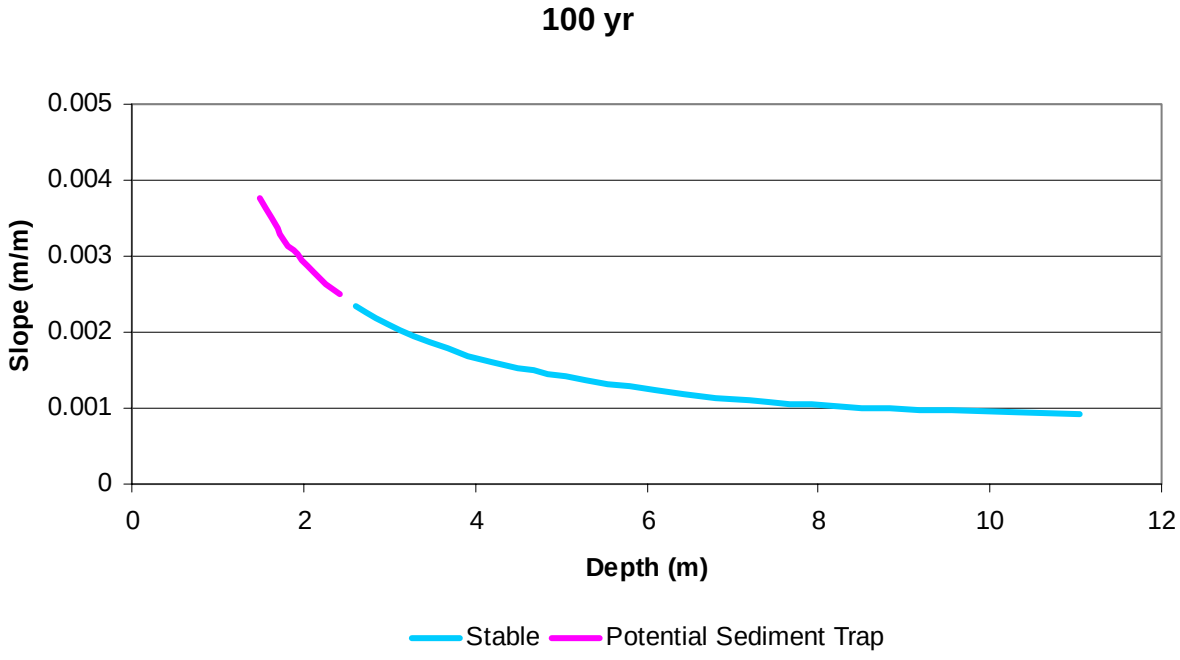

Figure G-10: Stable Channel Slope and Depth (100 yr)

APPENDIX H - Cross Sections

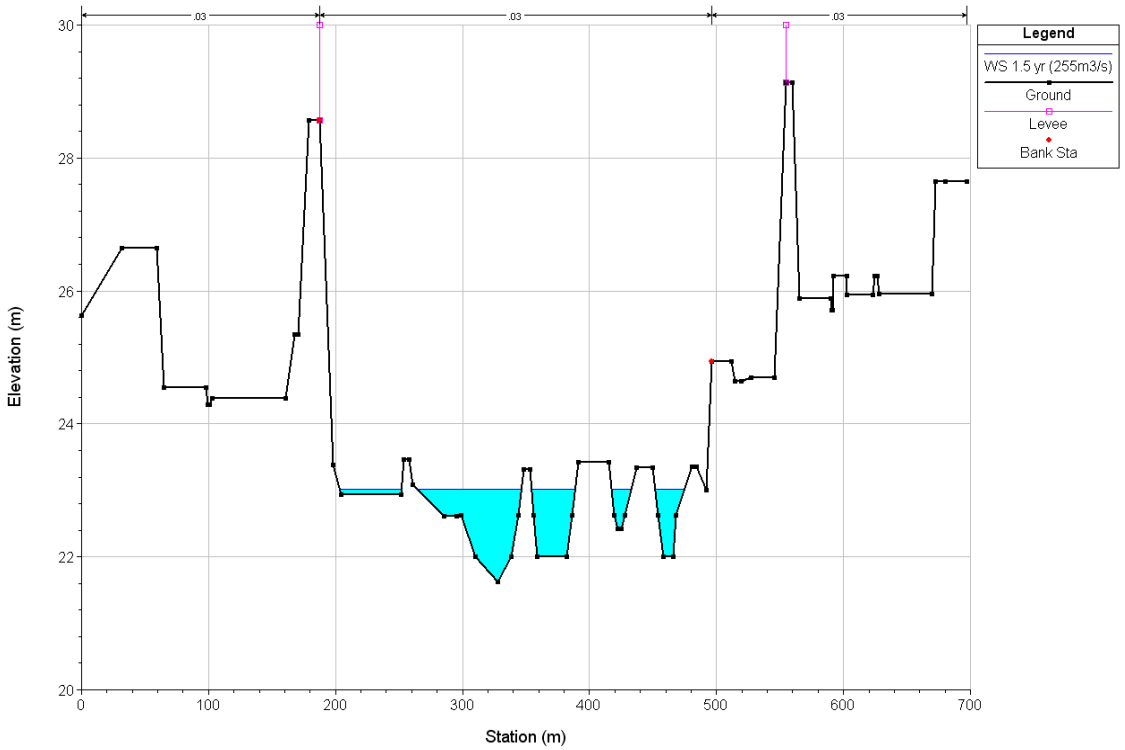

Figure H-1: Cross Section No. 104+000

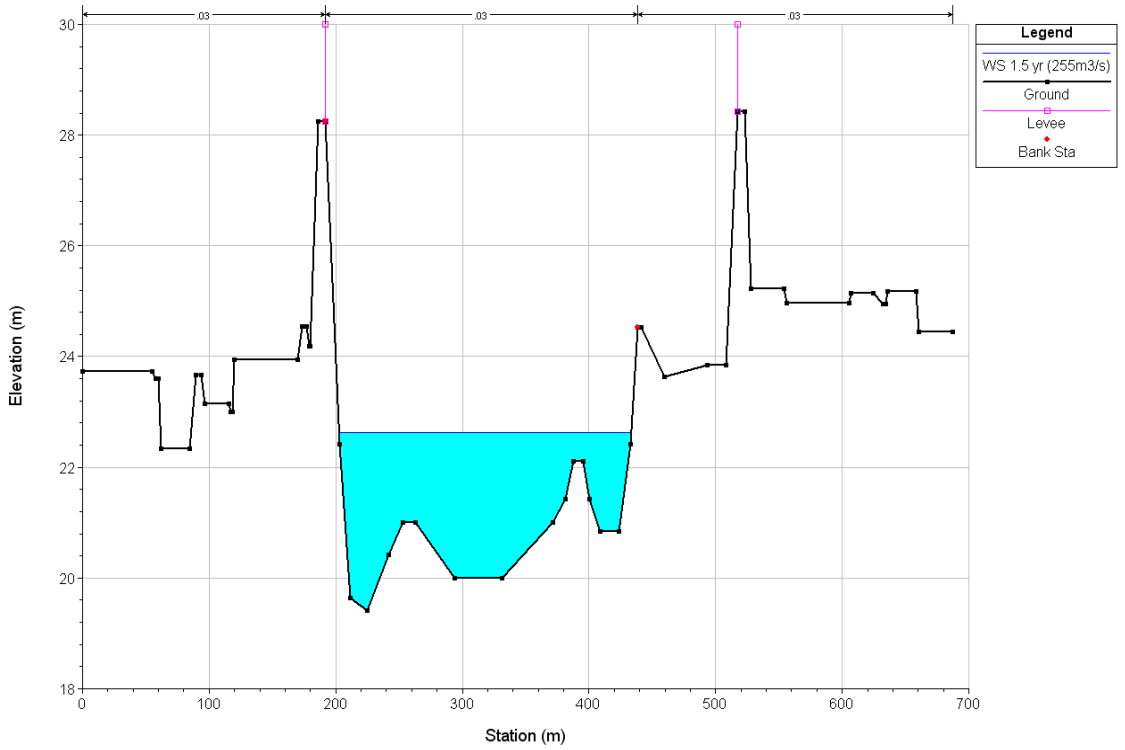

Figure H-2: Cross Section No. 103+000

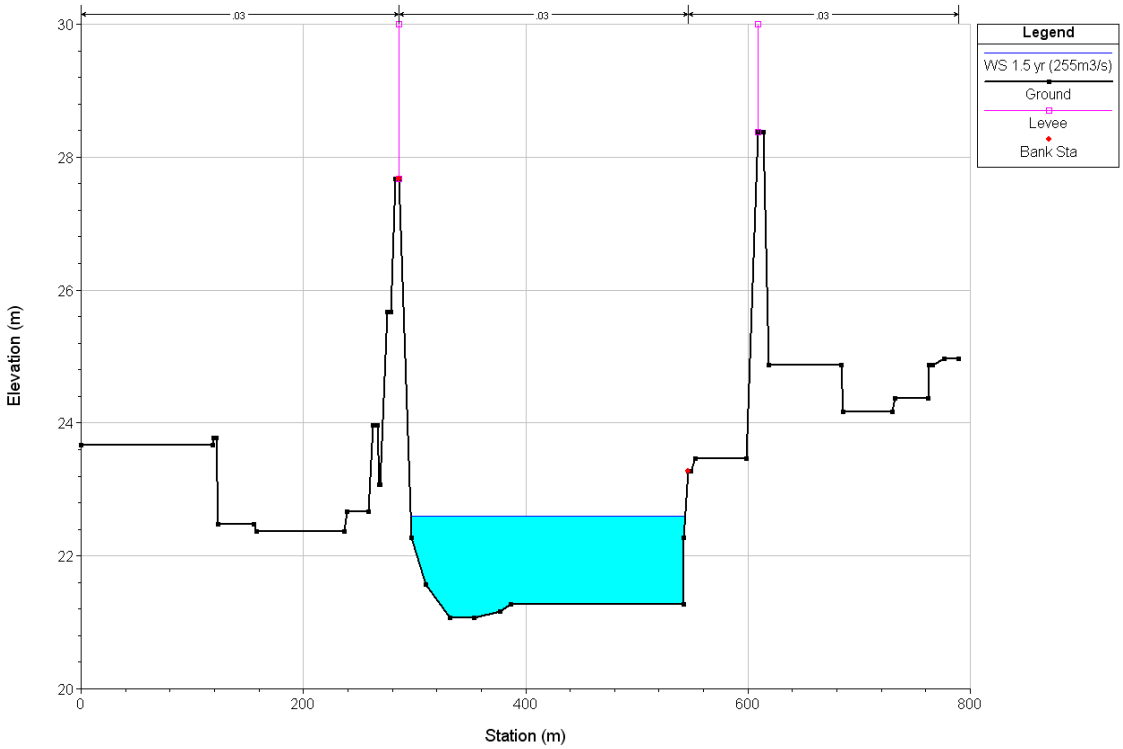

Figure H-3: Cross Section No. 100+176

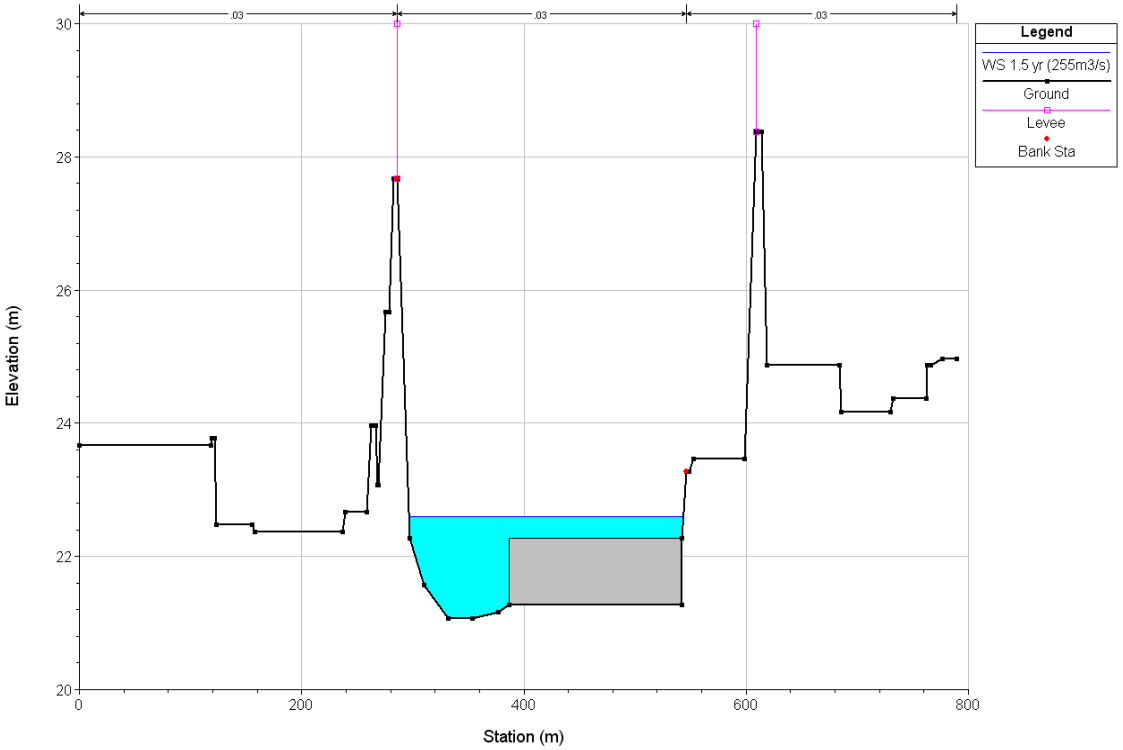

Figure H-4: Cross Section No. 102+175 IS

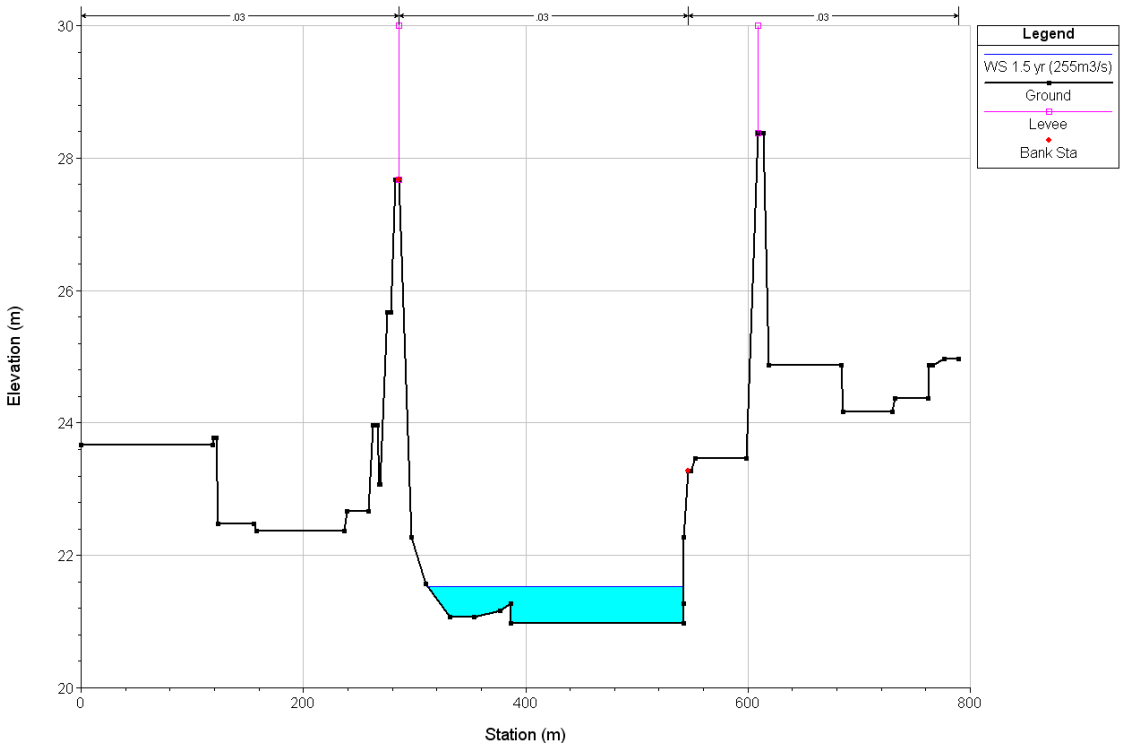

Figure H-5: Cross Section No. 102+163

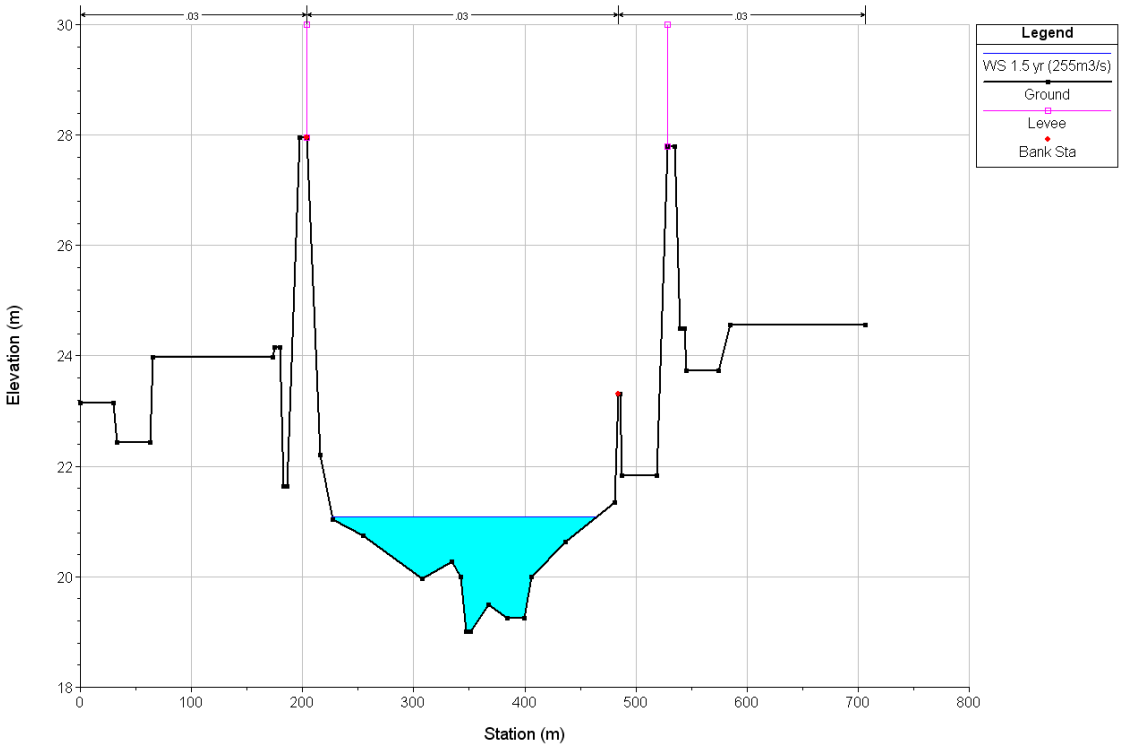

Figure H-6: Cross Section No. 102+000

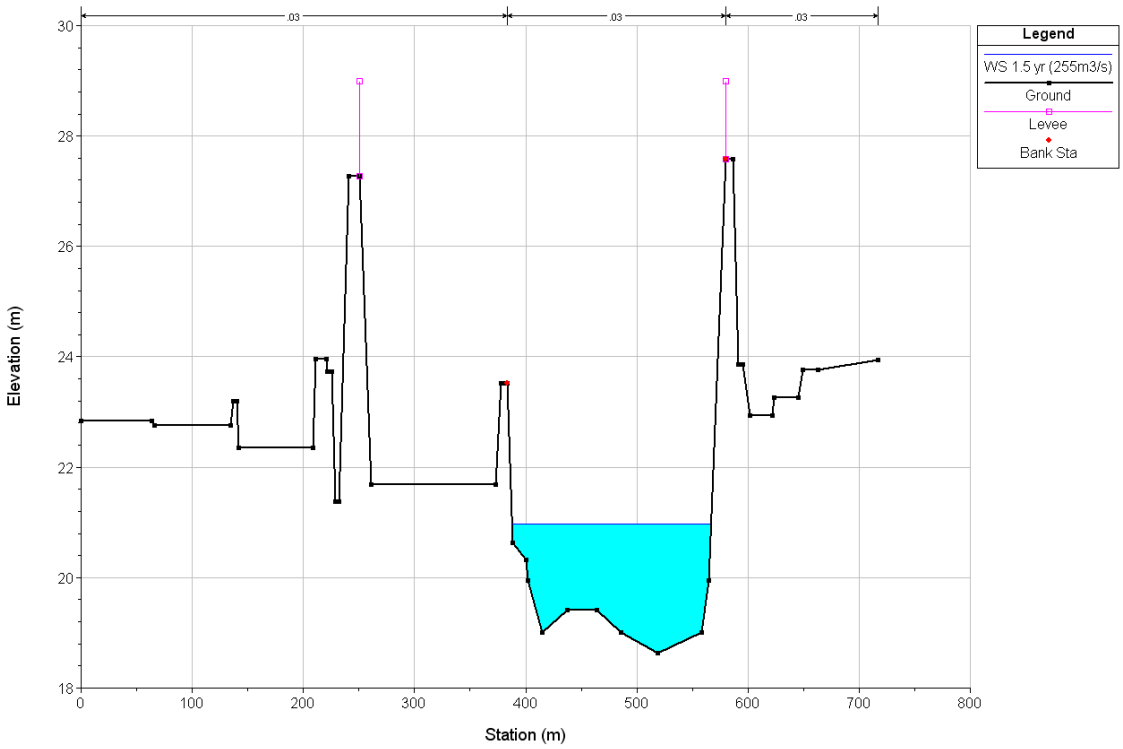

Figure H-7: Cross Section No. 101+000

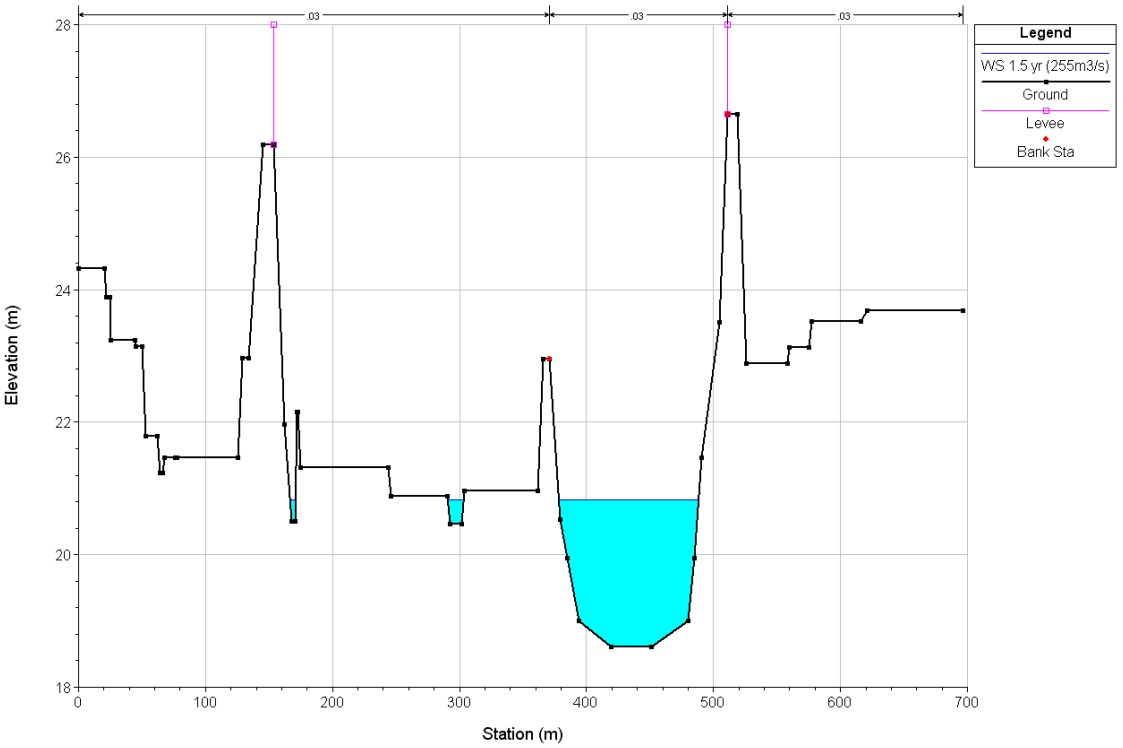

Figure H-8: Cross Section No. 100+000

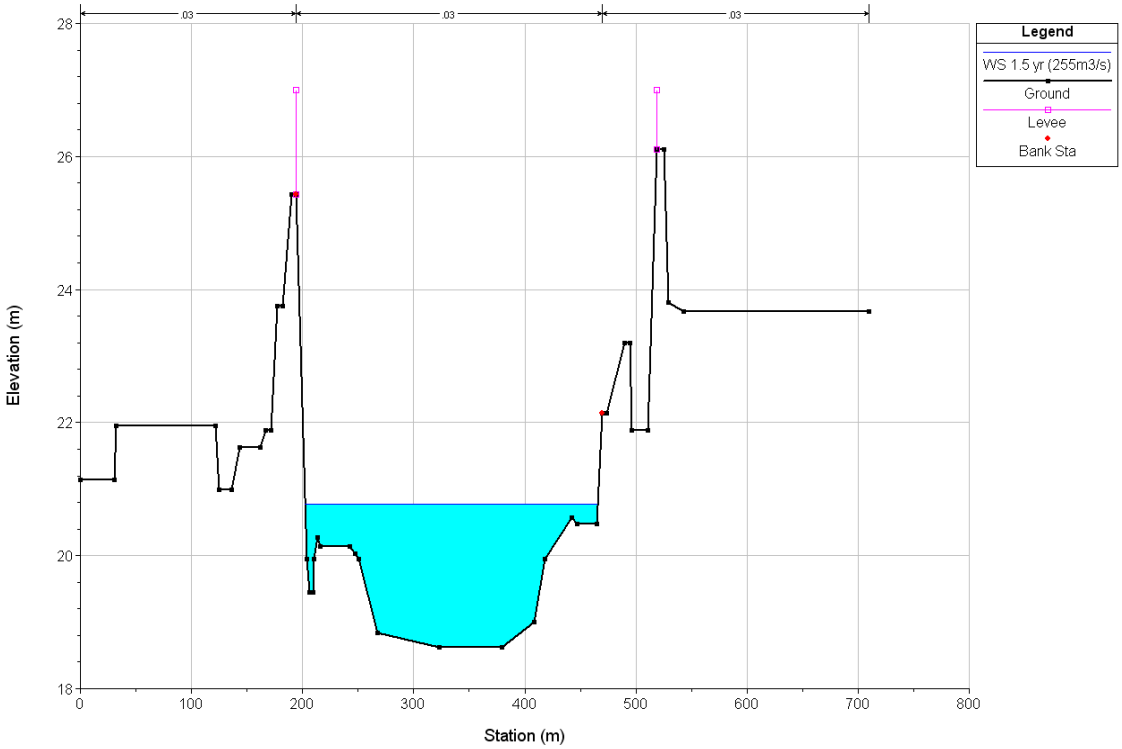

Figure H-9: Cross Section No. 99+000

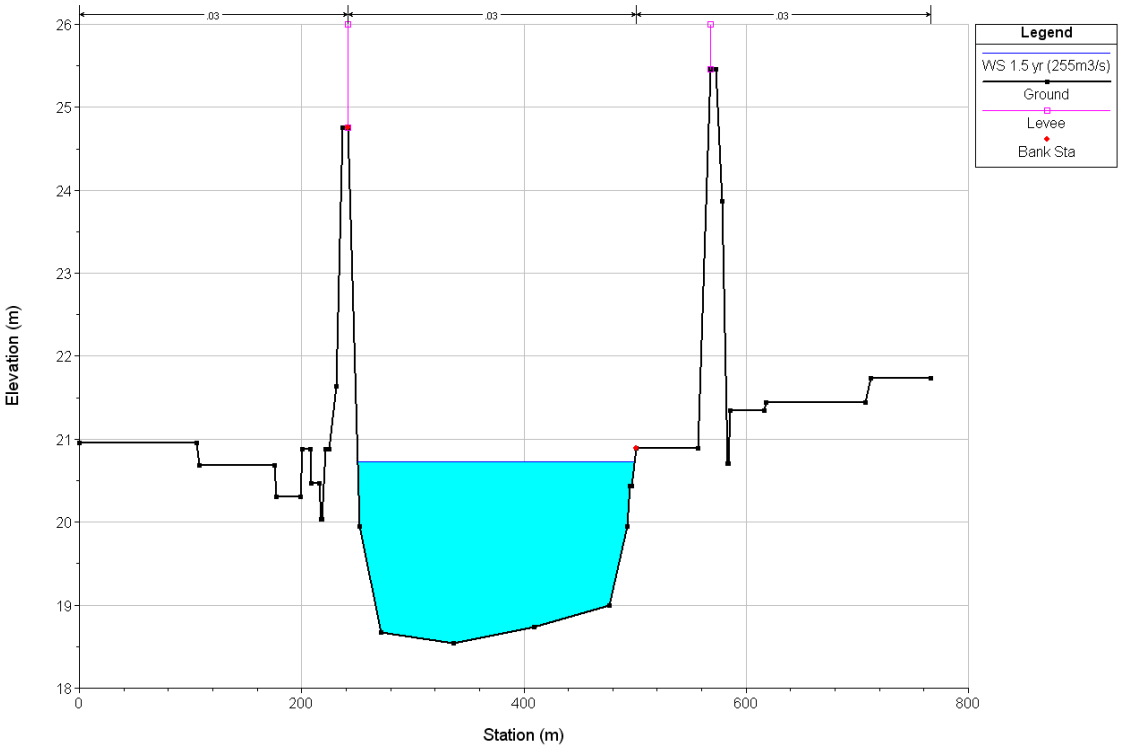

Figure H-10: Cross Section No. 98+000

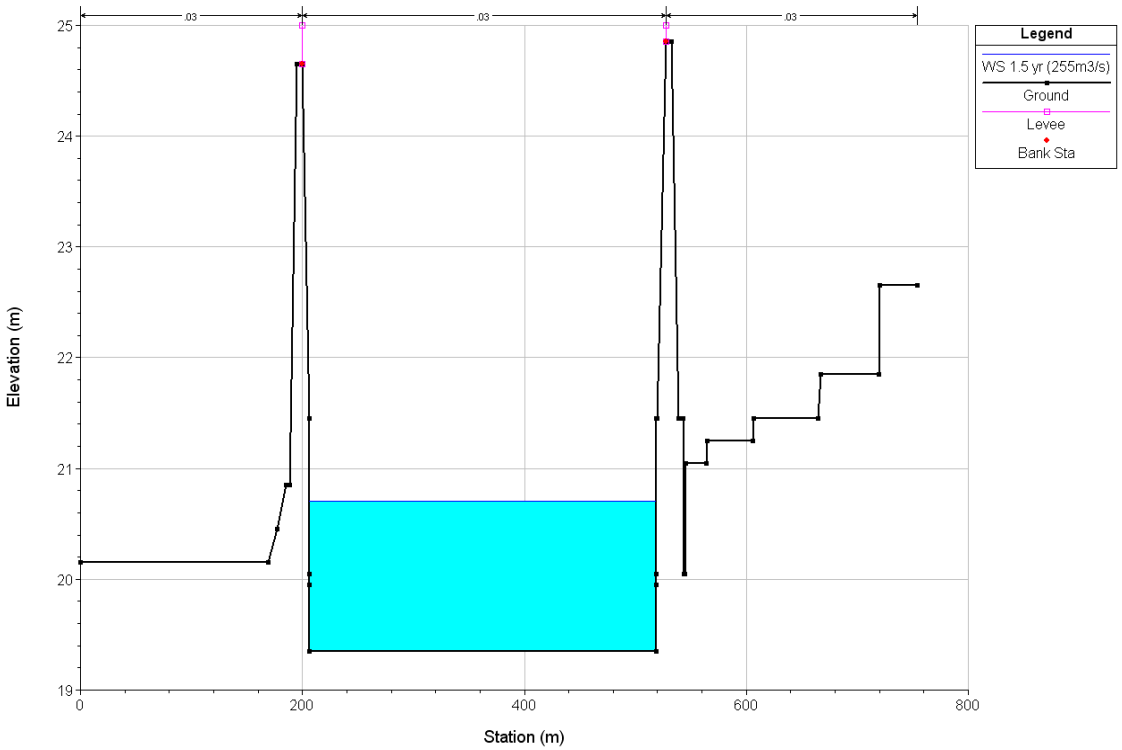

Figure H-11: Cross Section No. 97+093

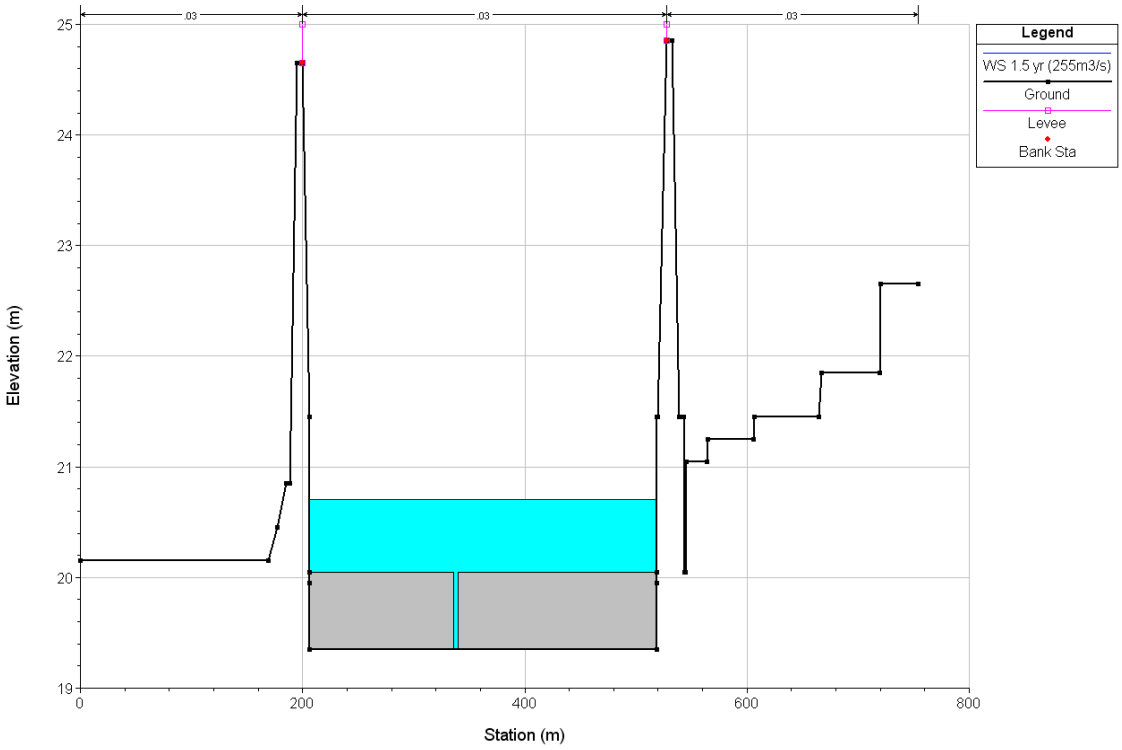

Figure H-12: Cross Section No. 97+092 IS

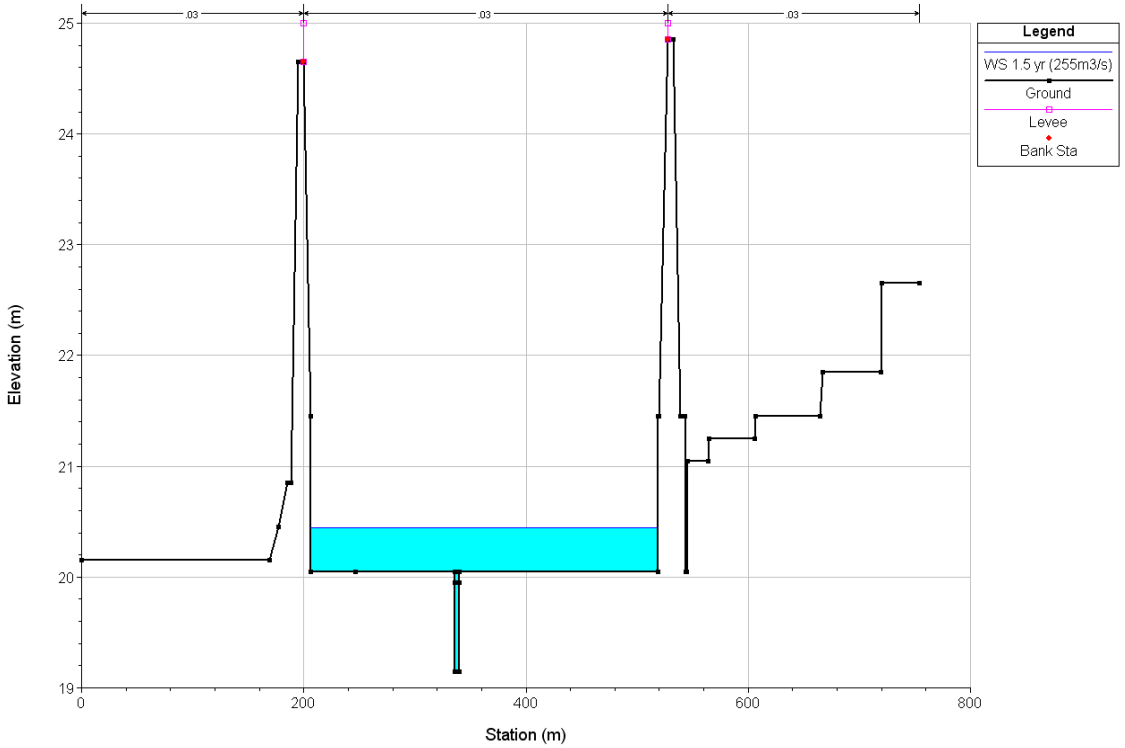

Figure H-13: Cross Section No. 97+084

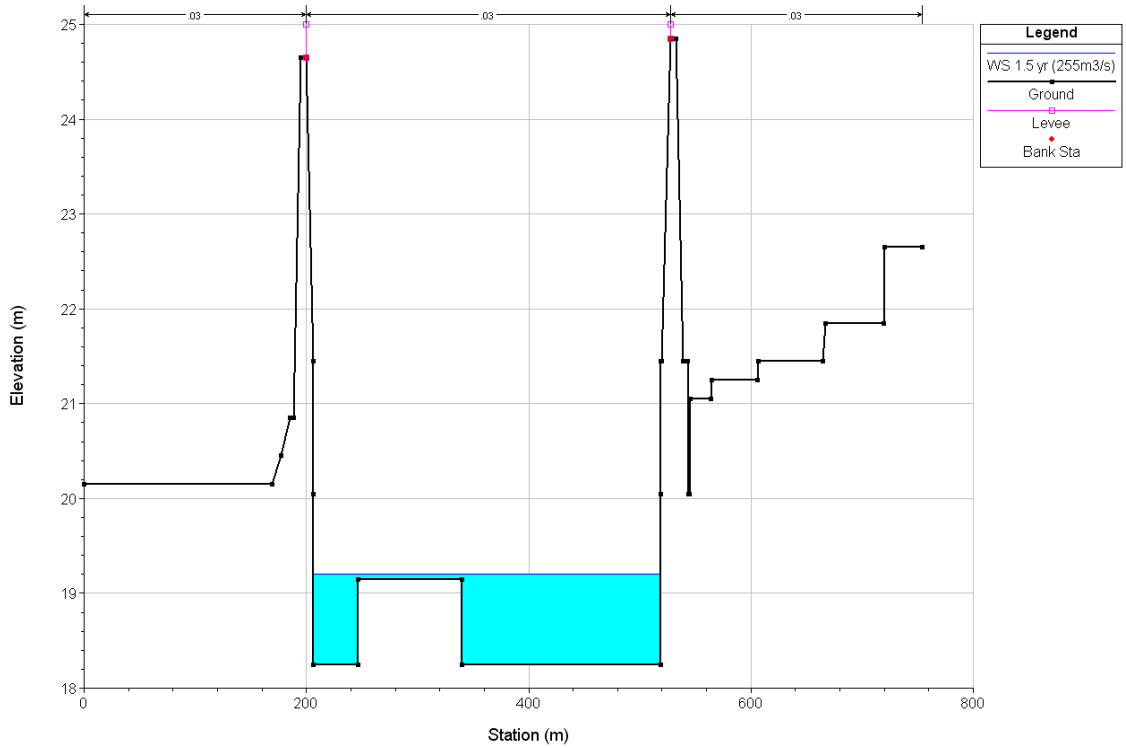

Figure H-14: Cross Section No. 97+081

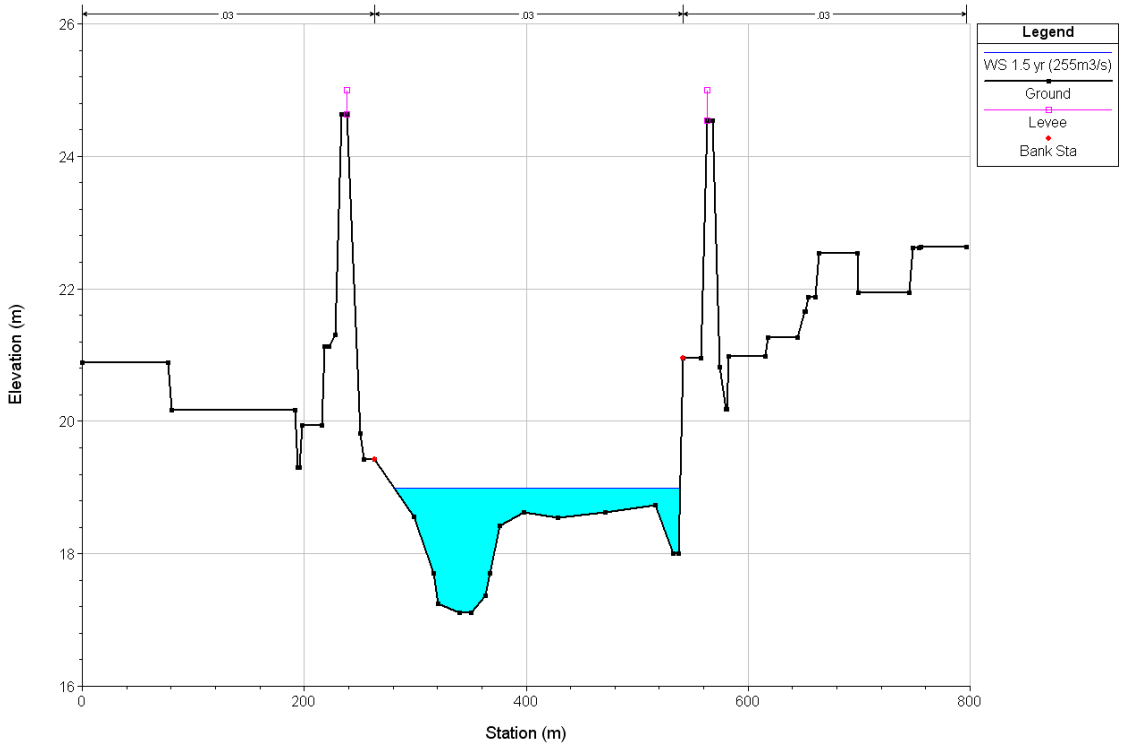

Figure H-15: Cross Section No. 97+000

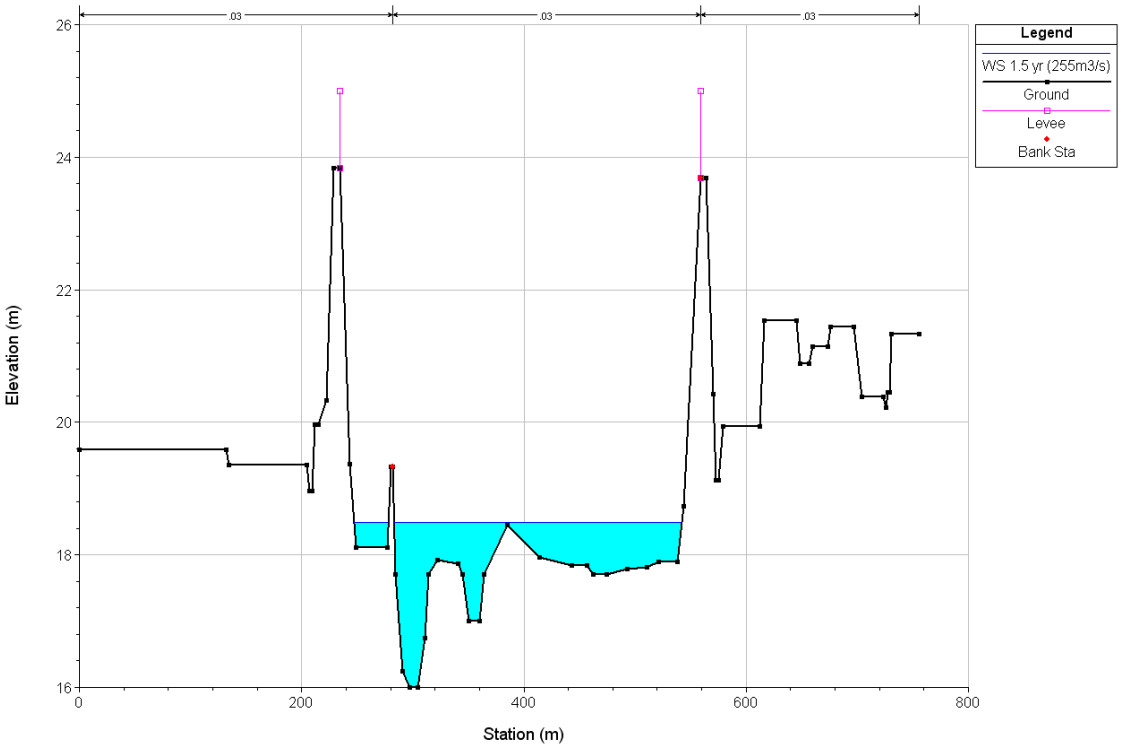

Figure H-16: Cross Section No. 96+000

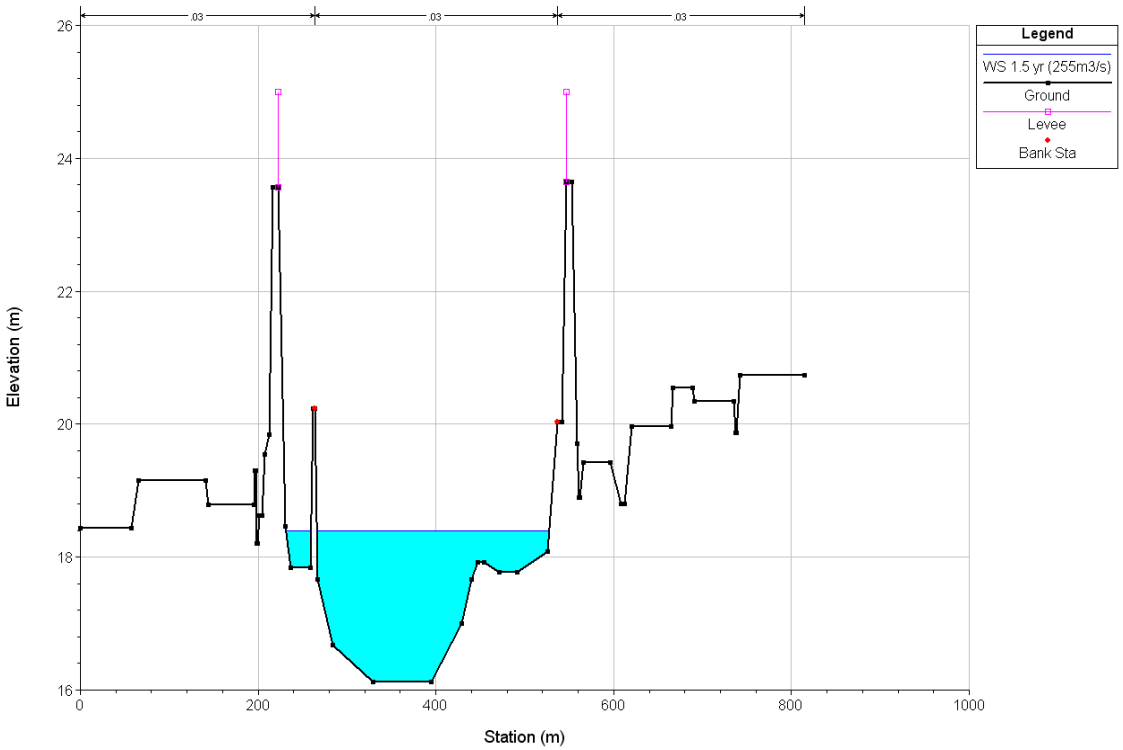

Figure H-17: Cross Section No. 95+000

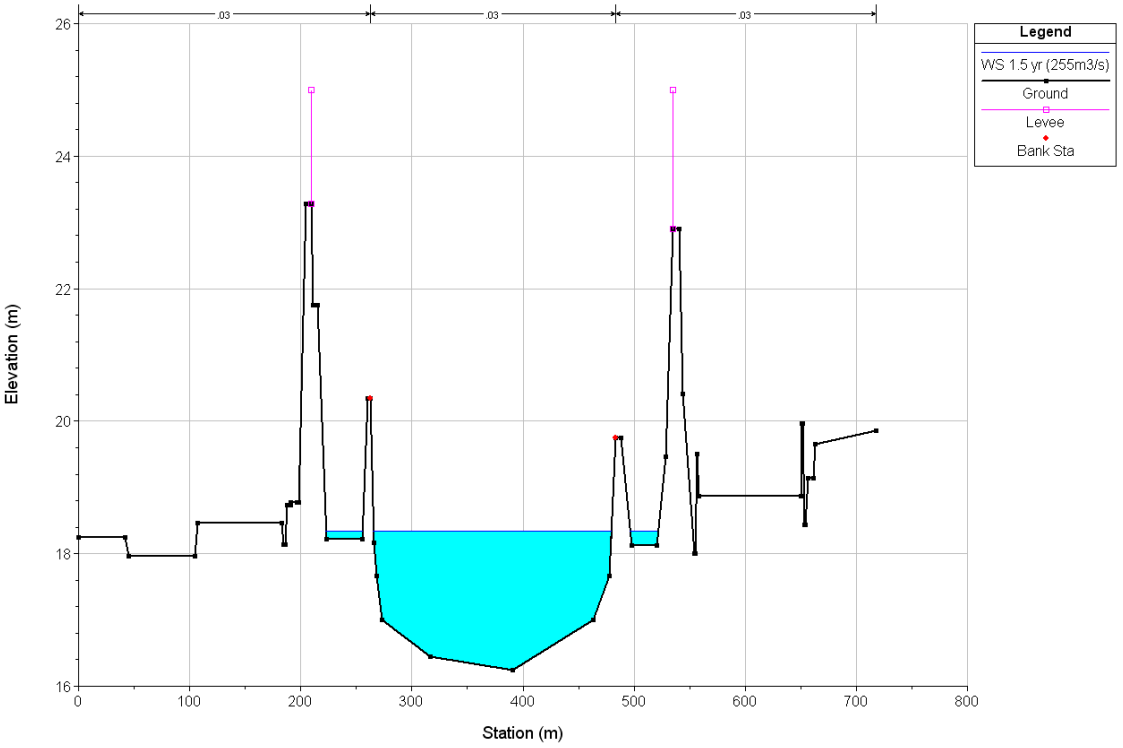

Figure H-18: Cross Section No. 94+000

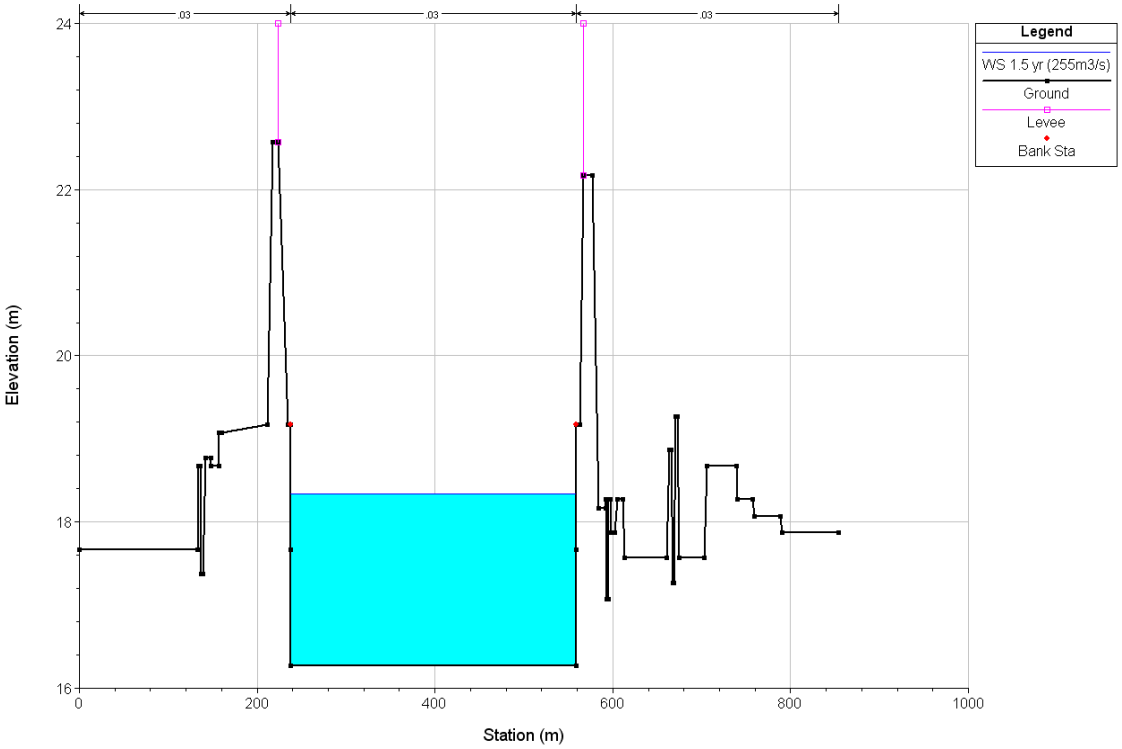

Figure H-19: Cross Section No. 93+071

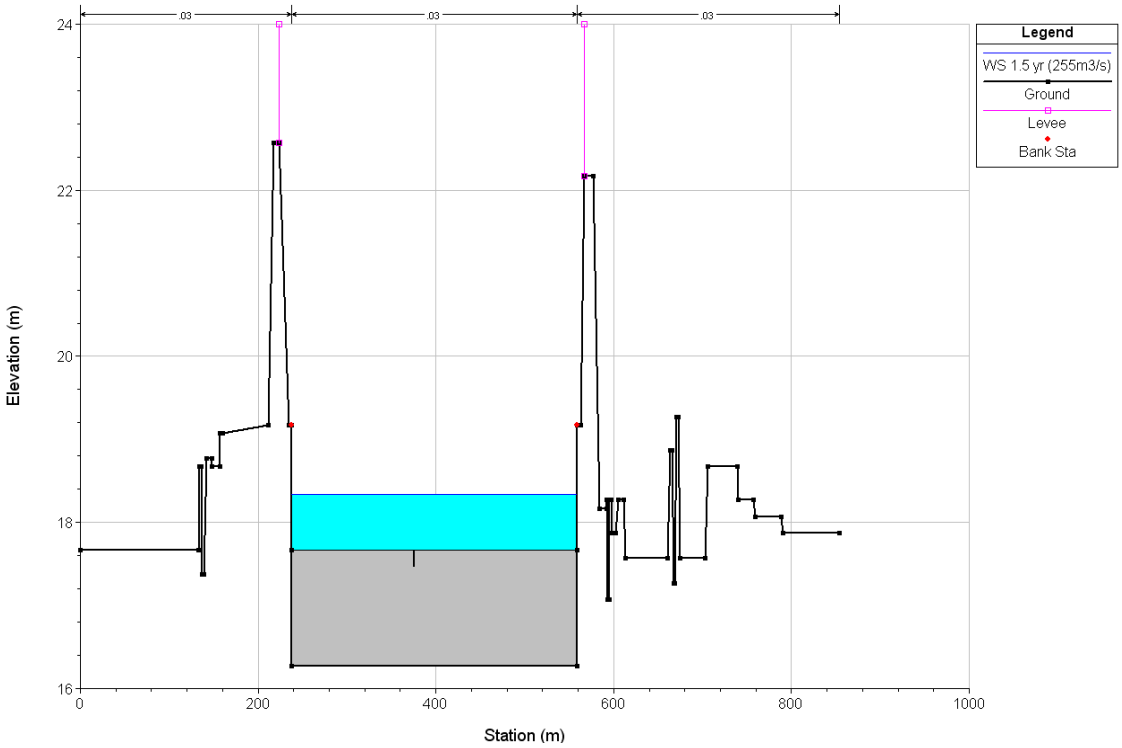

Figure H-20: Cross Section No. 93+070 IS

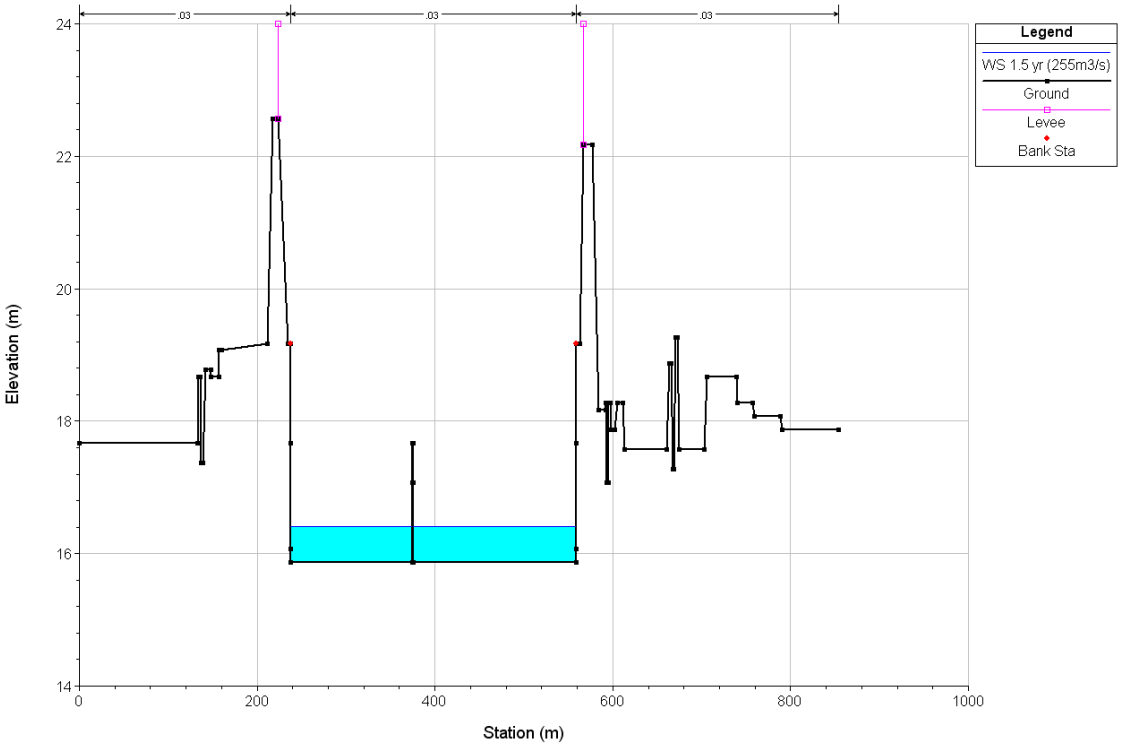

Figure H-21: Cross Section No. 93+056

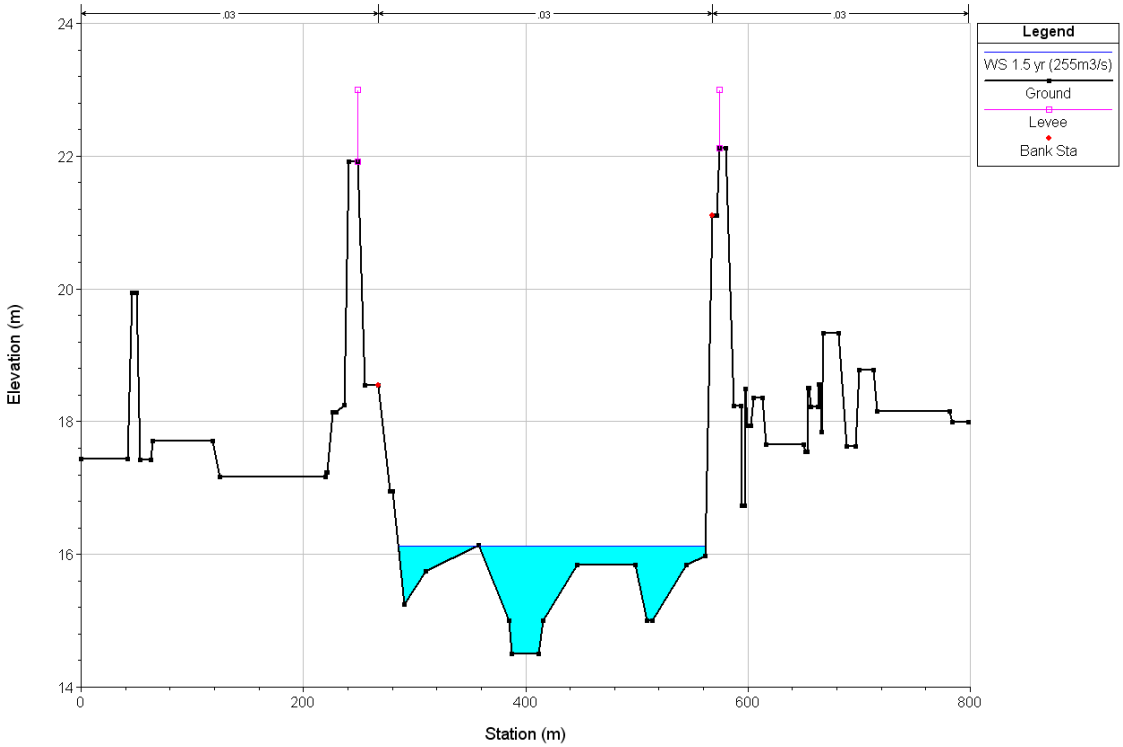

Figure H-22: Cross Section No. 93+000

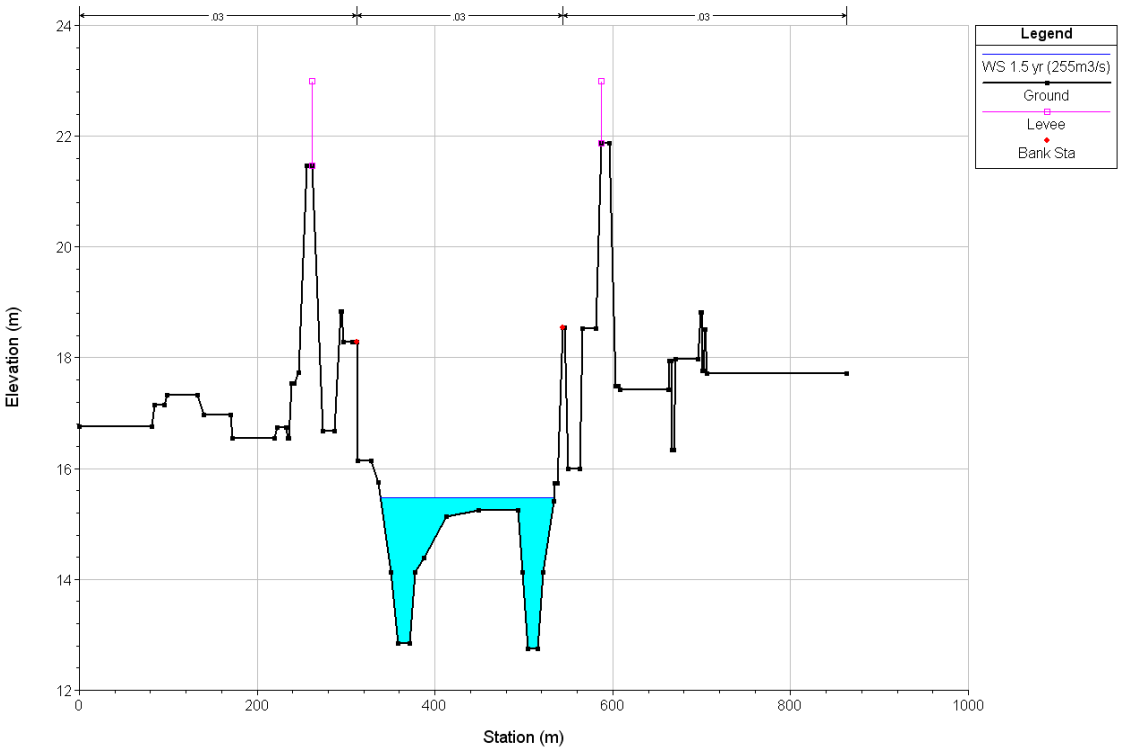

Figure H-23: Cross Section No. 92+000

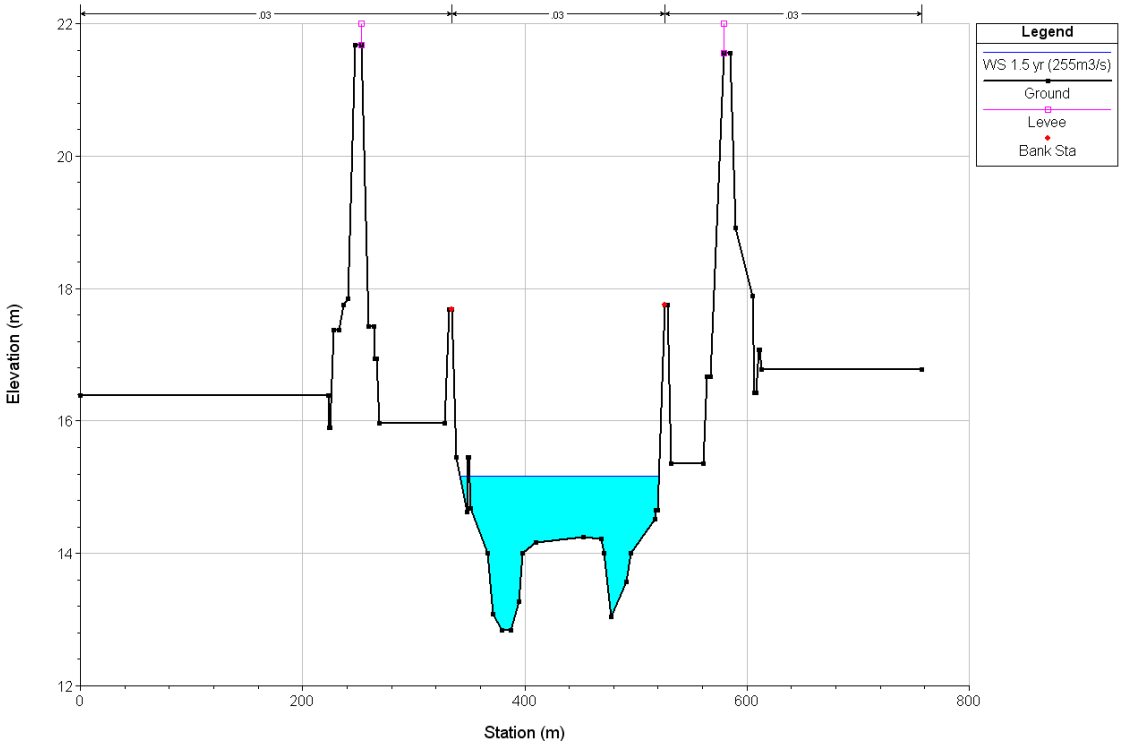

Figure H-24: Cross Section No. 91+000

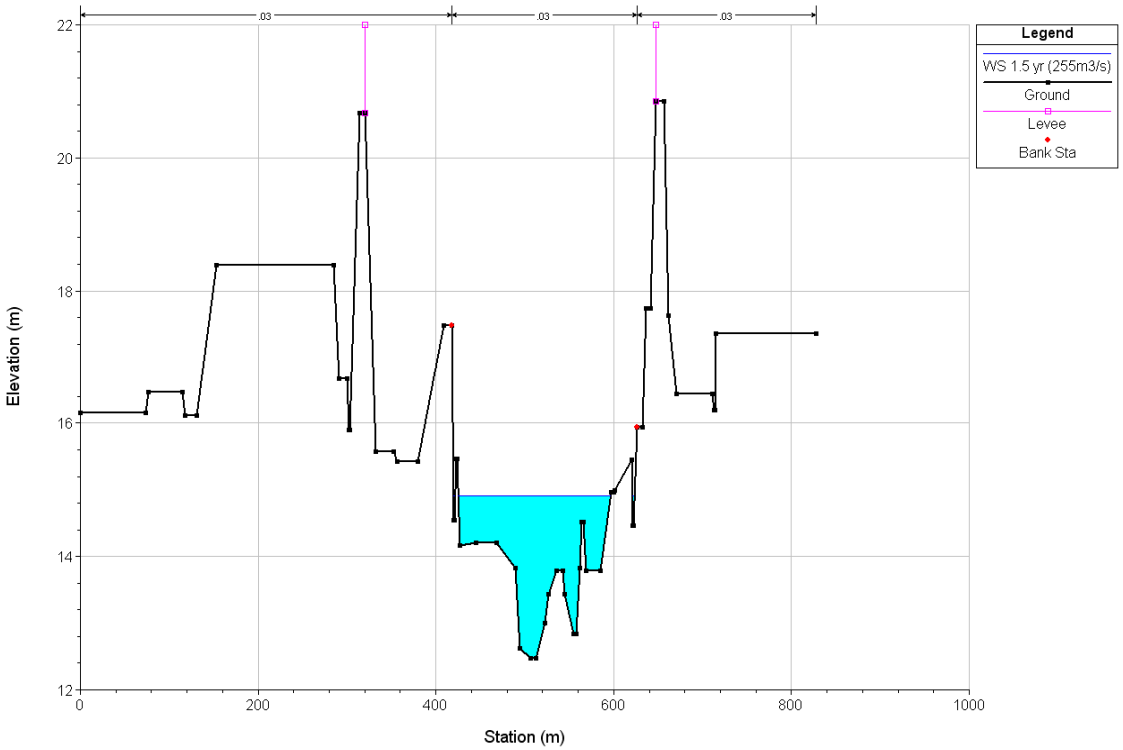

Figure H-25: Cross Section No. 90+000

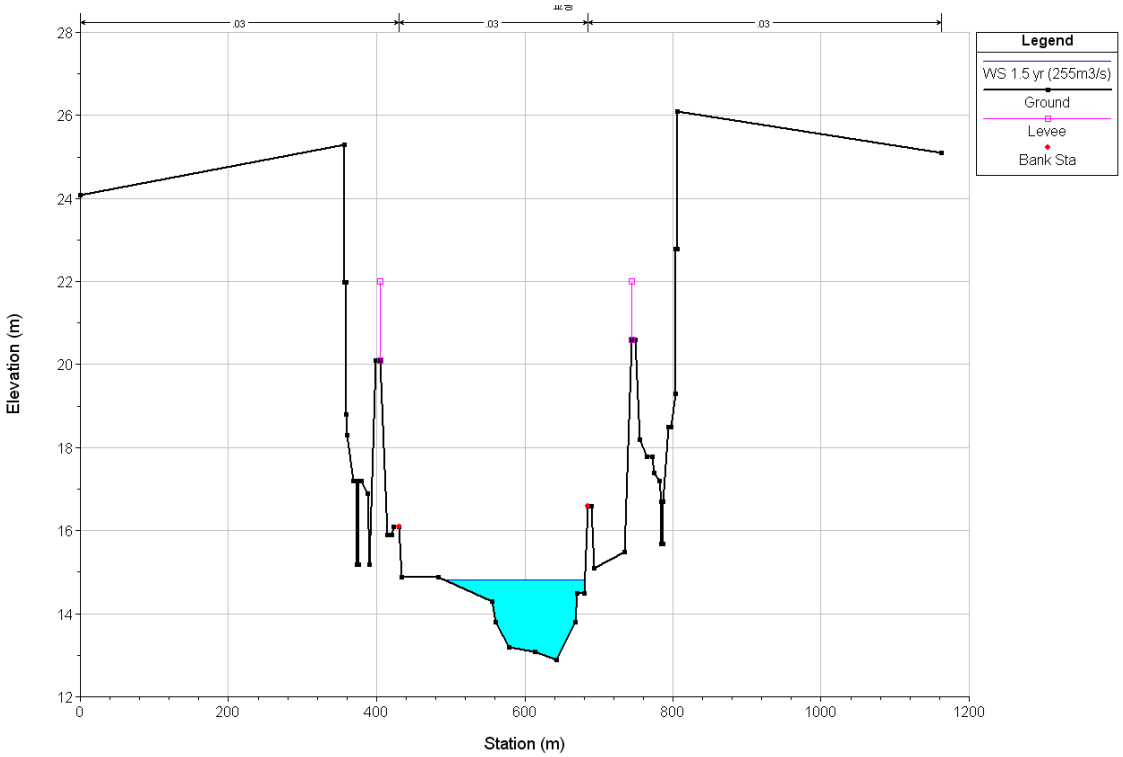

Figure H-26: Cross Section No. 89+182

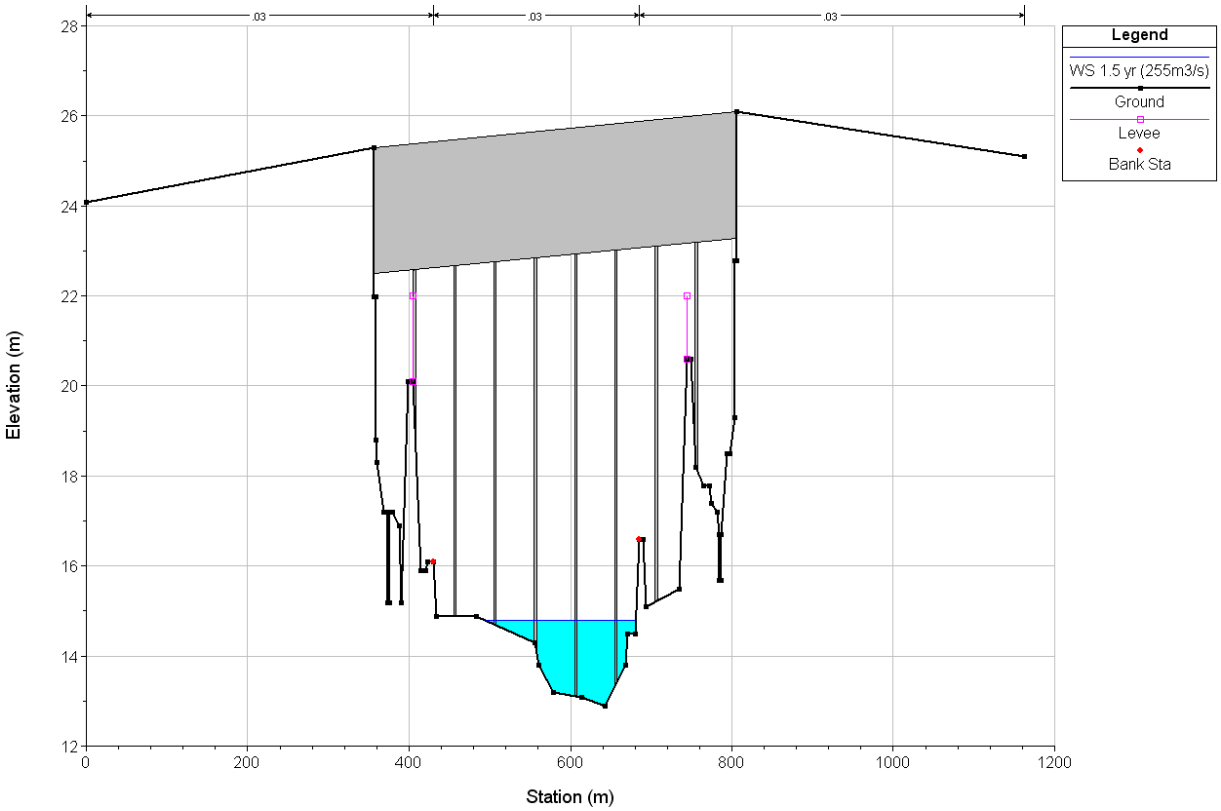

Figure H-27: Cross Section No. 89+170 BR U

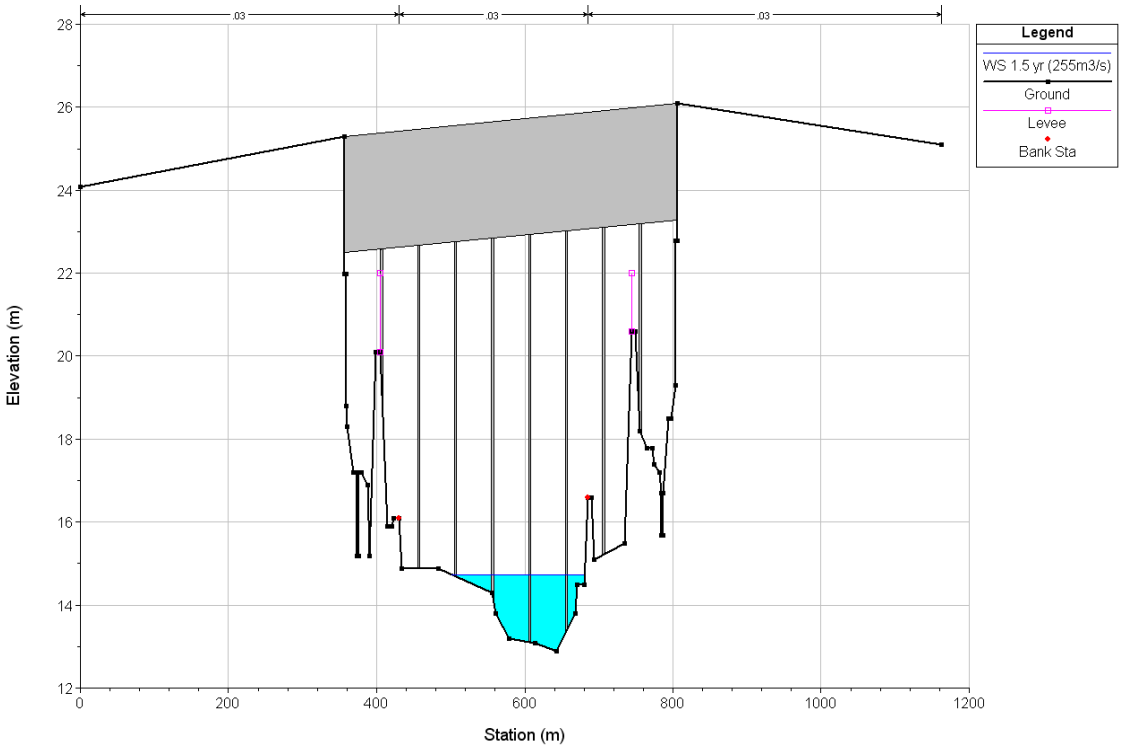

Figure H-28: Cross Section No. 89+170 BR D

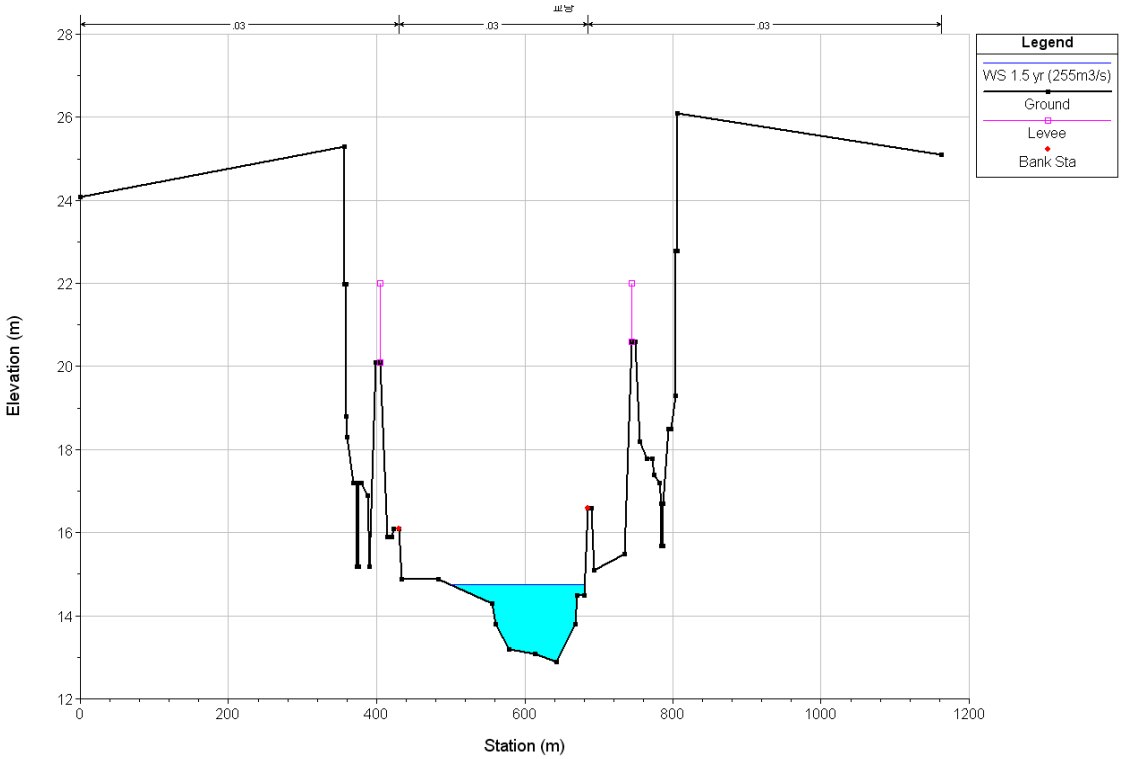

Figure H-29: Cross Section No. 89+158

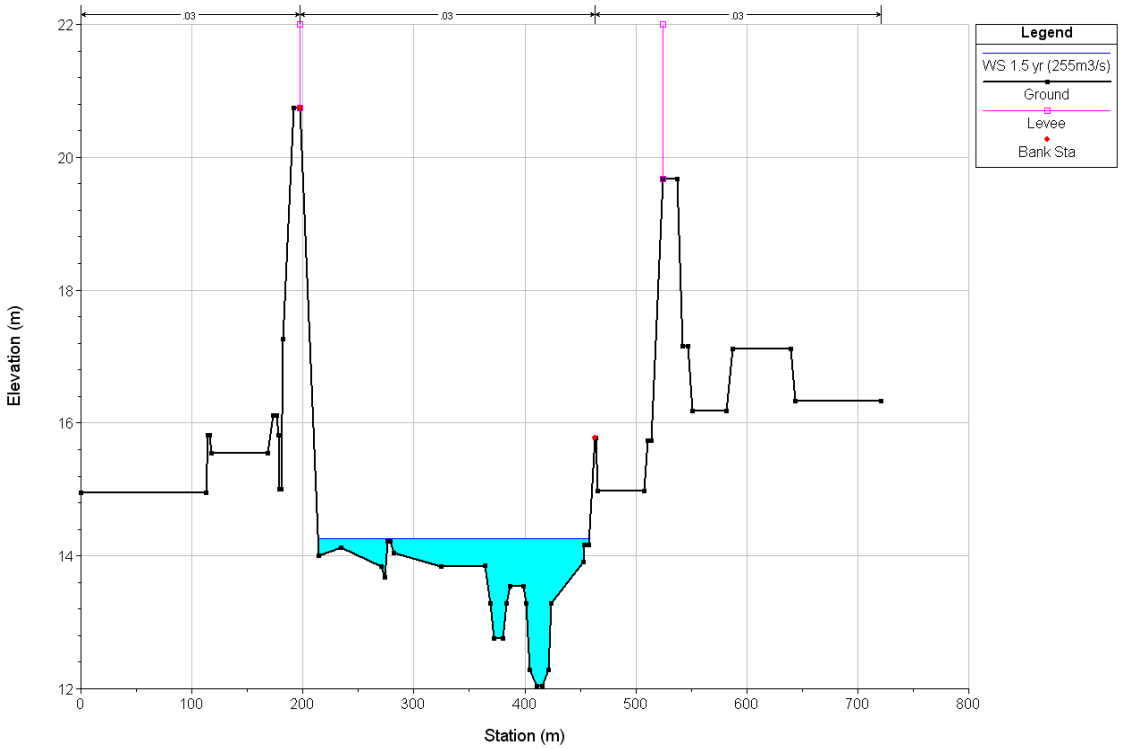

Figure H-30: Cross Section No. 89+000

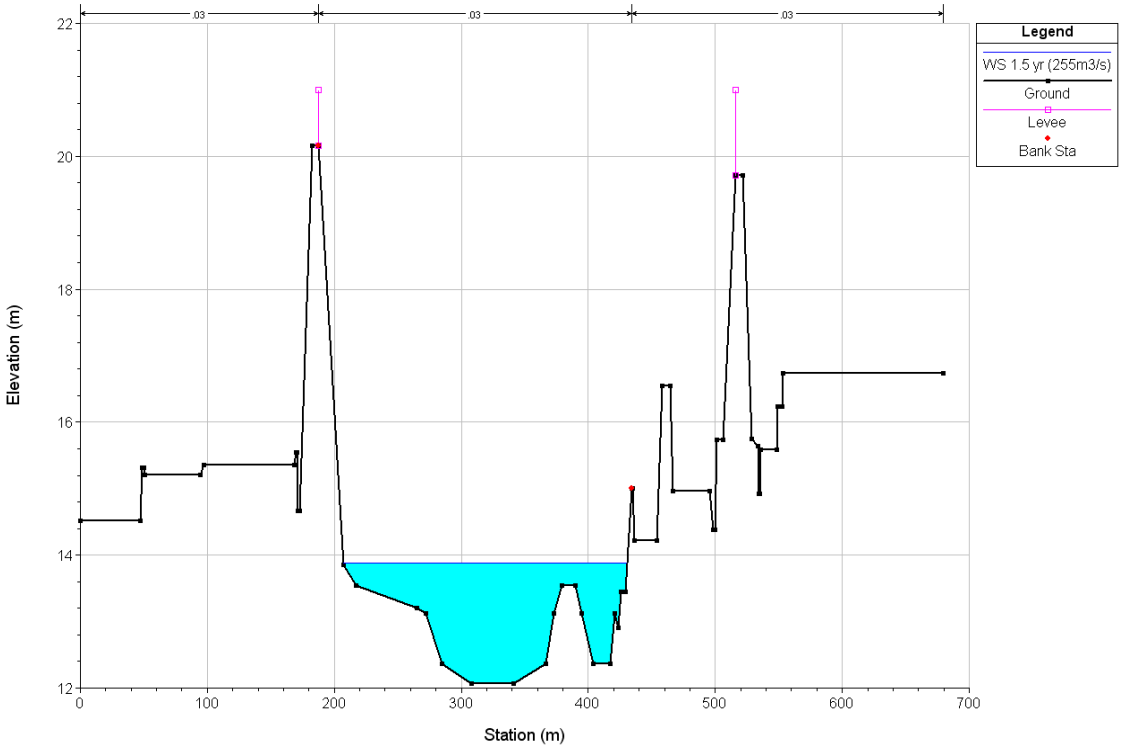

Figure H-31: Cross Section No. 88+000

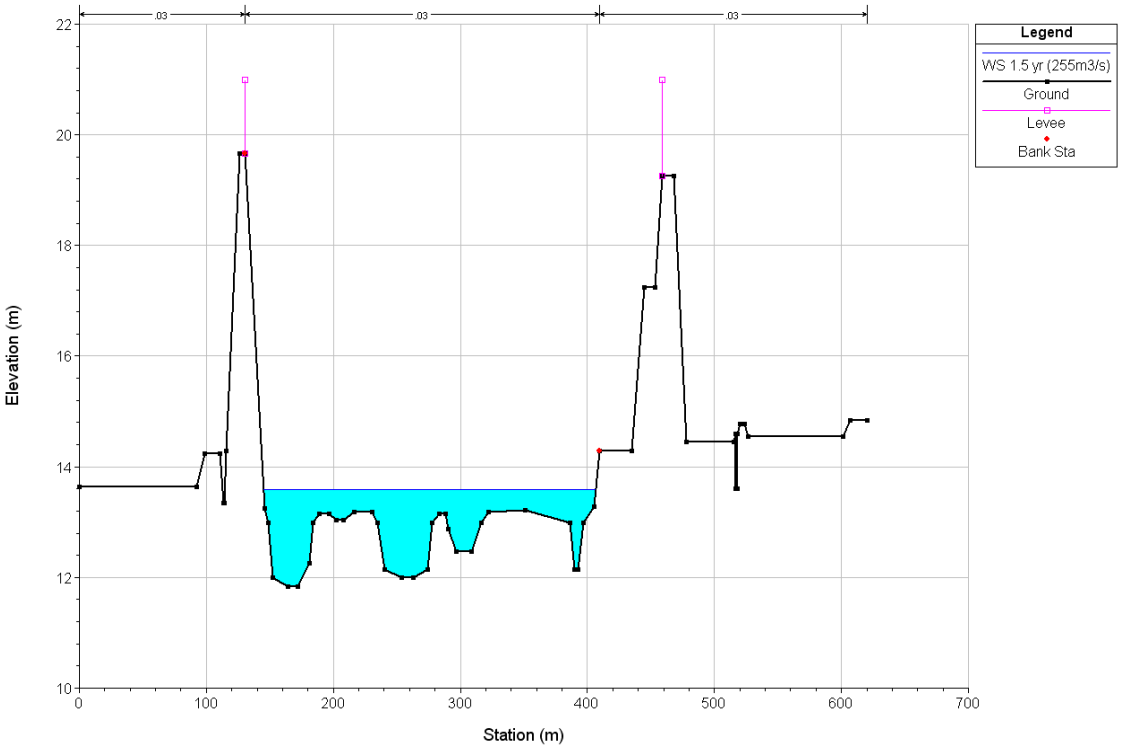

Figure H-32: Cross Section No. 87+000